MeteorNews

ISSN 2570-4745 VOL 8 / ISSUE 1 / JANUARY 2023

Fireball recorded at Hárskút (Hungary) on 26th October 2022, at 01h43m UT (the camera clock was not adjusted for a long time so the time is not very accurate). Despite the thin clouds the persistent train of the fireball was visible for more than 10 minutes. (Credit Monika Landy-Gyebnar).

- October Camelopardalids
- Orionids
- Geminids
- CAMS reports
- Radio meteor work
- Fireball reports

Contents

October Camelopardalids (OCT#281) recorded by Global Meteor Network

Paul Roggemans[1], Damir Šegon[2] and Denis Vida[3]

[1] **Pijnboomstraat 25, 2800 Mechelen, Belgium**
paul.roggemans@gmail.com

[2] **Astronomical Society Istra Pula, Park Monte Zaro 2, 52100 Pula, Croatia**

[3] **Department of Earth Sciences, University of Western Ontario, London, Ontario, N6A 5B7, Canada**
denis.vida@gmail.com

In 2022, the Global Meteor Network identified 159 meteors as possible October Camelopardalids (OCT#281), 139 of these within a short time interval of 192.3° < $\lambda_{\odot}$ < 192.75°. The time of maximum activity occurred at $\lambda_{\odot}$ = 192.55° corresponding to 2022 October 06, 03^h15^m UT. The activity level at maximum with a ZHR of 5 should catch attention of experienced visual meteor observers watching under good circumstances. The radiant has a small diameter of only few degrees and the orbital element diagrams show a very compact concentration of orbits. With a Tisserand value relative to Jupiter, T_J of about 0.5 and an orbital period *P* of about 92 years, this meteoroid stream has all characteristics of a prograde long-period comet shower.

1 Introduction

The poorly known October Camelopardalid (OCT#281) meteor shower has been occasionally spotted in 1902, 1942, 1976 and 2005, it was first documented by Jenniskens (2006). In later years the shower occurred in the data collected by the major video meteor networks, EDMOND, SonotaCo and CAMS. When CAMS BeNeLux registered as many 37 orbits of this shower during a clear night on 5–6 October 2018, the available data was used for a detailed analysis. The history of the shower has been summarized at the occasion of this analysis (Roggemans et al., 2019b).

Meanwhile a few years more data became available for CAMS, SonotaCo as well as for the new Global Meteor Network. The October Camelopardalid activity displayed a distinct activity 5–6 October 2022 on the radiant distribution map obtained by the Global Meteor Network. The well covered activity recorded in 2022 justifies another analysis dedicated to this shower, using the knowledge obtained from previous returns. *Figure 1* shows the compact OCT#281 radiant as a bright spot on a 24-hour map, no trace of activity can be seen on the plots of one day before or one day later. Apart from some outliers the shower activity seems limited to about half a day.

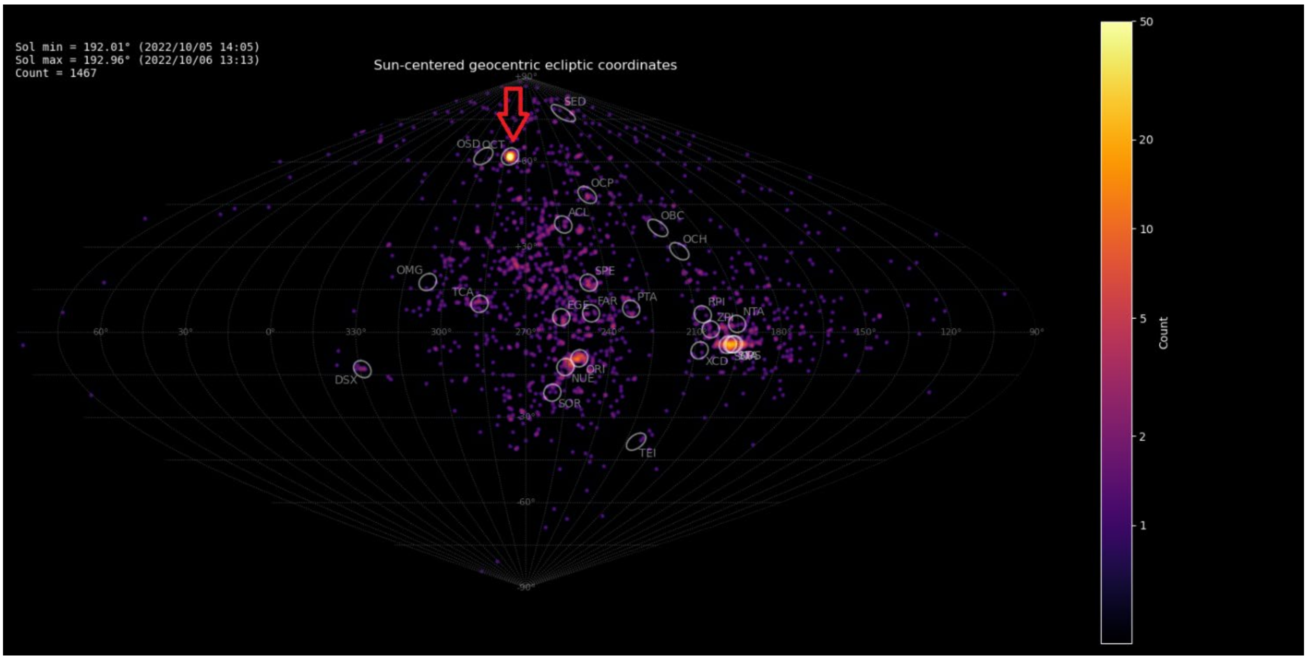

Figure 1 – The radiant map during the time interval 192.01° < $\lambda_{\odot}$ < 192.96° (2022 October 5, 14^h05^m to October 6, 13^h13^m UT). The red arrow indicates the bright spot of the very compact OCT#281 radiant in Sun-centered geocentric ecliptic coordinates.

Figure 2 – October Camelopardalid recorded by BE000E (Assenede, Belgium) at 2022 October 6, $02^h48^m54^s$ UT, trajectory solved with BE0001, BE0005 and BE000D.

Figure 3 – October Camelopardalid recorded by BE0007 (Genk, Belgium) at 2022 October 6, $00^h51^m26^s$ UT, multi-station with CZ0002 and FR0006.

Figure 4 – October Camelopardalid recorded by BE0005 (Grapfontaine, Belgium) at 2022 October 6, $02^h00^m09^s$ UT, multi-station with BE0008, UK0004, UK001P, UK002C, UK0034, UK0041, UK004C, UK005P, UK006B, UK006D, UK007B, UK007E, UK007H and UK007U.

Figure 5 – October Camelopardalid recorded by BE0008 (Genk, Belgium) at 2022 October 6, $02^h00^m09^s$ UT, same meteor as in *Figure 4*, triangulation based on as many as 15 camera stations!

Figure 6 – October Camelopardalid recorded by FR000X (Hagnicourt, France) at 2022 October 6, $04^h40^m31^s$ UT, triangulated with BE0001, BE0005, BE0009, BE000B, BE000C, BE000J, UK0004, UK003W and UK0007W.

Figure 7 – October Camelopardalid recorded by UK0004 (Eastbourne, United Kingdom) at 2022 October 6, 04h40m31s UT, triangulated with BE0001, BE0005, BE0009, BE000B, BE000C, BE000J, FR000X, UK003W and UK0007W.

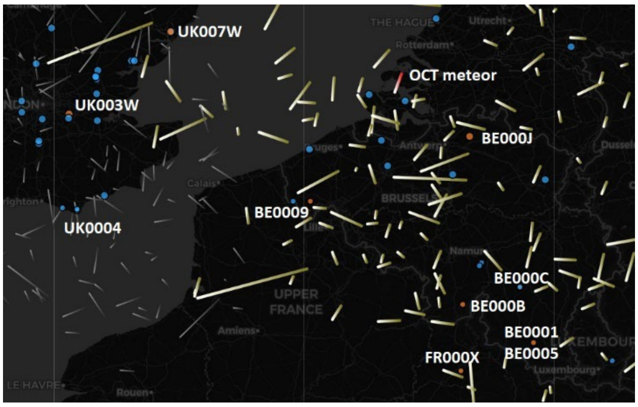

Figure 8 – Meteor map showing the trajectory for October 6, 04h40m31s UT and the stations that contributed to its triangulation.

The Global Meteor Network collected 1607 orbits during the night of 2022 October 5–6 (192.01° < $\lambda_{\odot}$ < 192.96°). The October Camelopardalids did not display any spectacular events. A selection of imaged OCT meteors is shown in *Figures 2 to 7*. Interested readers can find the trajectories and contributing camera stations on the Meteor Map[1] provided by Tammo-Jan Dijkema. *Figure 8* shows a screenshot of the Meteor Map with the trajectory obtained for the meteor shown in *Figures 6 and 7*. All details about the Meteor Map and how to use this has been presented in an article (Dijkema, 2022).

2 The GMN data

The Global Meteor Network identified 254 orbits as October Camelopardalids since 2019. This identification has been made based on a list of known meteor showers (Jenniskens et al., 2018) for orbits recorded within 1° in solar longitude of the known activity period, with the radiant within 3° relative to the known radiant position and with a geocentric velocity v_g within an interval of 10% relative to the reference geocentric velocity (Moorhead et al., 2020). Details about the methodology, theory and results of the Global Meteor Network can be found in Vida et al. (2019; 2020; 2021).

In 2022 alone, as many as 159 OCT#281 orbits were counted while the numbers in previous years were more modest with 57 in 2021, only 11 in 2020 and 27 orbits in 2019. Weather circumstances as well as the number of contributing GMN cameras may explain the variation from year to year. Short duration showers can be easily missed; therefore, cameras are needed at as many sites as possible.

The shower identification based on a reference list, radiant position and velocity, is not absolute, but has a good probability that the meteor may belong to the shower. This shower association still risks including sporadics. To eliminate these, we should look at the orbits to remove outliers that deviate too much from the mean orbit. This can be due to errors, mainly the velocity determination being very sensitive to measurement inaccuracies, or just 'noise' caused by look-alike sporadics. Whatever the cause may be, such outliers or noise should be removed to establish a reliable mean orbit.

When the 2018 analysis was made our knowledge about this shower was almost nonexistent. The samples to search for possible OCT-orbits were taken over a rather long range in solar longitude, a wide radiant area in equatorial coordinates and a large interval in velocity. Meanwhile we know that the activity of the shower is very short, therefore in this study we limited the period to search for OCT orbits to only 3 degrees in solar longitude. With a declination between 74° and 84°, the equatorial coordinates were not the best choice to define the radiant area to search for orbits. The Sun-centered coordinates offer a better alternative. To search for OCT orbits, we selected our sample within the following intervals:

- 191° < $\lambda_{\odot}$ < 194°
- 273° < $\lambda - \lambda_{\odot}$ < 290°
- +57° < β < +67°
- 39 km/s < v_g < 51 km/s

The GMN data[2] has 266 orbits that fulfill these conditions. This sample has been searched with an iterative procedure to locate the best fitting mean orbit for a concentration of similar orbits. The method used for this has been described before (Roggemans et al., 2019a) and combines three classic discrimination criteria, considering different classes for the degree of similarity. The discrimination criteria used in this method are that of Southworth and Hawkins (1963), identified as D_{SH}, Drummond (1981), identified as D_D, and Jopek (1993), identified as D_H. The method to compute the mean orbit during the iteration process has been described by Jopek et al. (2006).

We define five different classes with specific threshold levels of similarity:

- Low: D_{SH} < 0.25 & D_D < 0.105 & D_H < 0.25;
- Medium low: D_{SH} < 0.2 & D_D < 0.08 & D_H < 0.2;
- Medium high: D_{SH} < 0.15 & D_D < 0.06 & D_H < 0.15;
- High: D_{SH} < 0.1 & D_D < 0.04 & D_H < 0.1.
- Very high: D_{SH} < 0.05 & D_D < 0.02 & D_H < 0.05.

[1] https://tammojan.github.io/meteormap/

[2] https://globalmeteornetwork.org/data/traj_summary_data/

These classes allow us to distinguish the degree of concentration and dispersion of the particles within the meteoroid stream. The iterative search identifies 239 orbits with low threshold similarity of which as many as 121 fit the very high threshold similarity. The mean orbits for each threshold class of similarity are listed in *Table 1*. The values are almost identical regardless the class of similarity.

Table 1 – The mean orbits for the final selection of Global Meteor Network orbits with five different threshold levels on the D-criteria.

	Low	Medium low	Medium high	High	Very high
λ_O	192.53°	192.53°	192.53°	192.53°	192.53°
α_g	167.9°	167.9°	167.9°	167.9°	167.9°
δ_g	+78.6°	+78.6°	+78.6°	+78.6°	+78.6°
v_g	45.8	45.8	45.8	45.9	45.9
$\lambda - \lambda_O$	281.8°	281.8°	281.8°	281.8°	281.8°
β	+61.9°	+61.9°	+61.9°	+61.9°	+61.9°
H_b	108.3	108.3	108.3	108.4	108.4
H_e	95.5	95.4	95.5	95.4	95.1
a	17.9	18.3	19.0	19.5	20.4
q	0.9901	0.9903	0.9905	0.9907	0.9907
e	0.9447	0.9460	0.9479	0.9492	0.9516
ω	169.17°	169.24°	169.19°	169.05°	168.94°
Ω	192.54°	192.54°	192.54°	192.53°	192.53°
i	77.77°	77.72°	77.81°	77.86°	77.91°
Π	1.71°	1.77°	1.73°	1.58°	1.46°
T_j	0.55	0.54	0.53	0.52	0.51
N	239	229	211	172	121

19 of the 254 orbits classified as OCT#281 by GMN fail to fit the low threshold similarity. In all these cases a too large or too small value for the eccentricity e makes the orbit fail to fit with the mean orbit derived by the iterative procedure. The eccentricity depends mainly on the velocity and the uncertainties on the velocities are rather small, in the order of ±0.01 to ±1.2 km/s at most, suggesting that these may be sporadics mistaken as OCT shower members at the initial shower classification. On the other hand, two orbits classified by the GMN as sporadics, and two orbits classified as October 6-Draconids (OSD#745) are considered as OCT#281 orbits as these fit the similarity criteria. Taking a preliminary defined radiant position and velocity range to make a first assessment of the shower association risks to include some sporadic events fitting these criteria by chance, while real shower members may be missed as the radiant size is not exactly known.

Most of the October Camelopardalid activity seems to be concentrated within about half a day of activity. *Figure 10* shows the flux and corresponding zenithal hourly rate for all years together (2019–2022), assuming a population index $r = 2.5$ as there weren't enough meteors from single stations to determine a population index. *Figure 11* shows the profile based on 2022 only. The flux at low levels and outside the peak is probably completely caused by sporadics, as there is no sporadic contamination suppression applied to the flux plots. The methodology to compute the flux and derived ZHR values has been explained in Vida et al. (2022). With a maximum ZHR of about 5, the shower activity should catch the attention of any experienced visual observers. However, any uninformed casual observer will most likely not notice anything unusual at all.

All OCT-orbits that fit the similarity criteria were detected in the interval $191.25° < \lambda_O < 193.58°$ which includes all outliers. The main activity of this shower was limited to $192.3° < \lambda_O < 192.75°$, or about 11 hours. This is in good agreement with Koseki (2021, page 166). The activity profile could be also reconstructed as a percentage of the number of OCT orbits relative to the number of sporadic orbits. In *Figure 12* the different classes of similarity contributing to the shower activity show that the main activity consists of very similar orbits. Short duration meteor showers like this can be easily missed when the observing window suffers bad weather interference or a lack of camera coverage.

The velocity range with 41.78 km/s < v_g < 48.77 km/s, is smaller than what we assumed to select the search sample. A range of 10% more or less than the mean geocentric velocity of 45.8 km/s definitely covers all possible orbits.

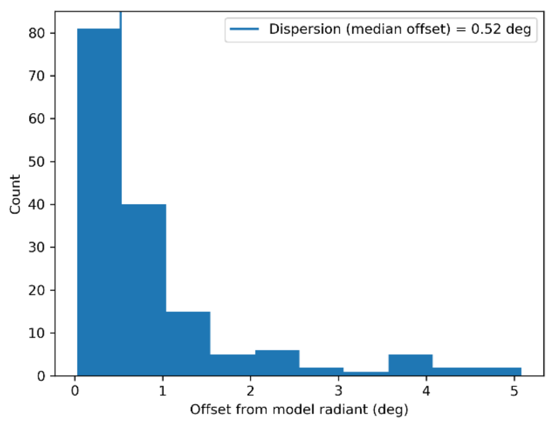

Figure 9 – The median offset from the mean radiant.

The median offset from the mean radiant as defined by Moorhead et al. (2021) is 0.52° (*Figure 9*). This makes the shower very compact and non-evolved, possibly young. The compactness of the shower appears also in the radiant plot with most orbits clustered within a radiant with few degrees in diameter. This is very well visible in the equatorial geocentric coordinates, although being at high declination (*Figure 13*). The compactness of the radiant is even more striking in Sun-centered ecliptic geocentric coordinates (*Figure 14*). Apart from some outliers with a low similarity threshold, most orbits share a very compact radiant area. Taking a close-up color coded for the geocentric velocity, we see that the outliers at higher ecliptic latitude are slower and those at lower ecliptic latitude faster compared to the concentration of orbits (*Figure 15*).

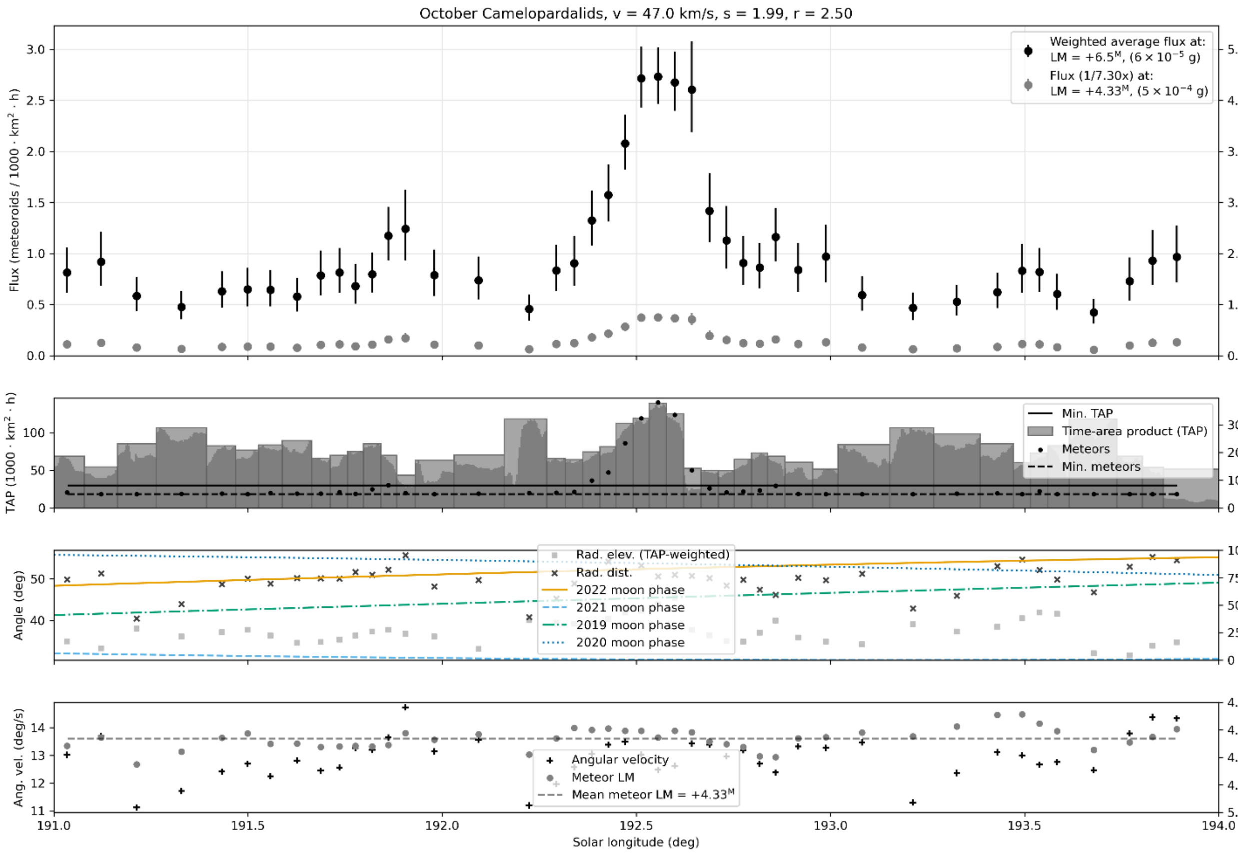

Figure 10 – The flux and corresponding ZHR profile for the October Camelopardalids (OCT#281) based on GMN data collected during the period 2019–2022.

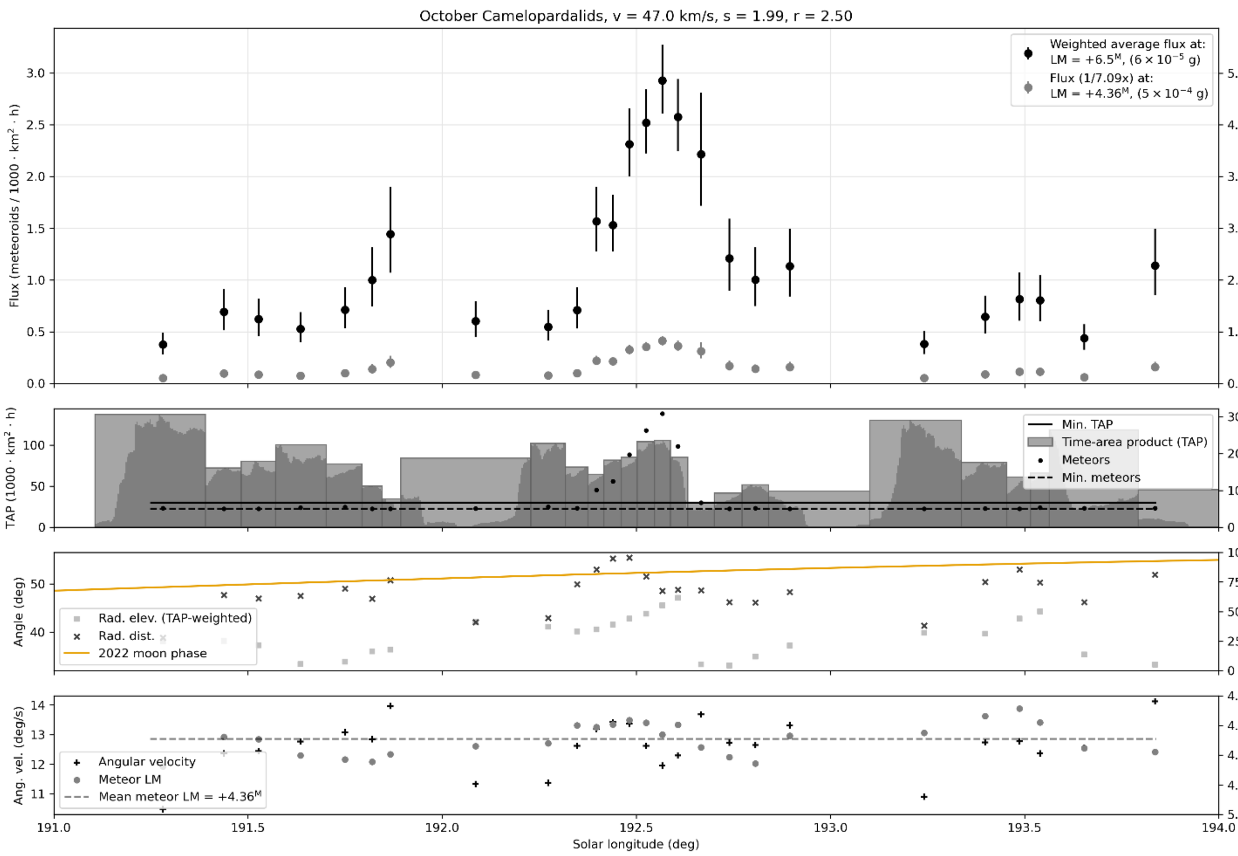

Figure 11 – The flux and corresponding ZHR profile for the October Camelopardalids (OCT#281) based on GMN data collected during 2022.

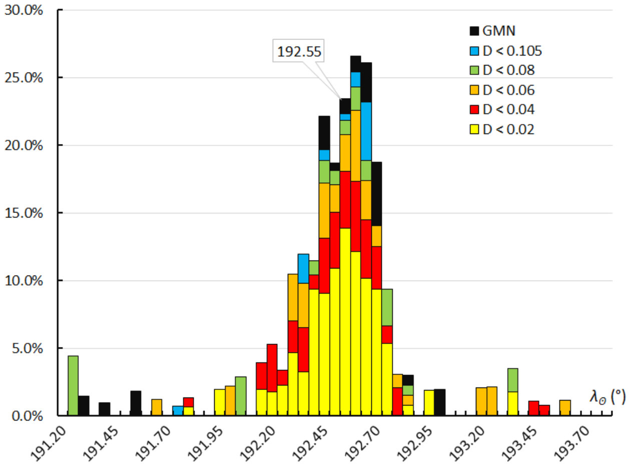

Figure 12 – Percentage of OCT#281 orbits relative to the number of sporadic orbits for the GMN shower identification and the different classes of similarity.

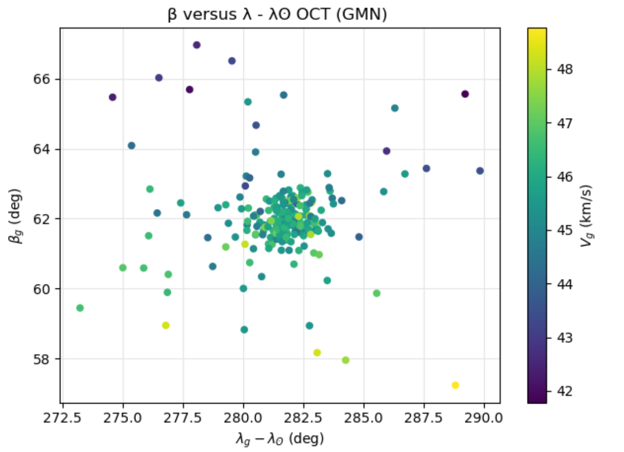

Figure 15 – The radiant plot for the OCT-orbits in Sun-centered ecliptic coordinates color coded for the geocentric velocity.

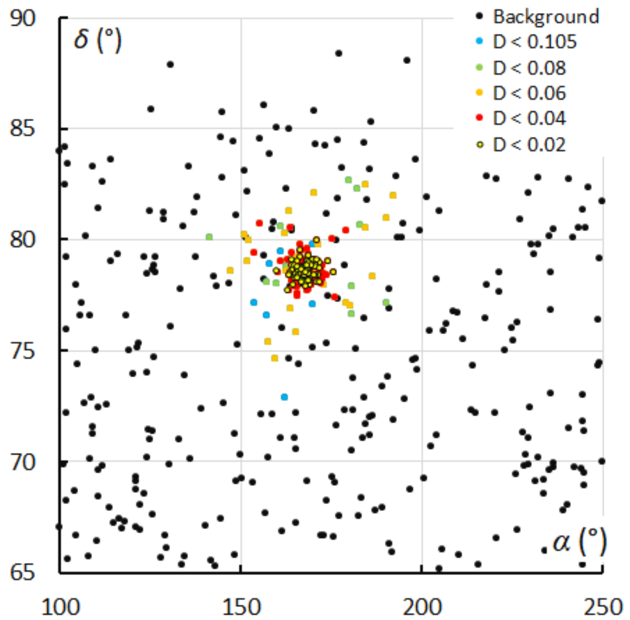

Figure 13 – The radiant plot for the OCT-orbits in equatorial geocentric coordinates, color coded according to the similarity classes.

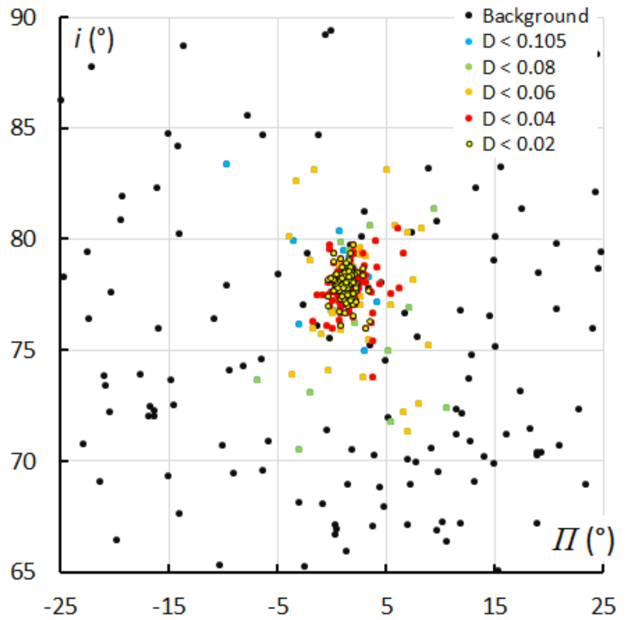

Figure 16 – The distribution of the inclination *i* against the longitude of perihelion *Π* for the OCT orbits, color coded according to the similarity classes.

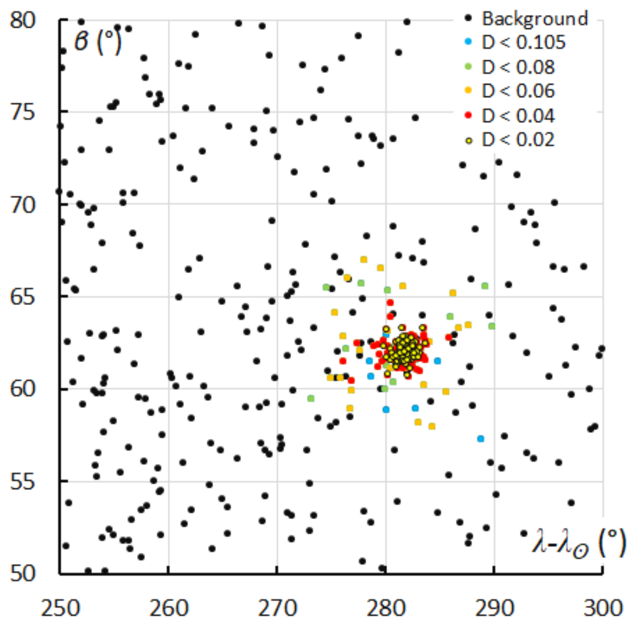

Figure 14 – The radiant plot for the OCT-orbits in Sun-centered ecliptic coordinates, color coded according to the similarity classes.

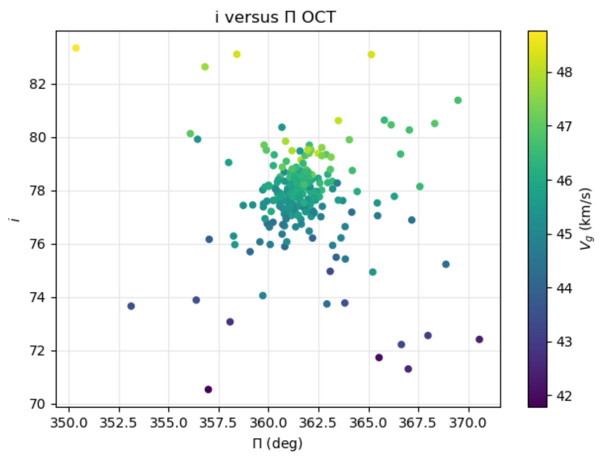

Figure 17 – The distribution of the inclination *i* against the longitude of perihelion *Π* for the OCT orbits, color coded for the geocentric velocity.

The distribution of inclination *i* against longitude of perihelion *Π* confirms the compactness of this meteoroid stream (*Figure 16*). A closer look at the velocity variation shows the faster OCT meteoroids at higher inclination and the slower meteoroids at lower inclination with a dense concentration near $i = 77.8°$. Also, the spread in longitude of perihelion is very narrow (*Figure 17*).

The distribution of the eccentricity e against the longitude of perihelion Π shows several outliers with $e > 1$ (*Figure 18*). With a mean eccentricity of about 0.95 we are close to the parabolic limit, even a small error in the velocity measurement can result in a hyperbolic orbit. The close up in *Figure 19* shows the spread in geocentric velocity, the higher the velocity, the higher the eccentricity value.

Figure 20 shows the distribution of the inclination i against the perihelion distance q. Apart from some outliers the bulk of the orbits are concentrated within a small range. *Figure 21* shows the corresponding velocity distribution with higher velocities at higher inclination.

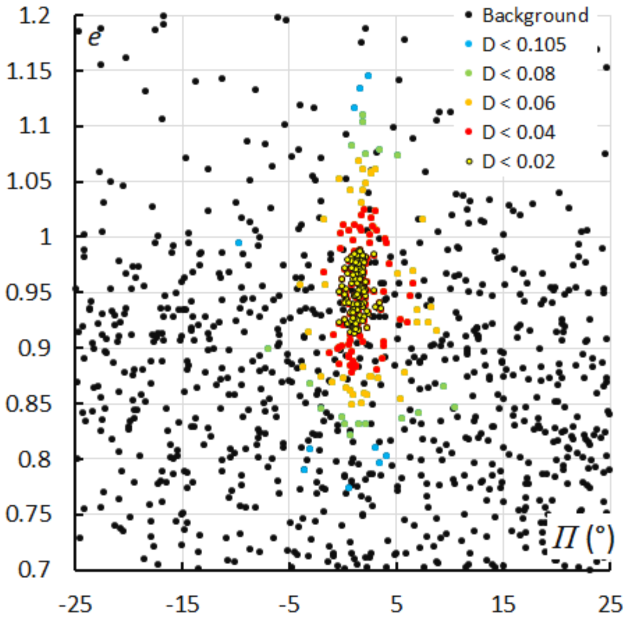

Figure 18 – The distribution of the eccentricity e against the longitude of perihelion Π for the OCT orbits, color coded according to the similarity classes.

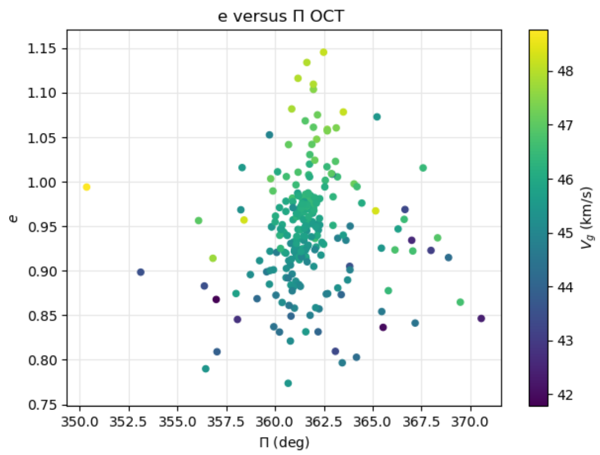

Figure 19 – The distribution of the eccentricity e against the longitude of perihelion Π for the OCT orbits, color coded for the geocentric velocity.

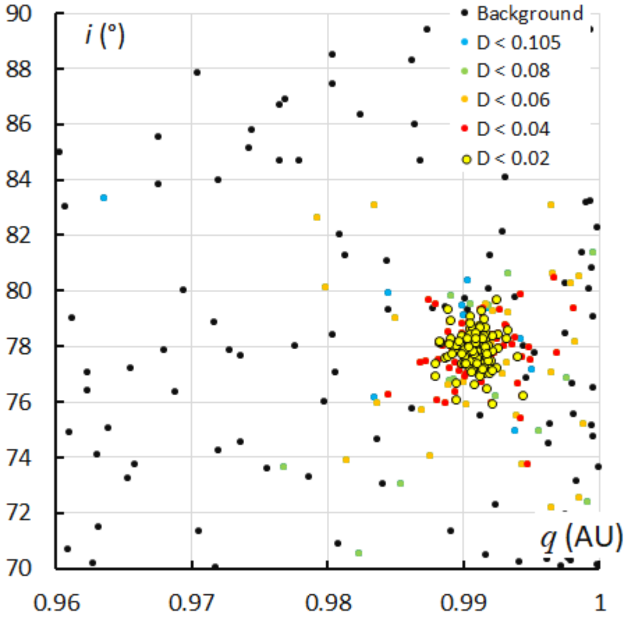

Figure 20 – The distribution of the inclination i against the perihelion distance q for the OCT orbits, color coded according to the similarity classes.

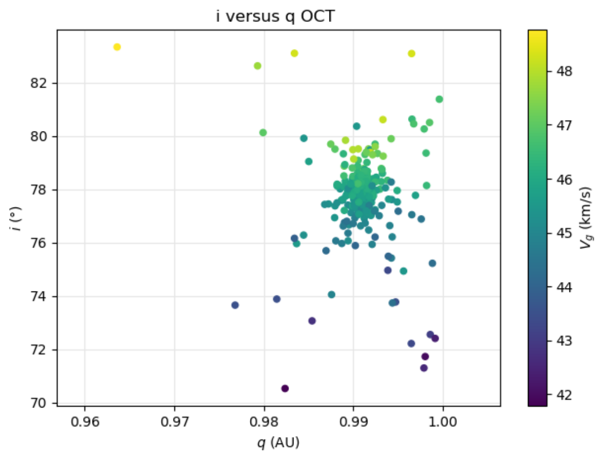

Figure 21 – The distribution of the inclination i against the perihelion distance q for the OCT orbits, color coded for the geocentric velocity.

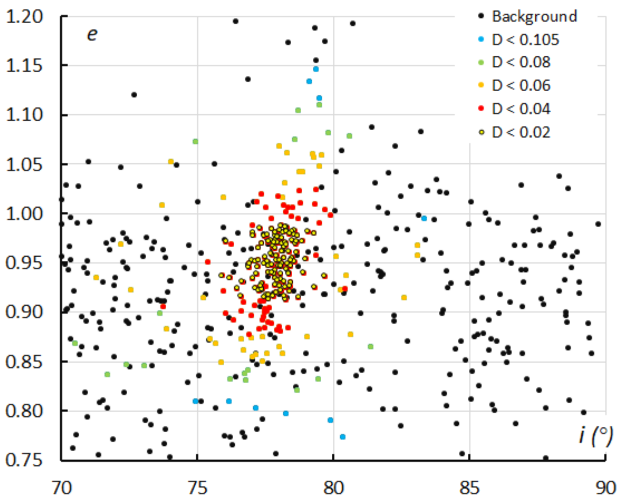

Figure 22 – The distribution of the eccentricity e against the inclination i for the OCT orbits, color coded according to the similarity classes.

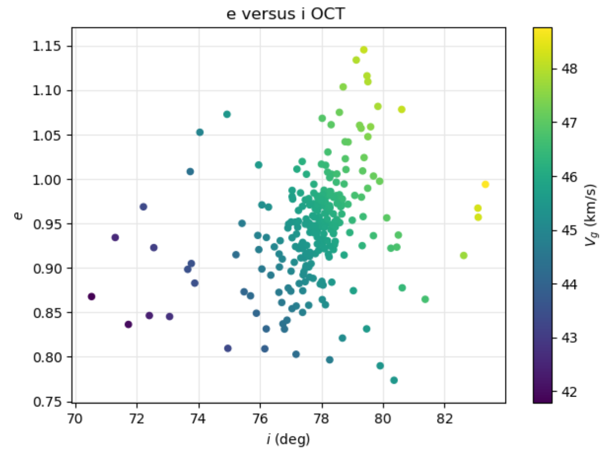

Figure 23 – The distribution of the eccentricity *e* against the inclination *i* for the OCT orbits, color coded for the geocentric velocity.

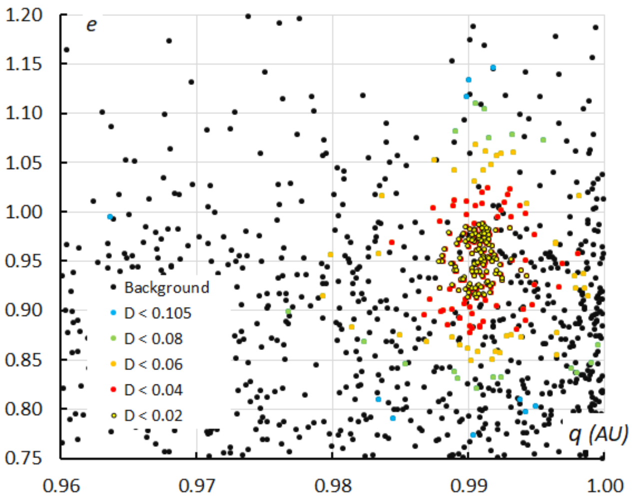

Figure 24 – The distribution of the eccentricity *e* against the perihelion distance *q* for the OCT orbits, color coded according to the similarity classes.

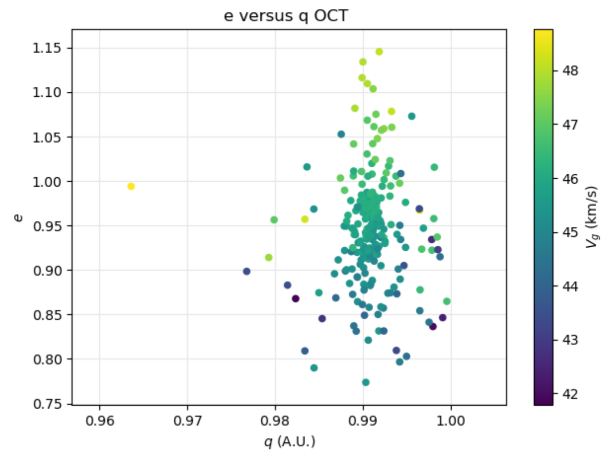

Figure 25 – The distribution of the eccentricity *e* against the perihelion distance *q* for the OCT orbits, color coded for the geocentric velocity.

The distribution of the eccentricity *e* against the inclination *i* (*Figure 22*), shows the same distorted pattern as in *Figure 18* affected by hyperbolic orbits caused by the uncertainties on the velocity measurement. The velocity distribution in *Figure 23* shows the spread from the left bottom corner with lower eccentricity and inclination towards the upper right corner with higher inclination and eccentricity. Most of the orbits are concentrated within a narrow range around the mean values.

The distribution of the eccentricity *e* against the perihelion distance *q* (*Figure 24*) also shows a compact concentration of orbits with outliers which were recorded with lower or higher velocities than the main concentration (*Figure 25*).

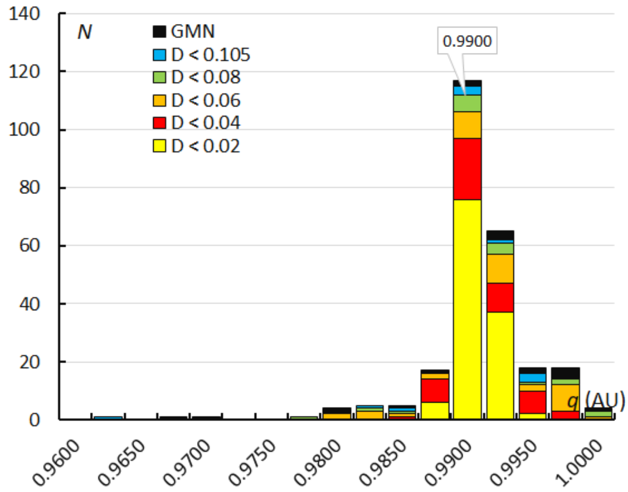

Figure 26 – The histogram for the distribution of the perihelion distance *q*.

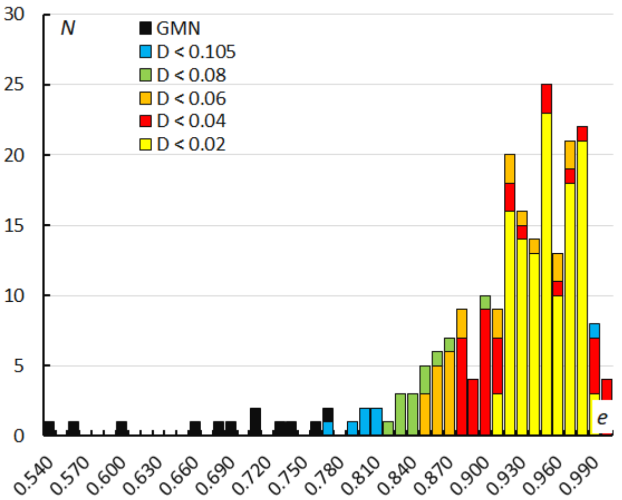

Figure 27 – The histogram for the distribution of the eccentricity *e*.

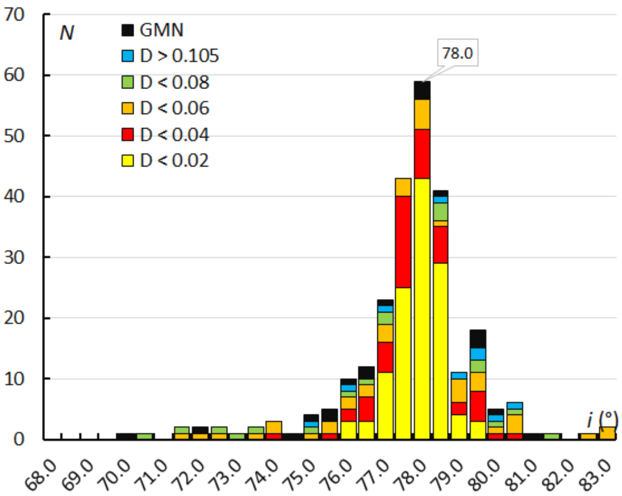

Figure 28 – The histogram for the distribution of the inclination *i*.

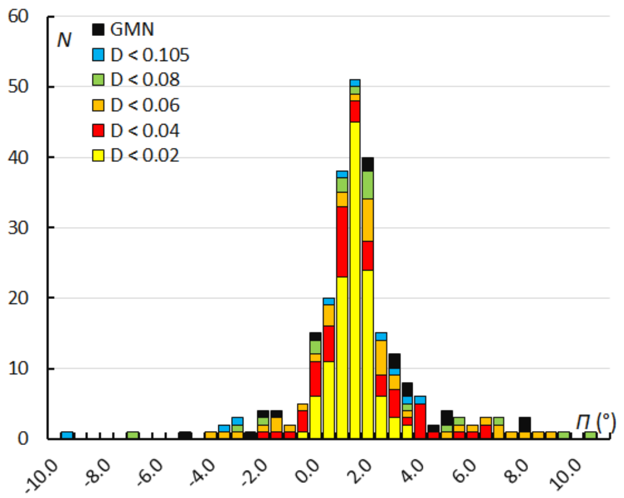

Figure 29 – The histogram for the distribution of the longitude of perihelion *Π*.

The spread in the main orbital elements *q* (*Figure 26*), *e* (*Figure 27*), *i* (*Figure 28*) and *Π* (*Figure 29*) also confirm the compactness of this meteoroid stream. Only the eccentricity appears more dispersed due to the effect of the velocity being close to the parabolic limit.

With a T_J value of about 0.5 and a long period orbit (*P* about 92 years) the OCT#281 appears to be of the type of prograde long-period comet showers. So far, no parent comet is known for this meteoroid stream. With a heliocentric velocity v_h close to the parabolic limit of 42.1 km/s at the Earth orbit, even small errors on the velocity determination can result in hyperbolic orbits.

3 Comparing to other networks

We can compare the results obtained by the Global Meteor Network with some other public available datasets of meteoroid orbits. For this purpose, we can search the orbit datasets made available for EDMOND (Kornos et al., 2014), CAMS (Jenniskens et al., 2011) and SonotaCo (SonotaCo, 2009). The same selection criteria and iterative procedure has been applied to locate the mean orbit for these datasets as described above for the GMN orbit data. We also checked older photographic meteor orbit lists, but we couldn't find any single orbit matching the October Camelopardalid orbit. For reason of cost effectiveness photographic meteor campaigns were limited in time, often covering mainly well-known shower activity. All year around all-sky coverage by fireball networks also produces orbit data, but this orbit data is a magnitude less in accuracy compared to the typical small field of view video optics. Radar orbits were not checked for the obvious reason that meteor orbits obtained by radar from the past tend to be rather inaccurate.

The CAMS network has 41 possible OCT orbits recorded between 2011 and 2016. Only 12 orbits fit the very high threshold similarity criteria, used for the final best fitting mean orbit for this dataset. SonotaCo has 56 possible OCT orbits recorded between 2007 and 2021 with 22 orbits fitting the very high threshold similarity criteria for its mean orbit. EDMOND has 69 possible OCT orbits collected between 2010 and 2016. 17 of these orbits could be used to compute a mean orbit based on the very high threshold similarity criteria. The results for the different datasets are in good agreement.

In *Table 2* we compare the final mean orbit for the different datasets with the very high similarity threshold ($D_{SH} < 0.05$ and $D_D < 0.02$). SonotaCo has rather few matching orbits for the October Camelopardalids mainly because this period of the year often brings bad weather circumstances in Japan. The main difference with the results of the 2018 analysis (Roggemans et al., 2019) is that the selection criteria for this study are reduced to the time interval of 3 degrees in solar longitude against 25 degrees in the 2018 analysis. Most matching orbits beyond the short activity interval are isolated events that can be regarded as noise, or with other words sporadics that resemble the OCT orbit by pure chance.

Table 2 – The mean orbit obtained by the Global Meteor Network compared to the mean orbits obtained for independent datasets with meteoroid orbits obtained by CAMS, SonotaCo and EDMOND, all for the very high threshold similarity class ($D_{SH} < 0.05$ & $D_D < 0.02$ & $D_H < 0.05$).

	GMN	CAMS	SonotaCo	EDMOND
$\lambda_{☉}$ (°)	192.53°	192.61°	192.57°	192.55°
α_g (°)	167.9°	169.1°	168.1°	168.7°
δ_g (°)	+78.6°	+78.6°	+78.6°	+78.6°
v_g (km/s)	45.9	46.0	45.7	45.3
$\lambda - \lambda_{☉}$ (°)	281.8°	282.2°	281.9°	281.9°
β (°)	+61.9°	+62.2°	+62.0°	+62.0
H_b (km)	108.4	109.1	107.9	107.2
H_e (km)	95.1	97.0	95.1	92.3
a (AU)	20.4	22.2	17.8	12.5
q (AU)	0.9907	0.9907	0.9906	0.9904
e	0.9516	0.9553	0.9445	0.9210
ω (°)	168.94°	168.94°	168.88°	168.88°
Ω (°)	192.53°	192.56°	192.57°	192.55°
i (°)	77.91°	77.84°	77.81°	77.36°
Π (°)	1.46°	1.50°	1.45°	1.43°
T_j	0.51	0.49	0.55	0.68
N	121	12	22	17

4 Conclusions

The October Camelopardalids (OCT#281) caught attention with 159 orbits identified by GMN in 2022. This long-period comet type shower displayed its main activity in the short interval $192.3° < \lambda_{☉} < 192.75°$. The time of maximum activity occurred at $\lambda_{☉} = 192.55°$ corresponding to 2022 October 06, 03^h15^m UT. The activity level at maximum with a ZHR of 5 should catch attention of experienced visual meteor observers watching under good circumstances.

The radiant has a small diameter of only few degrees. The median offset from the mean radiant is 0.52°. This makes the shower very compact and non-evolved, possibly young. The compact nature of this meteoroid stream appears also in different diagrams. Rather few dispersed outliers appear in the graphs with exception for the diagrams with the eccentricity *e* which is the most sensitive orbital parameter for the uncertainties on the measured velocity as the heliocentric velocity is close to the escape velocity from the Sun at the Earth orbit.

Showers with a short activity period of less than 1 degree in solar longitude are easily missed due to bad weather circumstances or poor camera coverage. So far there is no indication for a periodicity in strong October Camelopardalid activity. No parent body has been found for this meteoroid stream.

Acknowledgment

The authors thank all the camera operators and people involved in the Global Meteor Network. Orbits for this shower analysis were obtained by GMN RMS cameras. The Global Meteor Network (GMN) data are released under the following license[3].

The Global Meteor Network results were obtained thanks to the efforts of the following volunteers: *Richard Abraham, Victor Acciari, Rob Agar, Yohsuke Akamatsu, David Akerman, Daknam Al-Ahmadi, Jamie Allen, Alexandre Alves, Don Anderson, Željko Andreić, Martyn Andrews, Enrique Arce, Georges Attard, Chris Baddiley, David Bailey, Roger Banks, Hamish Barker, Jean-Philippe Barrilliot, Ricky Bassom, Richard Bassom, Alan Beech, Dennis Behan, Ehud Behar, Josip Belas, Alex Bell, Florent Benoit, Serge Bergeron, Denis Bergeron, Jorge Bermúdez Augusto Acosta, Steve Berry, Adrian Bigland, Chris Blake, Arie Blumenzweig, Ventsislav Bodakov, Robin Boivin, Claude Boivin, Bruno Bonicontro, Fabricio Borges, Ubiratan Borges, Dorian Božičević, David Brash, Stuart Brett, Ed Breuer, Martin Breukers, John W. Briggs, Gareth Brown, Peter G. Brown, Laurent Brunetto, Tim Burgess, Jon Bursey, Yong-Ik Byun, Ludger Börgerding, Sylvain Cadieux, Peter Campbell-Burns, Andrew Campbell-Laing, Pablo Canedo, Seppe Canonaco, Jose Carballada, Steve Carter, David Castledine, Gilton Cavallini, Brian Chapman, Jason Charles, Matt Cheselka, Enrique Chávez Garcilazo, Tim Claydon, Trevor Clifton, Manel Colldecarrera, Michael Cook, Bill Cooke, Christopher Coomber, Brendan Cooney, Jamie Cooper, Andrew Cooper, Edward Cooper, Paul Cox, Llewellyn Cupido, Christopher Curtis, Chris Dakin, Fernando Dall'Igna, James Davenport, Richard Davis, Steve Dearden, Christophe Demeautis, Bart Dessoy, Pat Devine, Miguel Diaz Angel, Paul Dickinson, Ivo Dijan, Pieter Dijkema, Tammo Dijkema Jan, Luciano Diniz Miguel, Marcelo Domingues, Stacey Downton, Stewart Doyle, Zoran Dragić, Iain Drea, Igor Duchaj, Jean-Paul Dumoulin, Garry Dymond, Jürgen Dörr, Robin Earl, Howard Edin, Ollie Eisman, Carl Elkins, Ian Enting Graham, Peter Eschman, Nigel Evans, Bob Evans, Bev M. Ewen-Smith, Seraphin Feller, Eduardo Fernandez Del Peloso, Andres Fernandez, Andrew Fiamingo, Barry Findley, Rick Fischer, Richard Fleet, Jim Fordice, Kyle Francis, Jean Francois Larouche, Patrick Franks, Stefan Frei, Gustav Frisholm, Jose Galindo Lopez, Pierre Gamache, Mark Gatehouse, Ivan Gašparić, Chris George, Megan Gialluca, Kevin Gibbs-Wragge, Marc Gilart Corretgé, Jason Gill, Philip Gladstone, Uwe Glässner, Chuck Goldsmith, Hugo González, Nikola Gotovac, Neil Graham, Pete Graham, Colin Graham, Sam Green, Bob Greschke, Daniel J. Grinkevich, Larry Groom, Dominique Guiot, Tioga Gulon, Margareta Gumilar, Peter Gural, Nikolay Gusev, Kees Habraken, Alex Haislip, John Hale, Peter Hallett, Graeme Hanigan, Erwin Harkink, Ed Harman, Marián Harnádek, Ryan Harper, David Hatton, Tim Havens, Mark Haworth, Paul Haworth, Richard Hayler, Andrew Heath, Sam Hemmelgarn, Rick Hewett, Nicholas Hill, Lee Hill, Don Hladiuk, Alex Hodge, Simon Holbeche, Jeff Holmes, Steve Homer, Matthew Howarth, Nick Howarth, Jeff Huddle, Bob Hufnagel, Roslina Hussain, Jan Hykel, Russell Jackson, Jean-Marie Jacquart, Jost Jahn, Nick James, Phil James, Ron James Jr, Rick James, Ilya Jankowsky, Alex Jeffery, Klaas Jobse, Richard Johnston, Dave Jones, Fernando Jordan, Romulo Jose, Edison José Felipe Pérezgómez Álvarez, Vladimir Jovanović, Alfredo Júnior Dal'Ava, Javor Kac, Richard Kacerek, Milan Kalina, Jonathon Kambulow, Steve Kaufman, Paul Kavanagh, Ioannis Kedros, Jürgen Ketterer, Alex Kichev, Harri Kiiskinen, Jean-Baptiste Kikwaya, Sebastian Klier, Dan Klinglesmith, John Kmetz, Zoran Knez, Korado Korlević, Stanislav Korotkiy, Danko Kočiš, Bela Kralj Szomi, Josip Krpan, Zbigniew Krzeminski, Patrik Kukić, Reinhard Kühn, Remi Lacasse, Gaétan Laflamme, Steve Lamb, Hervé Lamy, Jean Larouche Francois, Ian Lauwerys, Peter Lee, Hartmut Leiting, David Leurquin, Gareth Lloyd, Robert Longbottom, Eric Lopez, Paul Ludick, Muhammad Luqmanul Hakim Muharam, Pete Lynch, Frank Lyter, Guy Létourneau, Angélica López Olmos, Anton Macan, Jonathan Mackey, John Maclean, Igor Macuka, Nawaz Mahomed, Simon Maidment, Mirjana Malarić, Nedeljko Mandić, Alain Marin, Bob Marshall, Colin Marshall, Gavin Martin, José Martin Luis, Andrei Marukhno, José María García, Keith Maslin, Nicola Masseroni, Bob Massey, Jacques Masson, Damir Matković, Filip Matković, Dougal Matthews, Phillip Maximilian Grammerstorf Wilhelm, Michael Mazur, Sergio Mazzi, Stuart McAndrew, Lorna McCalman, Alex McConahay, Charlie McCormack, Mason McCormack, Robert McCoy, Vincent McDermott, Tommy McEwan, Mark McIntyre, Peter McKellar, Peter Meadows, Edgar Mendes Merizio, Aleksandar Merlak, Filip Mezak, Pierre-Michael Micaletti, Greg Michael, Matej Mihelčić, Simon Minnican, Wullie Mitchell, Georgi Momchilov, Dean Moore, Nelson Moreira, Kevin Morgan, Roger Morin, Nick Moskovitz, Daniela Mourão Cardozo, Dave Mowbray, Andrew Moyle, Gene Mroz, Brian Murphy, Carl Mustoe, Juan Muñoz Luis, Przemek Nagański, Jean-Louis Naudin,*

[3] https://creativecommons.org/licenses/by/4.0/

Damjan Nemarnik, Attila Nemes, Dave Newbury, Colin Nichols, Nick Norman, Philip Norton, Zoran Novak, Gareth Oakey, Perth Observatory Volunteer Group, Washington Oliveira, Jorge Oliveira, Jamie Olver, Christine Ord, Nigel Owen, Michael O'Connell, Dylan O'Donnell, Thiago Paes, Carl Panter, Neil Papworth, Filip Parag, Ian Parker, Gary Parker, Simon Parsons, Ian Pass, Igor Pavletić, Lovro Pavletić, Richard Payne, Pierre-Yves Pechart, Holger Pedersen, William Perkin, Enrico Pettarin, Alan Pevec, Mark Phillips, Anthony Pitt, Patrick Poitevin, Tim Polfliet, Renato Poltronieri, Derek Poulton, Janusz Powazki, Aled Powell, Alex Pratt, Miguel Preciado, Nick Primavesi, Paul Prouse, Paul Pugh, Chuck Pullen, Terry Pundiak, Lev Pustil'Nik, Dan Pye, Nick Quinn, Chris Ramsay, David Rankin, Steve Rau, Dustin Rego, Chris Reichelt, Danijel Reponj, Fernando Requena, Maciej Reszelsk, Ewan Richardson, Martin Richmond-Hardy, Mark Robbins, Martin Robinson, David Robinson, Heriton Rocha, Herve Roche, Paul Roggemans, Adriana Roggemans, Alex Roig, David Rollinson, Andre Rousseau, Jim Rowe, Nicholas Ruffier, Nick Russel, Dmitrii Rychkov, Robert Saint-Jean, Michel Saint-Laurent, Clive Sanders, Jason Sanders, Ivan Sardelić, Rob Saunders, John Savage, Lawrence Saville, Vasilii Savtchenko, Philippe Schaack, William Schauff, Ansgar Schmidt, Yfore Scott, James Scott, Geoff Scott, Jim Seargeant, Jay Shaffer, Steven Shanks, Mike Shaw, Jamie Shepherd, Angel Sierra, Ivo Silvestri, François Simard, Noah Simmonds, Ivica Skokić, Dave Smith, Ian A. Smith, Tracey Snelus, Germano Soru, Warley Souza, Mark Spink, Denis St-Gelais, James Stanley, Radim Stano, Laurie Stanton, Robert D. Steele, Yuri Stepanychev, Graham Stevens, Richard Stevenson, Thomas Stevenson, Peter Stewart, William Stewart, Paul Stewart, Con Stoitsis, Andrea Storani, Andy Stott, David Strawford, Claude Surprenant, Rajko Sušanj, Jeremy Taylor, Yakov Tchenak, John Thurmond, Stanislav Tkachenko, Eric Toops, Torcuill Torrance, Steve Trone, Wenceslao Trujillo, John Tuckett, Sofia Ulrich, Jonathan Valdez Aguilar Alexis, Edson Valencia Morales, Myron Valenta, Jean Vallieres, Paraksh Vankawala, Neville Vann, Marco Verstraaten, Arie Verveer, Jochen Vollsted, Predrag Vukovic, Aden Walker, Martin Walker, Bill Wallace, John Waller, Jacques Walliang, Didier Walliang, Christian Wanlin, Tom Warner, Neil Waters, Steve Welch, Tobias Westphal, Tosh White, Alexander Wiedekind-Klein, John Wildridge, Ian Williams, Mark Williams, Guy Williamson, Graham Winstanley, Urs Wirthmueller, Bill Witte, Jeff Wood, Martin Woodward, Jonathan Wyatt, Anton Yanishevskiy, Penko Yordanov, Stephane Zanoni, Pető Zsolt, Dario Zubović, Marcelo Zurita, Rob de Corday Long, Pierre de Ponthière, Jocimar Justino de Souza, Erwin van Ballegoij, Raoul van Eijndhoven, Ivica Ćiković, Dino Čaljkušić, Damir Šegon, Marko Šegon (list established 19 December 2022).

References

Dijkema T. J. (2022). "Visualizing meteor ground tracks on the meteor map". *eMetN*, **7**, 73–75.

Drummond J. D. (1981). "A test of comet and meteor shower associations". *Icarus*, **45**, 545–553.

Jenniskens P., Gural P. S., Grigsby B., Dynneson L., Koop M. and Holman D. (2011). "CAMS: Cameras for Allsky Meteor Surveillance to validate minor meteor showers". *Icarus*, **216**, 40–61.

Jenniskens P. (2006). Meteor Showers and their Parent Comets. ISBN 0521853494. Cambridge, UK: Cambridge University Press. Pages 528–530.

Jenniskens P., Baggaley J., Crumpton I., Aldous P., Pokorny P., Janches D., Gural P. S., Samuels D., Albers J., Howell A., Johannink C., Breukers M., Odeh M., Moskovitz N., Collison J. and Ganjuag S. (2018). "A survey of southern hemisphere meteor showers". *Planetary Space Science*, **154**, 21–29.

Jopek T. J. (1993). "Remarks on the meteor orbital similarity D-criterion". *Icarus*, **106**, 603–607.

Jopek T. J., Rudawska R. and Pretka-Ziomek H. (2006). "Calculation of the mean orbit of a meteoroid stream". *Monthly Notices of the Royal Astronomical Society*, **371**, 1367–1372.

Kornoš L., Matlovič P., Rudawska R., Tóth J., Hajduková M. Jr., Koukal J. and Piffl R. (2014). "Confirmation and characterization of IAU temporary meteor showers in EDMOND database". In Jopek T. J., Rietmeijer F. J. M., Watanabe J., Williams I. P., editors, Proceedings of the Meteoroids 2013 Conference, Poznań, Poland, Aug. 26-30, 2013. A.M. University, pages 225–233.

Koseki M. (2021). "The activity of meteor showers recorded by SonotaCo Net video observations 2007–2018". *eMetN*, **6**, 91–246.

Moorhead A., Clements T.D. and Vida D. (2020). "Realistic gravitational focusing of meteoroid streams". *Monthly Notices of the Royal Astronomical Society*, **494**, 2982–2994.

Moorhead A. V., Clements T. and Vida D. (2021). "Meteor shower radiant dispersions in Global Meteor Network data". *Monthly Notices of the Royal Astronomical Society*, **508**, 326–339.

Roggemans P., Johannink C. and Cambell-Burns P. (2019a). "October Ursae Majorids (OCU#333)". *eMetN*, **4**, 55–64.

Roggemans P., Johannink C. and Cambell-Burns P. (2019b). "October Camelopardalids (OCT#281)". *eMetN*, **4**, 65–73.

SonotaCo (2009). "A meteor shower catalog based on video observations in 2007–2008". *WGN, Journal of the IMO*, **37**, 55–62.

Southworth R. B. and Hawkins G. S. (1963). "Statistics of meteor streams". *Smithsonian Contributions to Astrophysics*, **7**, 261–285.

Vida D., Gural P., Brown P., Campbell-Brown M., Wiegert P. (2019). "Estimating trajectories of meteors: an observational Monte Carlo approach - I. Theory". *Monthly Notices of the Royal Astronomical Society*, **491**, 2688–2705.

Vida D., Gural P., Brown P., Campbell-Brown M., Wiegert P. (2020). "Estimating trajectories of meteors: an observational Monte Carlo approach - II. Results". *Monthly Notices of the Royal Astronomical Society*, **491**, 3996–4011.

Vida D., Šegon D., Gural P. S., Brown P. G., McIntyre M. J., Eschman P., Roggemans P., Merlak A., Zubrović D. (2021). "The Global Meteor Network – Methodology and first results". *Monthly Notices of the Royal Astronomical Society*, **506**, 5046–5074.

Vida D., Blaauw Erskine R. C., Brown P. G., Kambulow J., Campbell-Brown M., Mazur M. J. (2022). "Computing optical meteor flux using global meteor network data". *Monthly Notices of the Royal Astronomical Society*, **515**, 2322–2339.

Orionids 2022 by worldwide radio meteor observations

Hiroshi Ogawa[1] **and Hirofumi Sugimoto**[2]

[1] **The International Project for Radio Meteor Observations**
h-ogawa@amro-net.jp

[2] **The Nippon Meteor Society**
hiro-sugimoto@kbf.biglobe.ne.jp

The Orionids are one of the major meteor showers in October. It is known that the annual maximum occurs around $\lambda_{\odot} = 208°$. In 2022, some possible unusual activity was detected around $\lambda_{\odot} = 205.2°$ (October 18, 22ʰ30ᵐ UT) by the International Project for Radio Meteor Observations (IPRMO). The calculated activity level was 0.7 ± 0.2 and the estimated ZHR_r was 39 ± 4. Besides there were more long echoes in 2022 than past years.

1 Introduction

The Orionids are one of the major meteor showers during the month of October. The peak occurs at $\lambda_{\odot} = 208°$ with a ZHR = 20 for visual observations (Rendtel, 2021). Although high activity has been observed in 2006–2008 (Arlt et al., 2008) and strong activity was also detected in radio meteor observation (Steyaert, 2014), a very weak activity has been detected in recent years.

Radio meteor observations make it possible to observe even with bad weather and during daytime. The International Project for Radio Meteor Observations (IPRMO)[4] was organized in 2001 (Ogawa et al., 2001). It has as purpose to monitor and analyze meteor shower activity continuously. Besides, Radio Meteor Observations Bulletin (RMOB)[5] is providing worldwide radio meteor data on its website.

Although there was no unusual activity predicted for 2022, this paper reports a possible unusual activity.

2 Method

This research adopted two methods for estimating meteor shower activity. One is the Activity Level Index which is used by IPRMO (Ogawa et al., 2001). Another method is the estimated ZHR_r (Sugimoto, 2017). This index is estimated by using the Activity Level index and a factor named S_{bas} which translates this to the ZHR_r. This method is very useful to compare radio meteor observations to visual observations.

3 Results

3.1 Activity Level Index

Figure 1 shows the result based on the calculation of the Activity Level using 46 sets of observing data from 14 countries. The solid line shows the average value for the period of 2004–2021. The peak occurred at $\lambda_{\odot} = 205.21°$ (October 18, 22ʰ30ᵐ UT).

Figure 2 displays the estimated components by using the Lorentz profile (Jenniskens et al., 2000). One is the usual annual activity which had a peak around $\lambda_{\odot} = 208.77°$. The other component shows a possible unusual activity. The maximum activity level was 0.4 and the Full Width of Half Maximum (FWHM) had –3.0hours/+4.0hours.

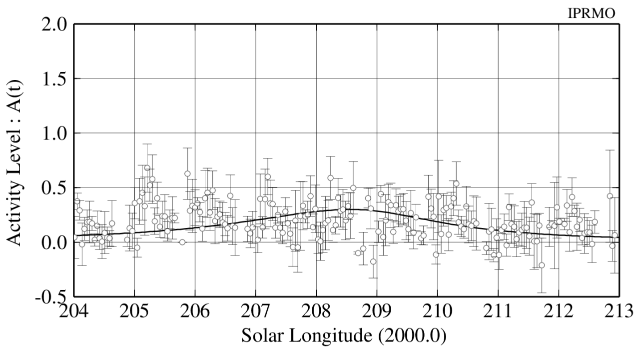

Figure 1 – Activity Level Index of the Orionids 2022. (the line is the average for the period of 2004–2021).

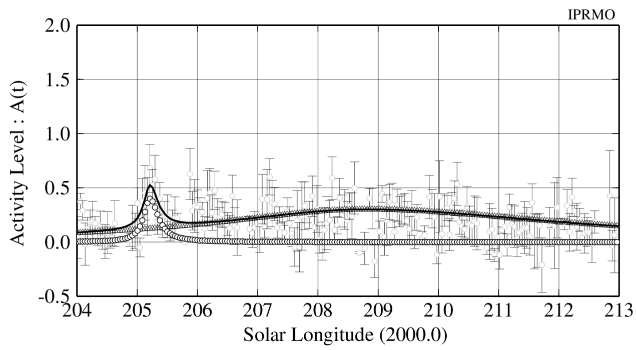

Figure 2 – Estimated Components using the Lorentz Profile (the curve with triangles represents the annual activity, the curve with the circles is the possible unusual activity. The line is the total of both components. Circles with error bars show the Orionids in 2022.

[4] https://www.iprmo.org

[5] https://www.rmob.org

3.2 Estimated ZHR_r

Figure 3 shows the result of the ZHR_r using 40 datasets of observations. The maximum ZHR_r reached 39 ± 4 at $\lambda_\Theta = 205.21°$. A solid line represents the average value for the period of 2012–2021. The beginning of the unusual activity was observed at $\lambda_\Theta = 205.05°$ (October 18, 18^h30^m UT). After the maximum, the unusual activity was over around $\lambda_\Theta = 205.46°$ (October 19, 04^h30^m UT). *Table 1* shows the numeric details for the profiles of the estimated ZHR_r and the Activity Level Index.

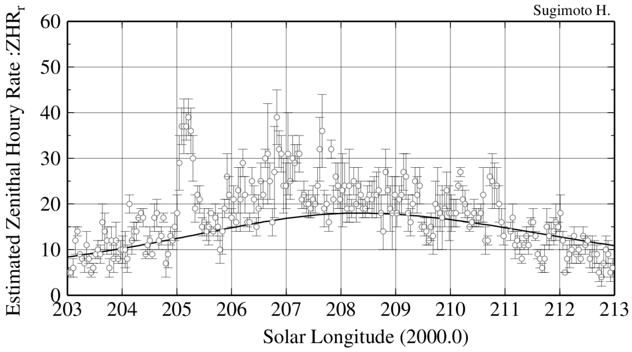

Figure 3 – The estimated ZHR_r of the Orionids 2022. (the line is the average for the period of 2004–2021).

Table 1 – The estimated ZHR_r and Activity Level Index (*AL*).

Time (UT)	λ_Θ (°)	ZHR_r *N*	ZHR_r	Activity Level *N*	*AL*
Oct. 18 15^h30^m	204.922	8	12±2	13	0.1±0.2
Oct. 18 16^h30^m	204.963	9	15±3	12	0.1±0.2
Oct. 18 17^h30^m	205.005	9	18±4	12	0.4±0.1
Oct. 18 18^h30^m	205.046	9	29±6	11	-0.1±0.1
Oct. 18 19^h30^m	205.087	10	37±4	12	0.4±0.2
Oct. 18 20^h30^m	205.129	10	37±6	14	0.5±0.3
Oct. 18 21^h30^m	205.170	8	37±3	12	0.3±0.3
Oct. 18 22^h30^m	205.212	8	39±4	20	0.7±0.2
Oct. 18 23^h30^m	205.253	19	36±5	22	0.5±0.1
Oct. 19 0^h30^m	205.294	18	30±5	20	0.6±0.2
Oct. 19 1^h30^m	205.336	16	19±3	19	0.2±0.1
Oct. 19 2^h30^m	205.377	15	22±2	19	0.4±0.1
Oct. 19 3^h30^m	205.418	15	21±3	19	0.1±0.1
Oct. 19 4^h30^m	205.460	17	15±2	18	0.2±0.1
Oct. 19 5^h30^m	205.501	12	16±3	20	0.2±0.1

3.3 Long Echoes

A strong overdense meteor echo, also called "Long Echo" has been often observed. An echo during more than 20 seconds is defined as a Long Echo. *Figure 4* compares the number of long echoes per day in 2022 with past years in Japan. The number of long echoes was twice the average number during past years on October 19.

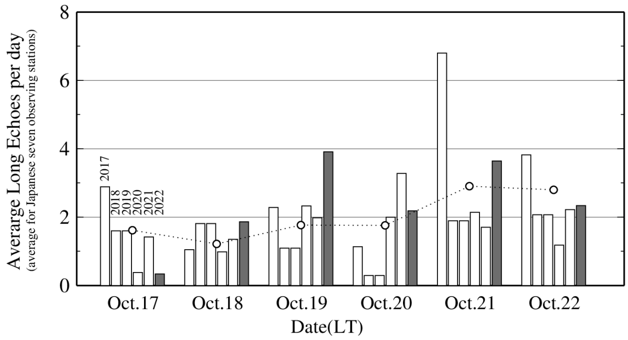

Figure 4 – Comparison of the number of long echoes for different days in 2022 and past years at Japanese observing stations. (circles means the average for the period of 2016–2020).

4 Discussion

Although radio meteor observations detected a possible unusual activity of the Orionids in 2022, there were no visual or video reports confirming this in the world. The best location in the world was Europe. The radiant elevation was around 20° at the time of the maximum. Therefore, it would have been possible to observe some activity. The reason why this is considered is that other meteor shower activity was detected. But it is too difficult to identify the kind of meteor shower in the case of forward scattering. It requires further research to discuss this result.

The activity level was also higher than past average values around $\lambda_\Theta = 207°$ in *Figure 3*. It remains uncertain whether the annual peak was shifted or if this was caused by another reason, such as an influence of Southern Taurids.

Acknowledgment

The worldwide data were provided by the Radio Meteor Observation Bulletin (RMOB) and Radio Meteor Observation in Japan (RMOJ). We wish to thank all radio meteor observers. Besides, we wish to thank *Pierre Terrier* for developing and hosting rmob.org.

References

Arlt R., Rendtel J., Barder P. (2008). "The 2007 Orionids from visual observations". *WGN, Journal of the IMO*, **36**, 55–60.

Jenniskens P., Crawford C., Butow S. J., Nugent D., Koop M., Holman D., Houston J., Jobse K., Kronk G., and Beatty K. (2000). "Lorentz shaped comet dust trail cross section from new hybrid visual and video meteor counting technique imprications for future Leonid storm encounters". *Earth, Moon and Planets*, **82–83**, 191–208.

Ogawa H., Toyomasu S., Ohnishi K., and Maegawa K. (2001). "The Global Monitor of Meteor Streams by Radio Meteor Observation all over the world". In, Warmbein Barbara, editor, *Proceeding of the Meteoroids 2001 Conference*, 6-10 August 2001, Swedish Institute of Space Physics, Kiruna, Sweden. ESA Publications Division, European Space Agency, Noordwijk, The Netherlands, 189–191.

Rendtel J. (2021). “2022 Meteor Shower Calendar”. International Meteor Organization.

Steyaert C. (2014). “The global radio Eta-Aquariids 2013”. *Proceedings of the International Meteor Conference, Poznan, Poland, 22-25 August 2013*, International Meteor Organization, 73–77.

Sugimoto H. (2017). “The New Method of Estimating ZHR using Radio Meteor Observations”. *eMetN*, **2**, 109–110.

Photographic Geminid observations on 13 December 2022

Mikhail Maslov

skjeller@yandex.ru

A presentation is given with photographic records obtained during the 2022 Geminids.

1 Introduction

Here are the results of photographic Geminid observation on 13 December from 12^h10^m to 22^h12^m UT. The images were taken with the Pentax KP camera and 8.5 mm lens, without guiding. Most part of the night was with the gibbous waning Moon in the sky, only the first evening hours were dark, but with lower radiant heights for the Geminids. The results are presented in the text below and in the form of composite images for every hour of observations:

- 12^h10^m–13^h10^m UT, 3 GEM, 1 SPO, Geminids radiant altitude: 14°, Moon: below horizon.
- 13^h10^m–14^h10^m UT, 2 GEM, Geminids radiant altitude: 21°, Moon: below horizon.
- 14^h10^m–15^h10^m UT, 8 GEM, Geminids radiant altitude: 29°, Moon: below horizon.
- 15^h10^m–16^h10^m UT, 7 GEM, 1 SPO, Geminids radiant altitude: 37°, Moon: altitude 6°, phase 75%.
- 16^h10^m–17^h10^m UT, 5 GEM, 2 SPO, Geminids radiant altitude: 46°, Moon: altitude 14°, phase 75%.
- 17^h10^m–18^h10^m UT, 9 GEM, Geminids radiant altitude: 54°, Moon: altitude 22°, phase 74%.
- 18^h10^m–19^h10^m UT, 8 GEM, Geminids radiant altitude: 61°, Moon: altitude 31°, phase 74%.
- 19^h10^m–20^h10^m UT, 7 GEM, 1 SPO, Geminids radiant altitude: 67°, Moon: altitude 38°, phase 74%.
- 20^h10^m–21^h10^m UT, 5 GEM, 1 SPO, Geminids radiant altitude: 68°, Moon: altitude 45°, phase 73%.
- 21^h10^m–22^h12^m UT, 8 GEM, 1 SPO, Geminids radiant altitude: 64°, Moon: altitude 50°, phase 73%.

2 The images

Figure 1 – 12^h10^m–13^h10^m UT, 3 GEM, 1 SPO, Geminid radiant altitude: 14 degrees, Moon: below horizon.

Figure 2 – 13^h10^m–14^h10^m UT, 2 GEM, Geminid radiant altitude: 21 degrees, Moon: below horizon.

Figure 3 – 14^h10^m–15^h10^m UT, 8 GEM, Geminid radiant altitude: 29 degrees, Moon: below horizon.

Figure 4 – 15^h10^m–16^h10^m UT, 7 GEM, 1 SPO, Geminids radiant altitude: 37 degrees, Moon: altitude 6 degrees, phase 75%.

Figure 5 – 16^h10^m–17^h10^m UT, 5 GEM, 2 SPO, Geminids radiant altitude: 46 degrees, Moon: altitude 14 degrees, phase 75%.

Figure 6 – 17^h10^m–18^h10^m UT, 9 GEM, Geminids radiant altitude: 54 degrees, Moon: altitude 22 degrees, phase 74%.

Figure 7 – 18^h10^m–19^h10^m UT, 8 GEM, Geminids radiant altitude: 61 degrees, Moon: altitude 31 degrees, phase 74%.

Figure 8 – 19^h10^m–20^h10^m UT, 7 GEM, 1 SPO, Geminids radiant altitude: 67 degrees, Moon: altitude 38 degrees, phase 74%.

Figure 9 – 20^h10^m–21^h10^m UT, 5 GEM, 1 SPO, Geminids radiant altitude: 68 degrees, Moon: altitude 45 degrees, phase 73%.

Figure 10 – 21^h10^m–22^h12^m UT, 8 GEM, 1 SPO, Geminids radiant altitude: 64 degrees, Moon: altitude 50 degrees, phase 73%.

Spectrum of a −2 magnitude Geminid meteor on December 14, 2022

Takashi Sekiguchi

Nippon Meteor Society
SonotaCo network
ts007@mtj.biglobe.ne.jp

On December 14, 2022, the SonotaCo Network in Japan recorded a Geminid meteor with a radiant position at α = 114.3° and δ = +31.6° with a geocentric velocity v_g = 33.7 km/s (Equinox J2000). The parent body is Phaethon and the spectrum of the meteor shows dominance of iron. The ratio of iron meteors to all meteors during the recording period on the same camera was 2.6 %.

1 Observations

The SonotaCo Network in Japan has recorded the spectrum of a −2 magnitude meteor of the Geminids[6].

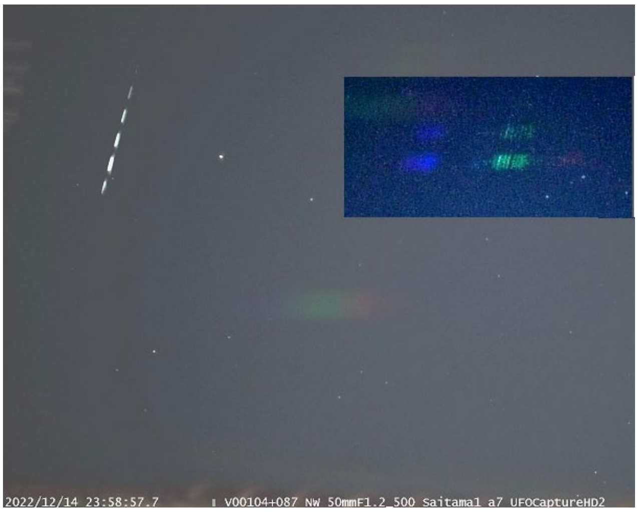

Figure 1 – Spectrum of a −2 magnitude meteor of the Geminids.

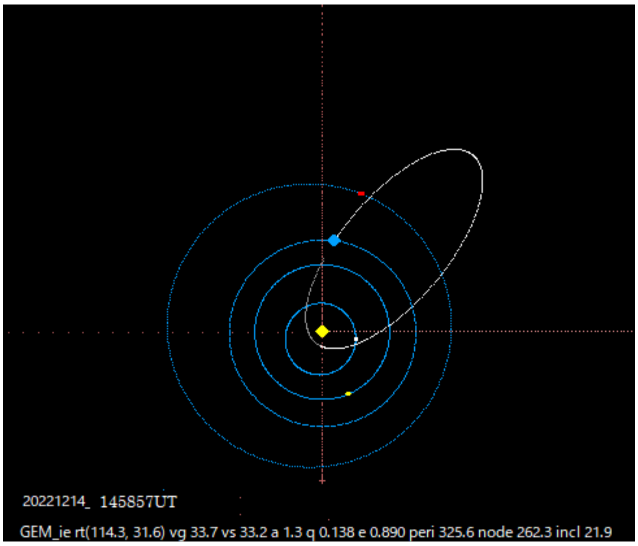

Figure 2 – Orbit of the Geminid meteor with the spectrum.

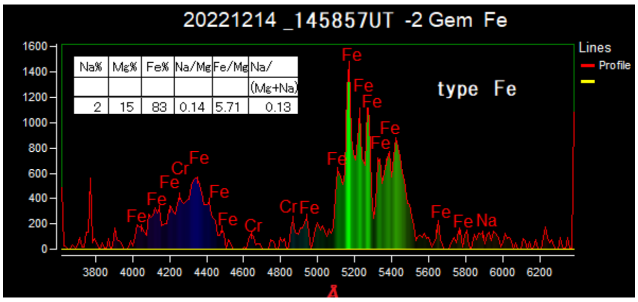

Figure 3 – Result of the spectrum analysis.

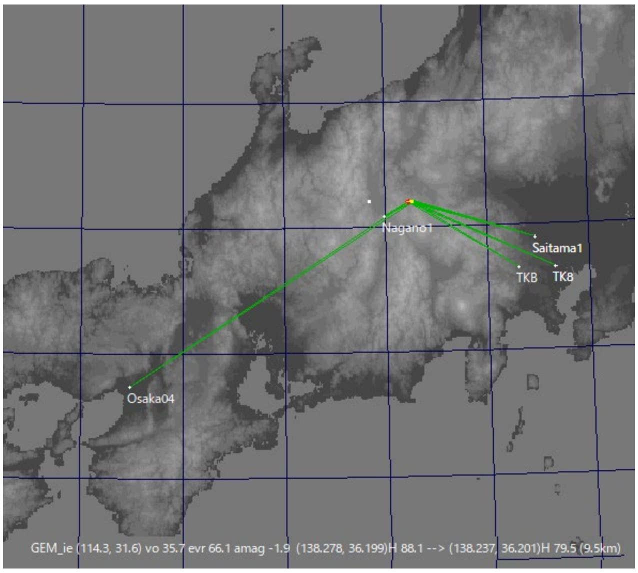

Figure 4 – The trajectory in the atmosphere and the ground track.

Table 1 – Comparing the orbits with parent body.

	a AU	*e*	*q* AU	*i* (°)	*ω* (°)	*Ω* (°)	D_{SH}	*Tj*
Meteor	1.25	0.890	0.138	21.9	325.6	262.30	0.00	4.56
Phaeton	1.27	0.890	0.140	22.3	322.2	265.22	0.02	4.50
Geminids	1.31	0.889	0.145	22.9	324.3	261.70	0.03	4.4

[6] https://sonotaco.jp/forum/viewtopic.php?t=5311

Analysis of bright bolides recorded between October and November 2022 by the Southwestern Europe Meteor Network

J.M. Madiedo[1], J.L. Ortiz[1], J. Izquierdo[2], P. Santos-Sanz[1], J. Aceituno[3], E. de Guindos[3], P. Yanguas[4], J. Palacián[4], A. San Segundo[5], D. Ávila[6], B. Tosar[7], A. Gómez-Hernández[8], Juan Gómez-Martínez[8], Antonio García[9], and A.I. Aimee[10]

[1] **Departamento de Sistema Solar, Instituto de Astrofísica de Andalucía (IAA-CSIC), 18080 Granada, Spain**
madiedo@cica.es, ortiz@iaa.es, psantos@iaa.es

[2] **Departamento de Física de la Tierra y Astrofísica, Universidad Complutense de Madrid, 28040 Madrid, Spain**
jizquierdo9@gmail.com

[3] **Observatorio Astronómico de Calar Alto (CAHA), E-04004, Almería, Spain**
aceitun@caha.es, guindos@caha.es

[4] **Departamento de Estadística, Informática y Matemáticas e Institute for Advanced Materials and Mathematics, Universidad Pública de Navarra, 31006 Pamplona, Navarra, Spain**
yanguas@unavarra.es, palacian@unavarra.es

[5] **Observatorio El Guijo (MPC J27), Galapagar, Madrid, Spain**
mpcj27@outlook.es

[6] **Estación de Meteoros de Ayora, Ayora, Valencia, Spain**
David_ayora007@hotmail.com

[7] **Casa das Ciencias. Museos Científicos Coruñeses. A Coruña, Spain**
borjatosar@gmail.com

[8] **Estación de Registro La Lloma, Olocau, Valencia, Spain**
curso88@gmail.com

[9] **Estación de Meteoros de Cullera (Faro de Cullera), Valencia, Spain**
antonio.garcia88@joseantoniogarcia.com

[10] **Southwestern Europe Meteor Network, 41012 Sevilla, Spain**
swemn.server@gmail.com

We present in this work the analysis of some of the bright fireballs spotted in the framework of the Southwestern Europe Meteor Network (SWEMN) between October and November 2022. They have been observed from the Iberian Peninsula and had a maximum brightness ranging from mag. –7 to mag. –15. Most meteors included in this report were linked to the sporadic background and also to the Southern Taurids.

1 Introduction

The Southwestern Europe Meteor Network (SWEMN) conducts the SMART project (Spectroscopy of Meteoroids by means of Robotic Technologies), which started operation in 2006 to analyze the physical and chemical properties of meteoroids ablating in the Earth's atmosphere. For this purpose we employ an array of automated cameras and spectrographs deployed at meteor-observing stations in Spain (Madiedo, 2014; 2017). This allows to derive the luminous path of meteors and the orbit of their progenitor meteoroids, and also to study the evolution of meteor plasmas from the emission spectrum produced by these events (Madiedo, 2015a; 2015b). SMART also provides important information for our MIDAS project, which is being conducted by the Institute of Astrophysics of Andalusia (IAA-CSIC) to study lunar impact flashes produced when large meteoroids impact the Moon (Madiedo et al., 2015; Madiedo et al., 2018; Madiedo et al. 2019; Ortiz et al., 2015).

Here we report a preliminary analysis of a series of remarkable fireballs recorded over Spain, France, and Portugal in the framework of the SWEMN network along October and November 2022. One of them was an Earth-grazer that ended over the Atlantic Ocean. This work has been fully written by AIMEE (acronym for Artificial Intelligence with Meteoroid Environment Expertise) from the records included in the SWEMN fireball database (Madiedo et al., 2021; Madiedo et al., 2022).

2 Equipment and methods

To record the events presented in this work we have used Watec 902H2 and Watec 902 Ultimate CCD cameras. Their field of view ranges from around 62×50 degrees to about 14×11 degrees. We have also employed digital CMOS color cameras (models Sony A7S and A7SII) operating in HD video mode (1920×1080 pixels). These cover a field of view of around 70×40 degrees. A detailed description of this hardware and the way it operates was given in previous works (Madiedo, 2017). Besides digital CMOS cameras manufactured by ZWO (model ASI185MC) were used. The atmospheric path of the events were triangulated by means of the SAMIA software, developed by J.M. Madiedo. This program employs the planes-intersection method (Ceplecha, 1987).

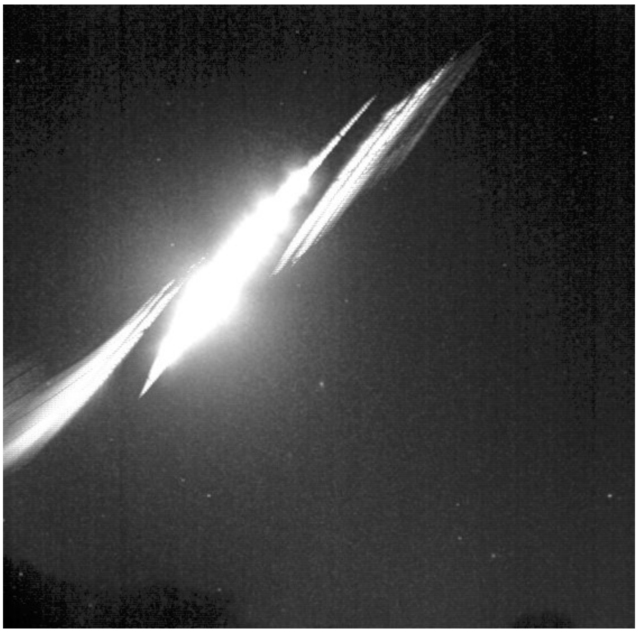

Figure 1 – Stacked image of the SWEMN20221005_221937 "Palomares del Campo" meteor as recorded from La Hita.

Figure 2 – Projection on the ground of the trajectory of the SWEMN20221005_221937 "Palomares del Campo" event.

3 Analysis of the 2022 October 5 event

This stunning bolide was recorded by our cameras at $22^h19^m37.0 \pm 0.1^s$ UT on 2022 October 5. The bright meteor, that exhibited a series of flares along its atmospheric trajectory, had a peak absolute magnitude of -12.0 ± 1.0 (*Figure 1*). These flares took place as a consequence of the sudden break-up of the meteoroid. The code assigned to the bolide in the SWEMN meteor database is SWEMN20221005_221937. A video showing this bolide was uploaded to YouTube[7].

Atmospheric trajectory, radiant and orbit

Having analyzed the atmospheric trajectory of the event it was deduced that this fireball overflew the province of Cuenca (Spain). The luminous event began at an altitude $H_b = 89.0 \pm 0.5$ km. The bolide penetrated the atmosphere till a final height $H_e = 67.6 \pm 0.5$ km. The equatorial coordinates found for the apparent radiant are $\alpha = 1.78°$, $\delta = +20.35°$. The pre-atmospheric velocity deduced for the meteoroid yields $v_\infty = 23.4 \pm 0.3$ km/s. *Figure 2* shows the calculated projection on the ground of the trajectory in the Earth's atmosphere of the fireball. *Figure 3* shows the orbit in the Solar System of its progenitor meteoroid.

Table 1 – Orbital data (J2000) of the progenitor meteoroid before its encounter with our planet.

a (AU)	2.35 ± 0.09	ω (°)	260.33 ± 00.07
e	0.72 ± 0.01	Ω (°)	192.348786 ± 10^{-5}
q (AU)	0.650 ± 0.003	i (°)	10.8 ± 0.2

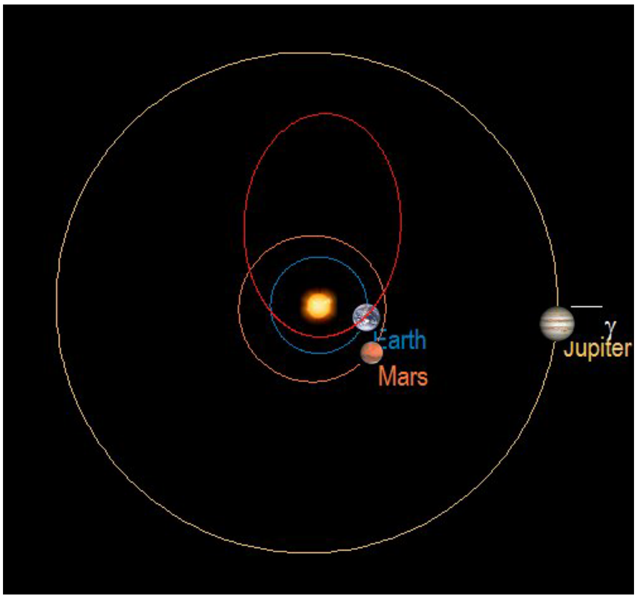

Figure 3 – Orbit of the SWEMN20221005_221937 "Palomares del Campo" fireball.

The bolide was named "Palomares del Campo", because the bright meteor was located over this locality during its initial phase. The parameters of the heliocentric orbit of the progenitor meteoroid before its encounter with our planet can be found in *Table 1*. The geocentric velocity obtained for the particle yields $v_g = 20.5 \pm 0.3$ km/s.

According to the value obtained for the Tisserand parameter referred to Jupiter ($T_J = 3.12$), before striking our planet's atmosphere the meteoroid was moving on an asteroidal

[7] https://youtu.be/qULk3ayDBu0

orbit. These data and the calculated radiant do not match any of the streams listed in the IAU meteor database. Consequently, it was concluded that the bright meteor was linked to the sporadic background.

Figure 4 – Stacked image of the SWEMN20221009_022441 event as recorded from CAHA.

Figure 5 – Atmospheric path of the SWEMN20221009_022441 fireball, and its projection on the ground.

4 Analysis of the 2022 October 9 meteor

We captured this bright event from the meteor-observing stations located at La Hita (Toledo), Calar Alto, Sierra Nevada, and La Sagra (Granada). The fireball was spotted on 2022 October 9, at $2^h24^m41.0 \pm 0.1^s$ UT. It had a peak absolute magnitude of -9.0 ± 1.0 (*Figure 4*), and showed various flares along its trajectory in the Earth's atmosphere as a consequence of the sudden disruption of the meteoroid. The code assigned to the fireball in the SWEMN meteor database is SWEMN20221009_022441.

Atmospheric path, radiant and orbit

It was deduced from the calculation of the trajectory in the Earth's atmosphere of the event that this fireball overflew the province of Valencia (Spain). The meteoroid started ablating at a height $H_b = 92.2 \pm 0.5$ km, and the terminal point of the luminous path was located at a height $H_e = 77.1 \pm 0.5$ km. From the analysis of the atmospheric path, we also deduced that the apparent radiant was located at the position $\alpha = 150.57°$, $\delta = +79.92°$. Besides, we inferred that the meteoroid stroke the atmosphere with a velocity $v_\infty = 23.7 \pm 0.2$ km/s. *Figure 5* shows the obtained atmospheric trajectory of the fireball. The heliocentric orbit of the meteoroid is drawn in *Figure 6*.

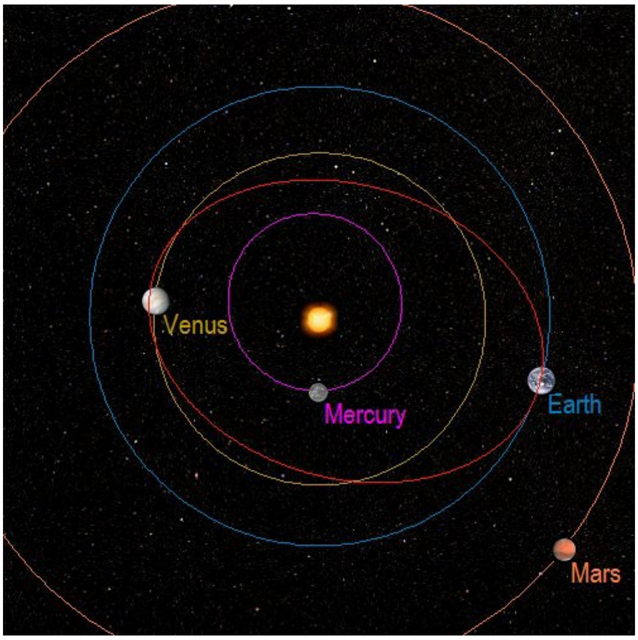

Figure 6 – Projection on the ecliptic plane of the orbit of the SWEMN20221009_022441 event.

The event was named "Gavarda", since the bright meteor overflew this locality during its final phase. The parameters of the orbit of the progenitor meteoroid before its encounter with our planet are listed in *Table 2*. The value calculated for the geocentric velocity was $v_g = 20.9 \pm 0.2$ km/s. From the value estimated for the Tisserand parameter referred to Jupiter ($T_J = 6.56$), we found that the meteoroid was moving on an asteroidal orbit before hitting the Earth's atmosphere. These parameters and the derived radiant do not match any of the streams listed in the IAU meteor database. Consequently, it was concluded that the bright meteor was linked to the sporadic background.

Table 2 – Orbital data (J2000) of the progenitor meteoroid before its encounter with our planet.

a (AU)	0.872 ± 0.002	ω (°)	9.4 ± 00.2
e	0.147 ± 0.003	Ω (°)	195.473854 ± 10^{-5}
q (AU)	0.743 ± 0.004	i (°)	42.2 ± 0.4

5 The 2022 October 12 event

This stunning bolide was recorded by the systems operated by the SWEMN network at $4^h50^m43.0 \pm 0.1^s$ UT on 2022 October 12 (*Figure 7*). Its maximum luminosity was equivalent to an absolute magnitude of -15.0 ± 1.0. It showed a series of flares along its luminous path as a consequence of the sudden break-up of the meteoroid. The code given to the event in the SWEMN meteor database is SWEMN20221012_045043. It can be viewed on this YouTube video[8].

Figure 7 – Stacked image of the SWEMN20221012_045043 bolide as recorded from CAHA.

Atmospheric path, radiant and orbit

It was deduced by calculating the luminous path of the fireball that this event overflew the province of Jaén (Spain). The initial altitude of the meteor yields $H_b = 80.5 \pm 0.5$ km, with the terminal point of the luminous phase located at a height $H_e = 75.2 \pm 0.5$ km. The equatorial coordinates concluded for the apparent radiant are $\alpha = 8.09°$, $\delta = +9.48°$. The entry velocity in the atmosphere inferred for the parent meteoroid was $v_\infty = 18.9 \pm 0.1$ km/s. *Figure 8* shows the obtained trajectory in the atmosphere of the fireball.

Figure 8 – Atmospheric path of the SWEMN20221012_045043 event, and its projection on the ground.

We named this fireball "Reculo", since the bright meteor passed near the zenith of this locality during its final phase. The orbital parameters of the progenitor meteoroid before its encounter with our planet can be found in *Table 3*, and the geocentric velocity derived in this case was $v_g = 15.7 \pm 0.1$ km/s. From the value calculated for the Tisserand parameter referred to Jupiter ($T_J = 2.99$), we found that the meteoroid followed a cometary (JFC) orbit before entering the Earth's atmosphere. These parameters and the derived radiant do not match any of the streams listed in the IAU meteor database. Consequently, it was concluded that this bolide was also linked to the sporadic background.

Table 3 – Orbital data (J2000) of the progenitor meteoroid before its encounter with our planet.

a (AU)	2.64 ± 0.03	ω (°)	239.5 ± 00.2
e	0.699 ± 0.005	Ω (°)	198.582920 ± 10^{-5}
q (AU)	0.795 ± 0.002	i (°)	1.21 ± 0.02

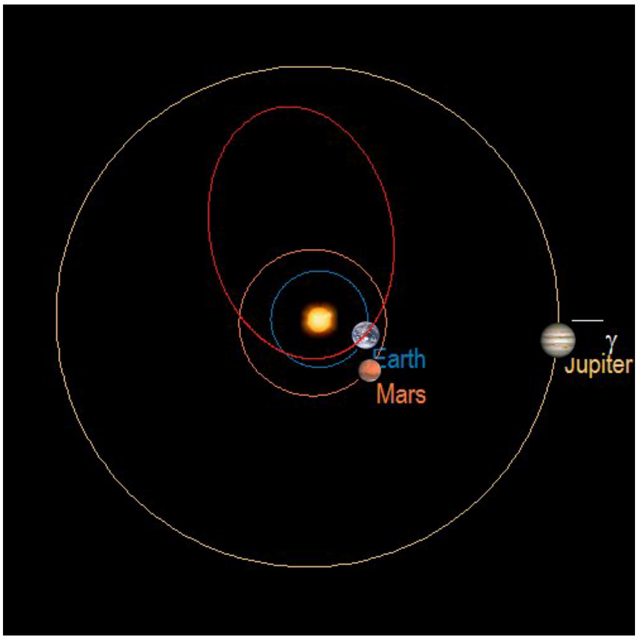

Figure 9 – Projection on the ecliptic plane of the orbit of the SWEMN20221012_045043 meteor.

6 Description of the 2022 October 16 meteor

We captured this bright event from the meteor-observing stations located at Huelva, La Hita (Toledo), Calar Alto, Sierra Nevada, La Sagra (Granada), Sevilla, and El Aljarafe (Sevilla). The fireball was spotted on 2022 October 16, at $2^h46^m41.0 \pm 0.1^s$ UT. Its maximum brightness was equivalent to an absolute magnitude of -9.0 ± 1.0 (*Figure 10*). It displayed a bright flare at the terminal stage of its atmospheric trajectory as a consequence of the sudden disruption of the meteoroid. The code given to the event in the SWEMN meteor database is SWEMN20221016_024641.

Atmospheric path, radiant and orbit

From the calculation of the atmospheric trajectory of the bright meteor it was found that this bolide overflew the province of Ciudad Real (Spain). The meteoroid started ablating at a height $H_b = 105.5 \pm 0.5$ km, and the terminal

[8] https://youtu.be/Sr_H9TZtiCg

point of the luminous path was located at a height $H_e = 59.2 \pm 0.5$ km. The equatorial coordinates of the apparent radiant yield $\alpha = 43.84°$, $\delta = +13.25°$. Besides, we inferred that the meteoroid entered the atmosphere with a velocity $v_\infty = 39.9 \pm 0.2$ km/s. The obtained atmospheric path of the bolide is shown in *Figure 11*.

Figure 10 – Stacked image of the SWEMN20221016_024641 event as recorded from CAHA.

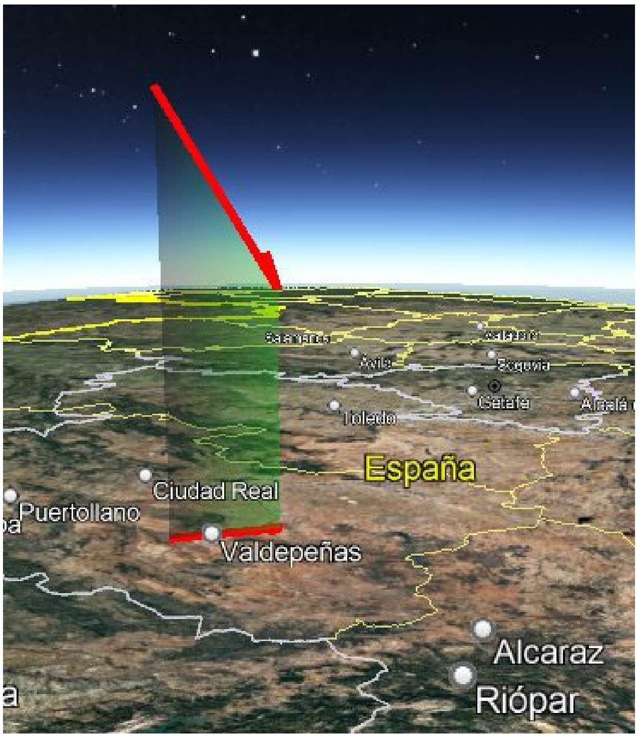

Figure 11 – Atmospheric path of the SWEMN20221016_024641 event, and its projection on the ground.

Figure 12 shows the orbit in the Solar System of the parent meteoroid, and *Table 4* shows the corresponding orbital parameters. The bolide was named "La Solana", because the bright meteor passed near the zenith of this locality during its final phase. *Table 4* shows the orbital parameters of the progenitor meteoroid before its encounter with our planet, and the geocentric velocity yields $v_g = 38.5 \pm 0.2$ km/s. From the value calculated for the Tisserand parameter referred to Jupiter ($T_J = 1.67$), we found that the particle followed a cometary (HTC) orbit before impacting our atmosphere. According to these parameters and the derived radiant, the event was produced by the sigma Arietids (IAU shower code SSA#0237), which peak around October 15 (Molau and Rendtel, 2009). So, the fireball was recorded near the activity peak of this meteor shower.

Table 4 – Orbital data (J2000) of the progenitor meteoroid before its encounter with our planet.

a (AU)	4.3 ± 0.2	ω (°)	137.1 ± 00.3
e	0.965 ± 0.002	Ω (°)	22.406612 ± 10^{-5}
q (AU)	0.148 ± 0.002	i (°)	8.6 ± 0.1

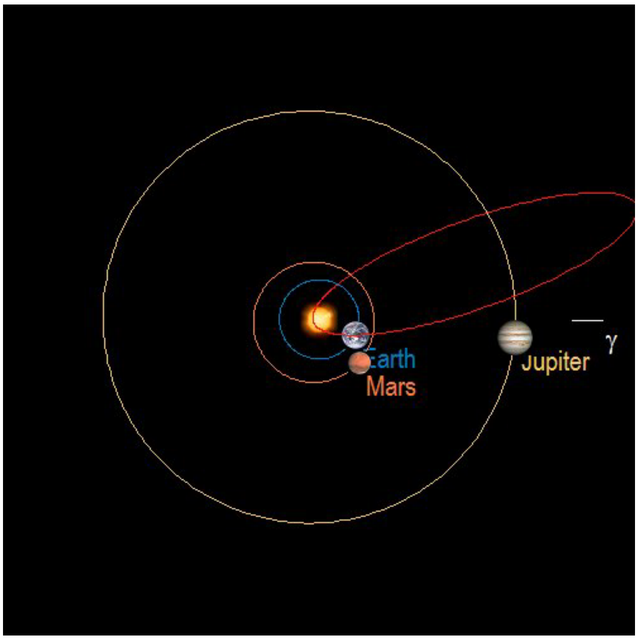

Figure 12 – Projection on the ecliptic plane of the orbit of the SWEMN20221016_024641 bolide.

7 Another fireball on 2022 October 16

This bright event was also captured on 2022 October 16, at $3^h00^m32.0 \pm 0.1^s$ UT (*Figure 13*). Its peak brightness was equivalent to an absolute magnitude of –7.0 ± 1.0. The code assigned to this fireball in the SWEMN meteor database is SWEMN20221016_030032.

Atmospheric path, radiant and orbit

By analyzing the trajectory in the Earth's atmosphere of the fireball it was deduced that this bright meteor was an Earth-grazer that overflew the north of Spain and the Atlantic Ocean. The luminous event began at an altitude $H_b = 128.7 \pm 0.5$ km over Spain. The bolide penetrated the atmosphere till a final height $H_e = 101.3 \pm 0.5$ km over the Atlantic. The position deduced for the apparent radiant correspond to the equatorial coordinates $\alpha = 138.67°$, $\delta = –10.62°$. The pre-atmospheric velocity concluded for the meteoroid yields $v_\infty = 61.1 \pm 0.2$ km/s. *Figure 14* shows the obtained atmospheric path of the meteor, which traveled a total distance in the atmosphere of around 311 km. The orbit in the Solar System of the meteoroid is shown in *Figure 15*.

Figure 13 – Stacked image of the SWEMN20221016_030032 meteor as recorded from El Guijo.

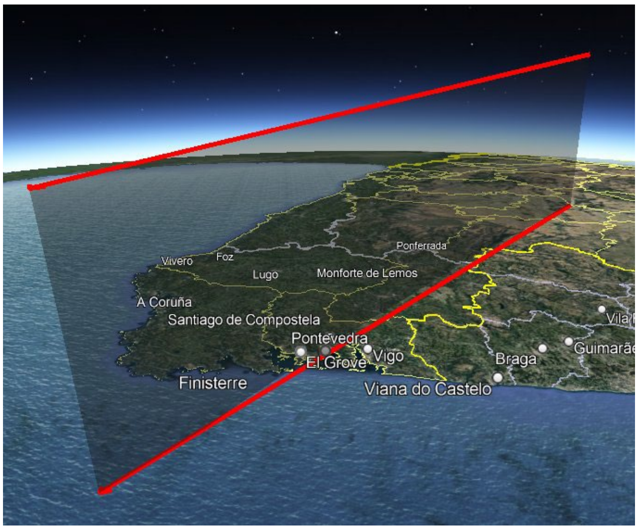

Figure 14 – Atmospheric path of the SWEMN20221016_030032 event, and its projection on the ground.

Table 5 – Orbital data (J2000) of the progenitor meteoroid before its encounter with our planet.

a (AU)	16.4 ± 4.5	*ω* (°)	271.6 ± 00.6
e	0.968 ± 0.008	Ω (°)	22.424283 ± 10^{-5}
q (AU)	0.520 ± 0.003	*i* (°)	120.7 ± 0.1

This fireball was named "Arquillinos", because the bolide was located over this locality during its initial phase. *Table 5* shows the orbital parameters of the parent meteoroid before its encounter with our planet, and the geocentric velocity yields $v_g = 59.8 \pm 0.2$ km/s. The Tisserand parameter with respect to Jupiter ($T_J = -0.14$) indicates that before striking our planet's atmosphere the meteoroid was moving on a cometary (HTC) orbit. These parameters and the derived radiant do not match any of the meteoroid streams in the IAU meteor database. So, it was concluded that the bright meteor was produced by a sporadic meteoroid.

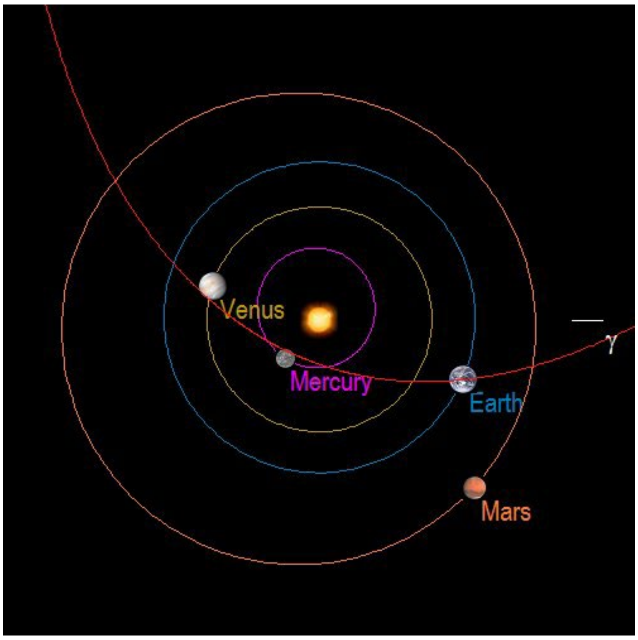

Figure 15 – Projection on the ecliptic plane of the orbit of the SWEMN20221016_030032 event.

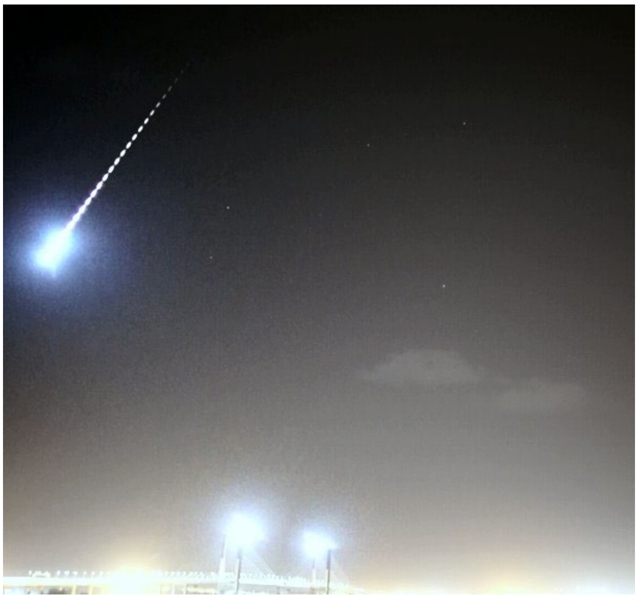

Figure 16 – Stacked image of the SWEMN20221027_045555 bolide as recorded from Sevilla.

8 Description of the 2022 October 27 bolide

This notable bright meteor was recorded on 2022 October 27 at $4^h55^m55.0 \pm 0.1^s$ UT from the meteor-observing stations located at Huelva, La Hita (Toledo), Calar Alto, Sierra Nevada, La Sagra (Granada), and Sevilla (*Figure 16*). Its maximum brightness was equivalent to an absolute magnitude of –12.0 ± 1.0. It exhibited a series of flares along its trajectory in the atmosphere as a consequence of the sudden disruption of the meteoroid. The code assigned to the bright meteor in the SWEMN meteor database is SWEMN20221027_045555. A video about this fireball can be viewed on YouTube[9].

[9] https://youtu.be/aHE0UKlwHhc

Figure 17 – Atmospheric path of the SWEMN20221027_045555 fireball, and its projection on the ground.

Atmospheric path, radiant and orbit

Following the analysis for the trajectory in the atmosphere of the event it was concluded that this bolide overflew Portugal. The luminous event began at an altitude $H_b = 135.8 \pm 0.5$ km. The bright meteor penetrated the atmosphere till a final height $H_e = 82.2 \pm 0.5$ km. The equatorial coordinates inferred for the apparent radiant are $\alpha = 164.97°$, $\delta = +47.00°$. The entry velocity in the atmosphere concluded for the progenitor meteoroid was $v_\infty = 60.3 \pm 0.4$ km/s. *Figure 17* shows the calculated trajectory in our atmosphere of the bolide. The orbit in the Solar System of the meteoroid is shown in *Figure 18*.

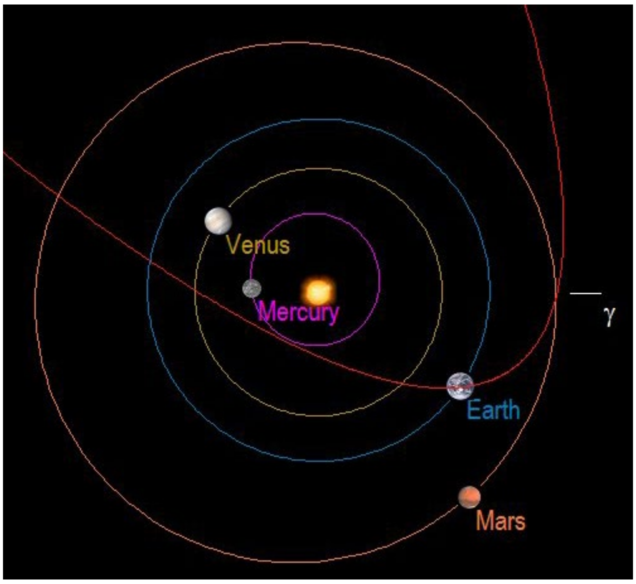

Figure 18 – Projection on the ecliptic plane of the orbit of the SWEMN20221027_045555 meteor.

The fireball was named "Nave do Barao", because the event was located over this locality during its final phase. *Table 6* shows the orbital parameters of the progenitor meteoroid before its encounter with our planet, and the geocentric velocity yields $v_g = 59.1 \pm 0.4$ km/s. From the value estimated for the Tisserand parameter referred to Jupiter ($T_J = -0.18$), we found that the meteoroid was moving on a cometary (HTC) orbit before entering our planet's atmosphere. By taking into account this orbit and the radiant position, the bright meteor was associated with the lambda Ursae Majorids (IAU meteor shower code LUM#0524). Since the lambda Ursae Majorids peak on October 28 (Jenniskens et al., 2016), the fireball was spotted during this activity peak.

Table 6 – Orbital data (J2000) of the progenitor meteoroid before its encounter with our planet.

a (AU)	23.7 ± 18.	ω (°)	131.2 ± 00.8
e	0.96 ± 0.02	Ω (°)	213.442207 ± 10^{-5}
q (AU)	0.827 ± 0.002	i (°)	111.1 ± 0.2

Figure 19 – Stacked image of the SWEMN20221102_224238 meteor as recorded from Sevilla.

9 Analysis of the 2022 November 2 meteor

This striking event was spotted on 2022 November 2 at $22^h42^m38.0 \pm 0.1^s$ UT from the meteor-observing stations located at Huelva, La Hita (Toledo), Calar Alto, Sierra Nevada, La Sagra (Granada), Sevilla, and El Aljarafe (Sevilla). The peak brightness of the bright meteor, which displayed a bright flare at the ending phase of its trajectory in the Earth's atmosphere, was equivalent to an absolute magnitude of –11.0 ± 1.0 (*Figure 19*). This flare appeared as a consequence of the sudden disruption of the meteoroid. The code given to the event in the SWEMN meteor database is SWEMN20221102_224238. A wide number of casual observers saw how the bolide crossed the sky, and reported the event on social networks. A video with images of the fireball and its trajectory in the atmosphere was uploaded to YouTube[10].

[10] https://youtu.be/_Yu2JfyZDwE

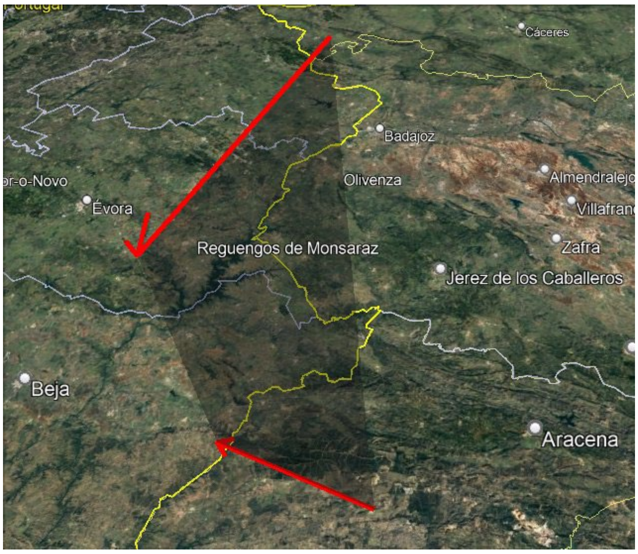

Figure 20 – Atmospheric path of the SWEMN20221102_224238 bolide, and its projection on the ground.

Atmospheric path, radiant and orbit

By analyzing the trajectory in the Earth's atmosphere of the event it was found that this fireball overflew Spain and Portugal. The initial altitude of the meteor yields $H_b = 98.6 \pm 0.5$ km over the south of Spain, and the bright meteor penetrated the atmosphere till a final height $H_e = 57.0 \pm 0.5$ km over the south of Portugal. The equatorial coordinates of the apparent radiant yield $\alpha = 54.00°$, $\delta = +14.32°$. Besides, we found that the meteoroid collided with the atmosphere with a velocity $v_\infty = 30.1 \pm 0.3$ km/s. *Figure 20* shows the calculated atmospheric trajectory of the bolide. The orbit in the Solar System of the meteoroid is shown in *Figure 21*.

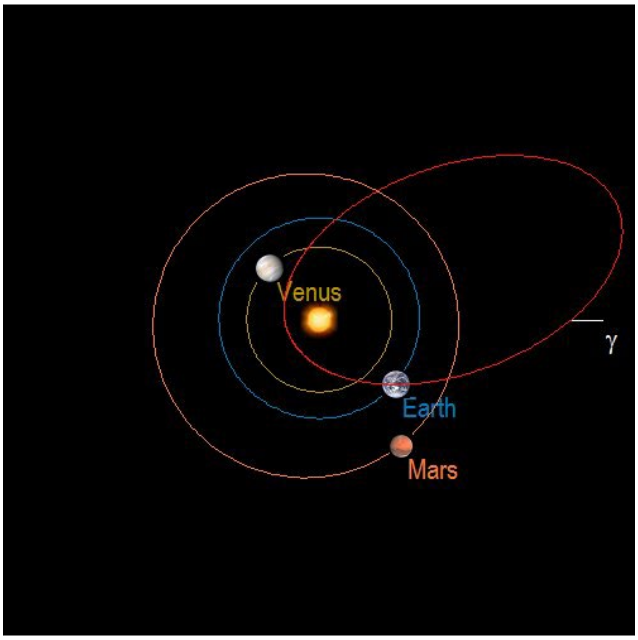

Figure 21 – Projection on the ecliptic plane of the orbit of the SWEMN20221102_224238 bolide.

Table 7 – Orbital data (J2000) of the progenitor meteoroid before its encounter with our planet.

a (AU)	1.76 ± 0.04	ω (°)	118.88 ± 00.03
e	0.811 ± 0.007	Ω (°)	40.163103 ± 10^{-5}
q (AU)	0.333 ± 0.003	i (°)	6.80 ± 0.07

The name given to the fireball was "El Cerro de Andévalo", since the bright meteor was located over this locality during its initial phase. The orbital parameters of the parent meteoroid before its encounter with our planet have been included in *Table 7*, and the geocentric velocity derived in this case was $v_g = 27.8 \pm 0.3$ km/s. These parameters and the derived radiant confirm that the bolide was associated with the Southern Taurids (IAU meteor shower code STA#0002). The proposed parent body of this shower, which peaks around November 6, is Comet 2P/Encke (Jenniskens et al., 2016).

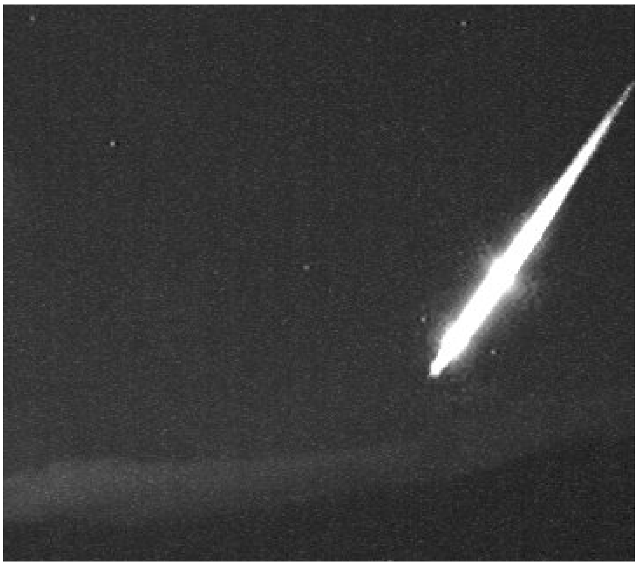

Figure 22 – Stacked image of the SWEMN20221103_205819 bolide as recorded from La Sagra.

10 The 2022 November 3 meteor

This bright event was captured on 2022 November 3 at $20^h58^m19.0 \pm 0.1^s$ UT from the meteor-observing stations located at Huelva, La Hita (Toledo), Calar Alto, Sierra Nevada, La Sagra (Granada), Sevilla, and El Aljarafe (Sevilla) (*Figure 22*). The peak luminosity of the fireball, that presented a series of flares along its trajectory in the atmosphere, was equivalent to an absolute magnitude of –9.0 ± 1.0. These flares took place as a consequence of the sudden break-up of the meteoroid. The code given to the bolide in the SWEMN meteor database is SWEMN20221103_205819. The event could also be observed by a wide number of causal eyewitnesses that reported the event on social networks. A video with images of the fireball and its trajectory in the atmosphere was uploaded to YouTube[11].

[11] https://youtu.be/Nh7H8LnNUow

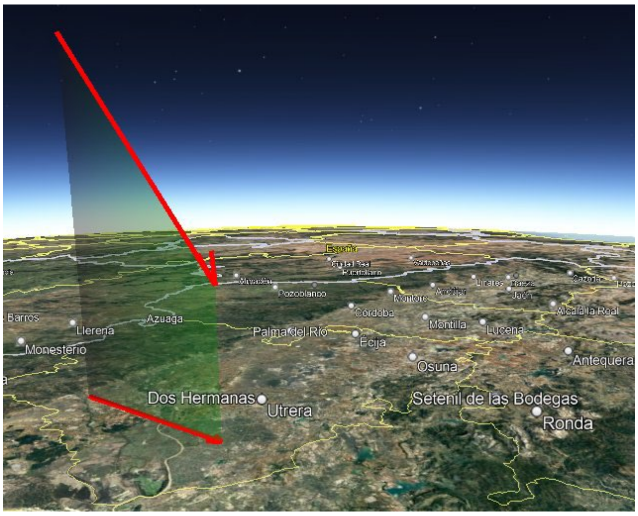

Figure 23 – Atmospheric path of the SWEMN20221103_205819 bolide, and its projection on the ground.

Atmospheric path, radiant and orbit

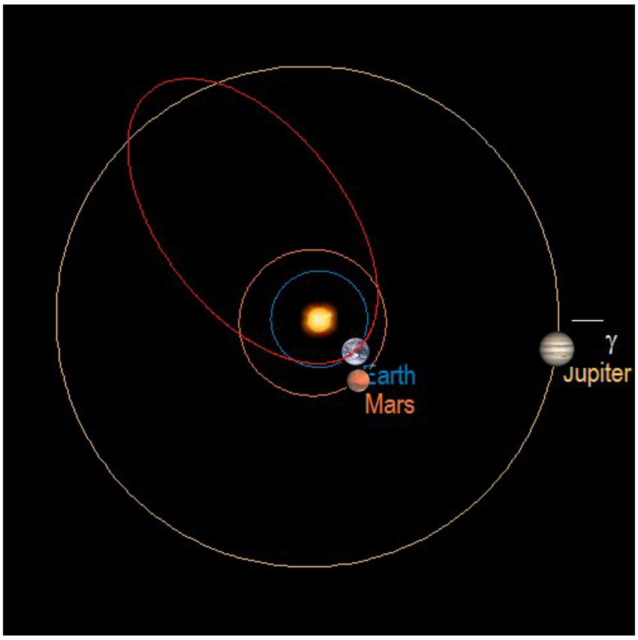

Figure 24 – Projection on the ecliptic plane of the orbit of the SWEMN20221103_205819 event.

By calculating the trajectory in the atmosphere of the bright meteor it was obtained that this fireball overflew the province of Sevilla (Spain). The ablation process of the meteoroid began at a height H_b = 99.3 ± 0.5 km, and ended at a height H_e = 77.5 ± 0.5 km. The equatorial coordinates of the apparent radiant yield α = 306.31°, δ = +71.81°. The meteoroid collided with the atmosphere with an initial velocity v_∞ = 27.3 ± 0.3 km/s. The obtained luminous path of the event is shown in *Figure 23*. The orbit in the Solar System of the meteoroid is shown in *Figure 24*.

Table 8 – Orbital data (J2000) of the progenitor meteoroid before its encounter with our planet.

a (AU)	3.4 ± 0.2	ω (°)	198.9 ± 00.5
e	0.72 ± 0.02	Ω (°)	221.110431 ± 10^{-5}
q (AU)	0.969 ± 0.001	i (°)	39.2 ± 0.3

The name given to the fireball was "San Leandro", because the bolide overflew this locality during its final phase. The orbital parameters of the parent meteoroid before its encounter with our planet are included in *Table 8*. The geocentric velocity of the meteoroid was v_g = 25.0 ± 0.3 km/s. From the value found for the Tisserand parameter with respect to Jupiter (T_J = 2.37), we found that before entering our planet's atmosphere the meteoroid was moving on a cometary (JFC) orbit. According to these values and the calculated radiant, the bright meteor was generated by the sporadic component.

11 The 2022 November 5 bolide

This striking event was recorded by the systems operated by the SWEMN network at $0^h00^m20.0 \pm 0.1^s$ UT on 2022 November 5. The fireball had a peak absolute magnitude of –12.0 ± 0.0 (*Figure 25*). The event was included in our meteor database with the code SWEMN20221105_000020. A video with images of the fireball and its trajectory in the atmosphere was uploaded to YouTube[12].

Figure 25 – Stacked image of the SWEMN20221105_000020 event.

Atmospheric path, radiant and orbit

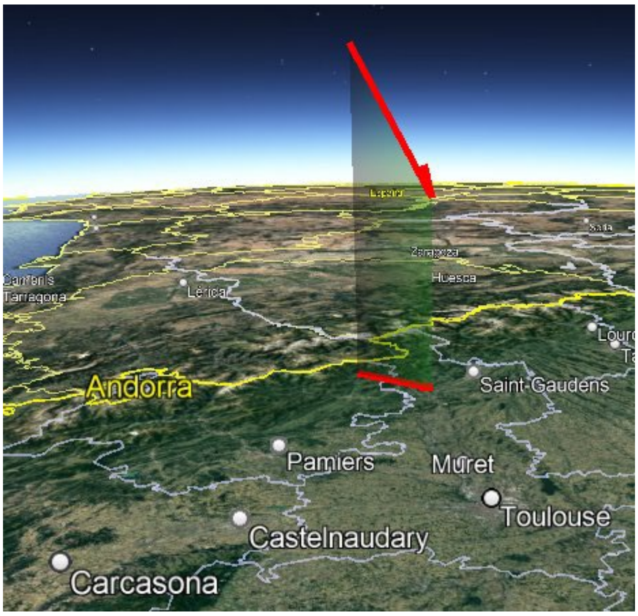

Figure 26 – Atmospheric path of the SWEMN20221105_000020 fireball, and its projection on the ground.

From the analysis of the atmospheric trajectory of the

[12] https://youtu.be/_aAcmNixt8I

fireball it was concluded that this event overflew the south of France. The luminous event began at an altitude $H_b = 95.0 \pm 0.5$ km. The bright meteor penetrated the atmosphere till a final height $H_e = 54.6 \pm 0.5$ km. The equatorial coordinates of the apparent radiant yield $\alpha = 54.19°$, $\delta = +12.41°$. Besides, we concluded that the meteoroid hit the atmosphere with a velocity $v_\infty = 30.8 \pm 0.3$ km/s. The obtained luminous path of the fireball is shown in *Figure 26*. The orbit in the Solar System of the meteoroid is shown in *Figure 27*.

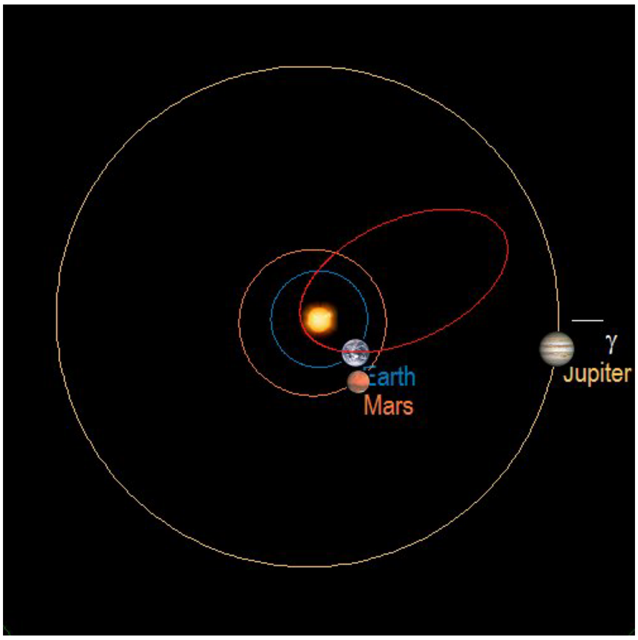

Figure 27 – Projection on the ecliptic plane of the orbit of the SWEMN20221105_000020 event.

Table 9 – Orbital data (J2000) of the progenitor meteoroid before its encounter with our planet.

a (AU)	2.32 ± 0.09	*ω* (°)	112.36 ± 00.03
e	0.842 ± 0.007	Ω (°)	42.223828 ± 10^{-5}
q (AU)	0.365 ± 0.003	*i* (°)	8.95 ± 0.09

The name given to the bright meteor was "Bonac-Irazein", since the event was located over this locality during its initial phase. The parameters of the heliocentric orbit of the parent meteoroid before its encounter with our planet have been listed in *Table 9*, and the geocentric velocity derived in this case was $v_g = 28.7 \pm 0.3$ km/s. From the value found for the Tisserand parameter with respect to Jupiter ($T_J = 2.95$), we found that before impacting the atmosphere the particle was moving on a cometary (JFC) orbit. By taking into account this orbit and the radiant position, the event was produced by the Southern Taurids (IAU code STA#0002). Since the Southern Taurids reach their peak around November 6, this bright meteor was captured during this activity peak. The parent body of this shower is Comet 2P/Encke (Jenniskens et al., 2016).

12 Description of the 2022 November 7 bolide

This bright meteor was captured on 2022 November 7, at $0^h53^m40.0 \pm 0.1^s$ UT (*Figure 28*). The fireball, which displayed different flares along its trajectory in the atmosphere, had a peak absolute magnitude of –9.0 ± 1.0. These flares arose as a consequence of the sudden disruption of the meteoroid. The code given to the bolide in the SWEMN meteor database is SWEMN20221107_005340. A video with images of the fireball and its trajectory in the atmosphere can be found on YouTube[13].

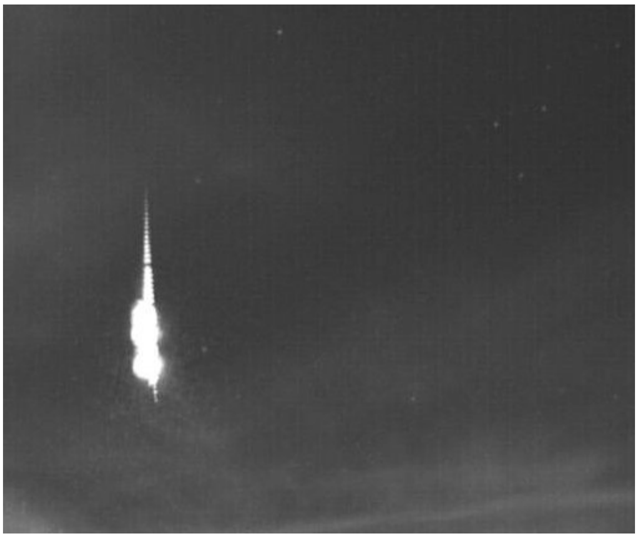

Figure 28 – Stacked image of the SWEMN20221107_005340 event as recorded from El Guijo.

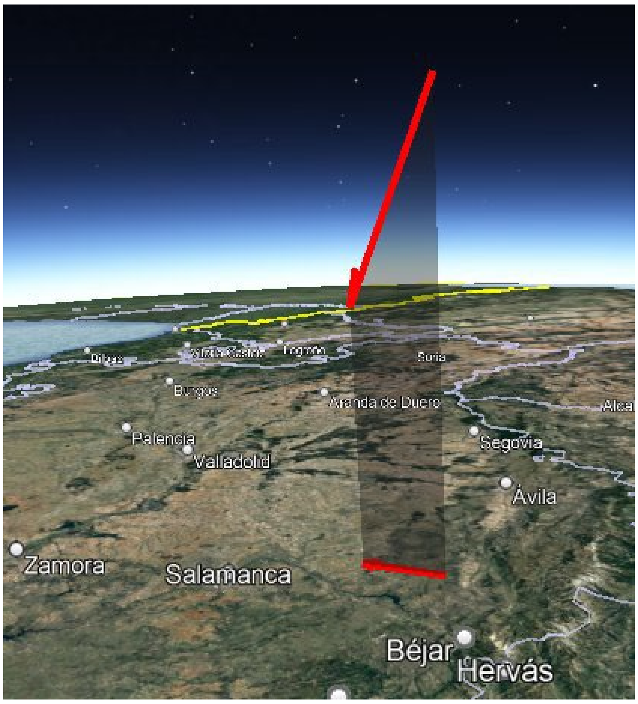

Figure 29 – Atmospheric path of the SWEMN20221107_005340 fireball, and its projection on the ground.

[13] https://youtu.be/a0Kttxhm494

Atmospheric path, radiant and orbit

Following the analysis of the trajectory in the atmosphere of the event it was obtained that this bolide overflew the provinces of Avila and Salamanca (Spain). The luminous event began at an altitude H_b = 113.0 ± 0.5 km over Avila. The bright meteor penetrated the atmosphere till a final height H_e = 63.5 ± 0.5 km over Salamanca. The equatorial coordinates of the apparent radiant yield α = 55.08º, δ = +16.70º. The pre-atmospheric velocity concluded for the meteoroid yields v_∞ = 30.3 ± 0.3 km/s. *Figure 29* shows the obtained trajectory in the Earth's atmosphere of the fireball. The orbit in the Solar System of the meteoroid is shown in *Figure 30*.

Table 10 – Orbital data (J2000) of the progenitor meteoroid before its encounter with our planet.

a (AU)	2.31 ± 0.08	ω (º)	111.79 ± 00.06
e	0.840 ± 0.007	Ω (º)	44.248643 ± 10^{-5}
q (AU)	0.370 ± 0.003	i (º)	3.91 ± 0.03

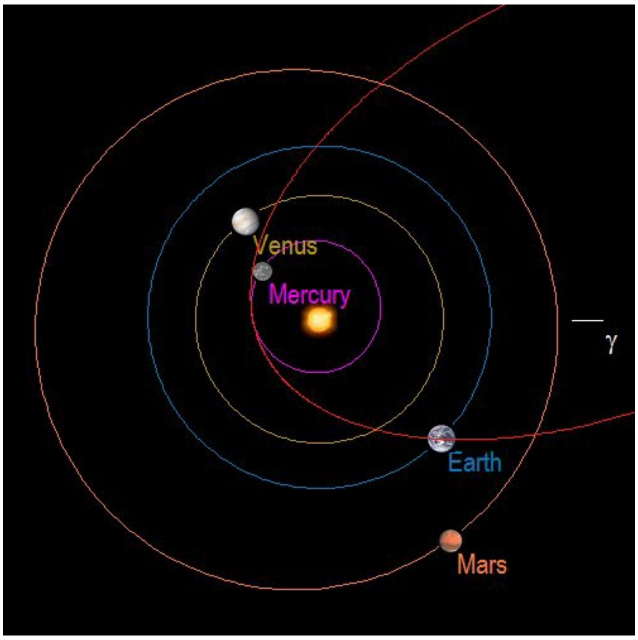

Figure 30 – Projection on the ecliptic plane of the orbit of the SWEMN20221107_005340 fireball.

This event was named "Carabias", since the fireball overflew this locality during its final phase. The parameters of the heliocentric orbit of the progenitor meteoroid before its encounter with our planet are listed in *Table 10*, and the geocentric velocity yields v_g = 28.3 ± 0.3 km/s. The value found for the Tisserand parameter with respect to Jupiter (T_J = 2.97) shows that the meteoroid followed a cometary (JFC) orbit before striking our atmosphere. These parameters and the derived radiant confirm that the bolide was also associated with the Southern Taurids (IAU meteor shower code STA#0002) (Jenniskens et al., 2016).

Figure 31 – Stacked image of the SWEMN20221112_001150 event as recorded from Sevilla.

13 The 2022 November 9 fireball

On 2022 November 12, at $0^h11^m50.0 \pm 0.1^s$ UT, the systems operated by the SWEMN network captured this bright event (*Figure 31*). The maximum luminosity of the bolide, that exhibited various flares along its trajectory in our atmosphere, was equivalent to an absolute magnitude of –9.0 ± 1.0. These flares arose as a consequence of the sudden disruption of the meteoroid. The bright meteor was included in our meteor database with the code SWEMN20221112_001150. A video with images of the fireball and its trajectory in the atmosphere was uploaded to YouTube[14].

Figure 32 – Atmospheric path of the SWEMN20221112_001150 fireball, and its projection on the ground.

Atmospheric path, radiant and orbit

This bright meteor overflew the Atlantic Ocean. The luminous event began at an altitude H_b = 116.4 ± 0.5 km. The event penetrated the atmosphere till a final height H_e = 62.6 ± 0.5 km. From the analysis of the atmospheric path, we also obtained that the apparent radiant was located at the position α = 55.81º, δ = +15.32º. The entry velocity in the atmosphere inferred for the parent meteoroid was

[14] https://youtu.be/Gm18KORg2as

$v_\infty = 28.4 \pm 0.3$ km/s. *Figure 32* shows the calculated trajectory in the Earth's atmosphere of the bright meteor. The orbit in the Solar System of the meteoroid is shown in *Figure 33*.

Table 11 – Orbital data (J2000) of the progenitor meteoroid before its encounter with our planet.

a (AU)	2.5 ± 0.1	ω (º)	101.57 ± 00.04
e	0.820 ± 0.009	Ω (º)	49.244600 ± 10^{-5}
q (AU)	0.454 ± 0.003	i (º)	4.74 ± 0.04

Table 11 shows the orbital parameters of the progenitor meteoroid before its encounter with our planet. The geocentric velocity obtained for the particle yields $v_g = 26.2 \pm 0.3$ km/s. The value estimated for the Tisserand parameter with respect to Jupiter ($T_J = 2.85$) reveals that the particle followed a cometary (JFC) orbit before striking our atmosphere. According to these parameters and the derived radiant, this bolide was also generated by the Southern Taurids (IAU meteor shower code STA#0002).

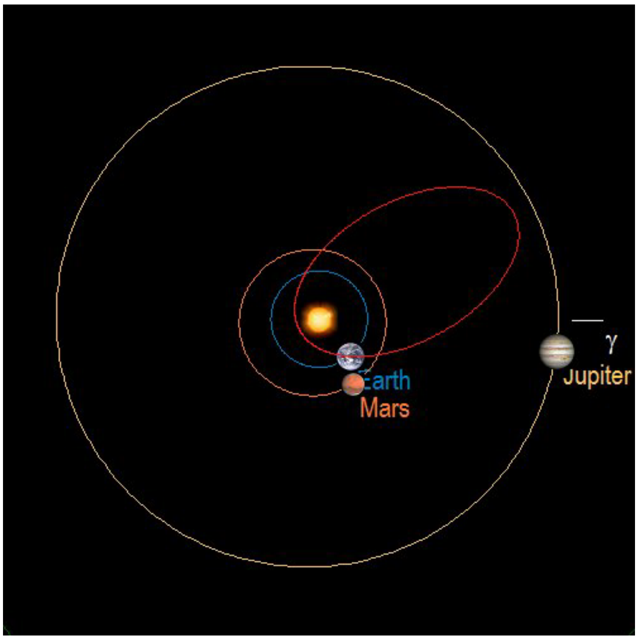

Figure 33 – Projection on the ecliptic plane of the orbit of the SWEMN20221112_001150 fireball.

14 Analysis of the 2022 November 13 event

On 2022 November 13, at $1^h42^m11.0 \pm 0.1^s$ UT, our meteor stations recorded this stunning bolide (*Figure 34*). It had a peak absolute magnitude of –11.0 ± 1.0, and exhibited a bright flare at the ending phase of its atmospheric path as a consequence of the sudden disruption of the meteoroid. The code given to the bright meteor in the SWEMN meteor database is SWEMN20221113_014211. A video describing the main features of the fireball and its trajectory in the atmosphere was uploaded to YouTube[15].

Figure 34 – Stacked image of the SWEMN20221113_014211 event as recorded from CAHA.

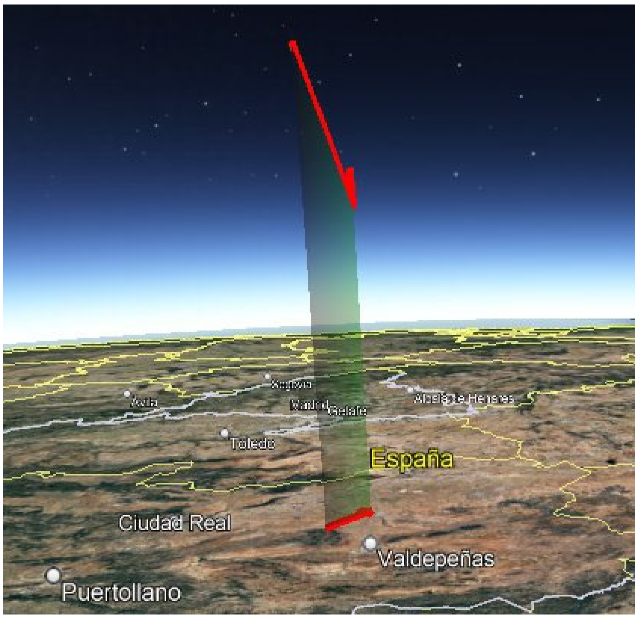

Figure 35 – Atmospheric path of the SWEMN20221113_014211 fireball, and its projection on the ground.

Atmospheric path, radiant and orbit

It was concluded by calculating the atmospheric path of the event that this bright meteor overflew the province of Ciudad Real (Spain). The meteoroid started ablating at a height $H_b = 109.5 \pm 0.5$ km, and ended at a height $H_e = 68.0 \pm 0.5$ km. The position concluded for the apparent radiant correspond to the equatorial coordinates $\alpha = 58.96°$, $\delta = +18.66°$. The pre-atmospheric velocity deduced for the meteoroid yields $v_\infty = 29.1 \pm 0.3$ km/s. *Figure 35* shows the obtained path in the atmosphere of the fireball. The orbit in the Solar System of the meteoroid is shown in *Figure 36*.

Table 12 – Orbital data (J2000) of the progenitor meteoroid before its encounter with our planet.

a (AU)	2.37 ± 0.09	ω (º)	106.71 ± 00.07
e	0.826 ± 0.008	Ω (º)	50.286116 ± 10^{-5}
q (AU)	0.413 ± 0.003	i (º)	2.40 ± 0.02

[15] https://youtu.be/azjpzyP7Ncc

The bright meteor was named "Llanos del Caudillo", because the event was located near the zenith of this locality during its final phase. The parameters of the orbit of the parent meteoroid before its encounter with our planet are listed in *Table 12*, and the geocentric velocity yields $v_g = 27.0 \pm 0.3$ km/s. From the value derived for the Tisserand parameter with respect to Jupiter ($T_J = 2.95$), we found that the meteoroid was moving on a cometary (JFC) orbit before entering the atmosphere. According to these data and the calculated radiant, the bolide was linked to the Southern Taurids (IAU shower code STA#0002).

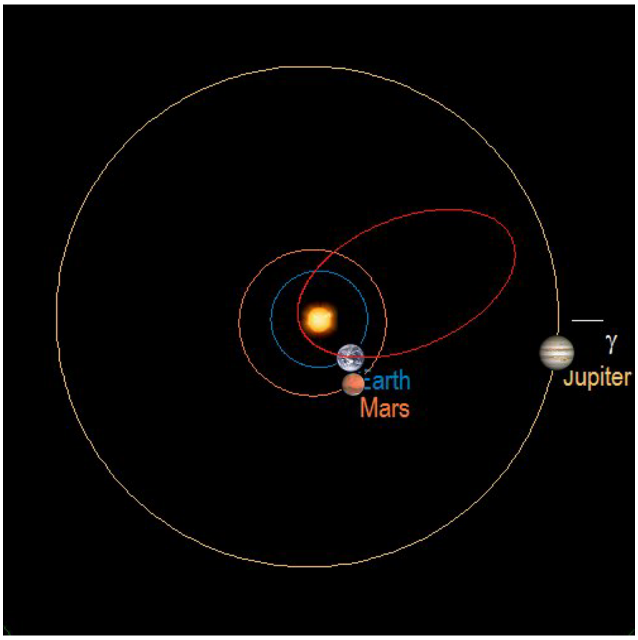

Figure 36 – Projection on the ecliptic plane of the orbit of the SWEMN20221113_014211 bolide.

15 Conclusions

Some of the most notable fireballs recorded by SWEMN from October to November 2022 have been described in this report. Their maximum absolute luminosity ranges from mag. –7 to mag. –15. Most of them were linked to the Southern Taurids and the sporadic component.

The "Palomares del Campo" event was recorded on October 5. The peak magnitude of this sporadic bolide, which overflew the province of Cuenca (Spain), was –12.0. The particle followed an asteroidal orbit before colliding with the atmosphere.

The second bright meteor presented here was the "Gavarda" fireball. This was recorded on October 9. The peak absolute magnitude of this sporadic, which overflew the province of Valencia (Spain), was –9.0. Its parent meteoroid followed an asteroidal orbit before impacting the Earth's atmosphere.

The third event in this report was the "Reculo" bolide, which was recorded on October 12. This sporadic meteor had a peak absolute magnitude of –15.0 and overflew the province of Jaén (Spain). The meteoroid followed a cometary (JFC) orbit before striking the Earth's atmosphere.

The fourth bolide presented in this work was named "La Solana". It was recorded on October 16 and reached a peak absolute magnitude of –9.0. This fireball was associated with the sigma Arietids (SSA#0237) and overflew the province of Ciudad Real (Spain). Before entering the atmosphere the meteoroid was moving on a cometary (HTC) orbit.

Next, we have analyzed an Earth-grazer bolide recorded on October 16 and named "Arquillinos". It reached a peak absolute magnitude of –7.0, and belonged to the sporadic background. This meteor overflew Spain and the Atlantic Ocean. The meteoroid followed a cometary (HTC) orbit before hitting our atmosphere.

The bright meteor recorded on October 27, which was named "Nave do Barao", belonged to the lambda Ursae Majorids (LUM#0524) and reached a peak absolute magnitude of –12.0. This fireball overflew Portugal and the parent meteoroid was also moving on a cometary (HTC) orbit before entering the atmosphere.

The "El Cerro de Andévalo" bolide, recorded on November 2, was produced by the Southern Taurids (STA#0002). It overflew Spain and Portugal with a peak absolute magnitude of –11.0.

A sporadic meteoroid moving on a cometary (JFC) orbit gave rise to the "San Leandro" bright meteor, which was recorded on November 3. It reached a peak absolute magnitude of –9.0 and overflew the province of Sevilla (Spain).

The next bright event presented here was a fireball recorded on November 5 named "Bonac-Irazein". This Southern Taurid (STA#0002) meteor had a peak absolute magnitude of –12.0 and overflew the south of France.

The "Carabias" fireball, which was generated by a meteoroid moving on a JFC orbit, was recorded on November 7. It belonged to the Southern Taurids (STA#0002). Its peak magnitude was –9.0 and overflew the provinces of Avila and Salamanca (Spain).

The next fireball analyzed here was a bolide recorded on November 12. It was also associated with the Southern Taurids (STA#0002). Its peak magnitude was –9.0 and overflew the Atlantic Ocean.

And the last bolide discussed in this work was the "Llanos del Caudillo" bolide, which was recorded on November 13. Its peak absolute magnitude was –11.0. The fireball was also a Southern Taurid (STA#0002) and overflew the province of Ciudad Real (Spain).

Acknowledgment

We acknowledge support from the Spanish Ministry of Science and Innovation (project PID2019-105797GB-I00). We also acknowledge financial support from the State Agency for Research of the Spanish MCIU through the "Center of Excellence Severo Ochoa" award to the Instituto de Astrofísica de Andalucía (SEV-2017-0709). P.S-S. acknowledges financial support by the Spanish grant AYA -RTI2018–098657–J-I00 "LEO-SBNAF" (MCIU / AEI / FEDER, UE). The first author is very grateful to Casa das Ciencias (Museos Científicos Coruñeses) for their helpful support in the setup and operation of the automated meteor-observing station located at their facilities in A Coruña.

References

Ceplecha Z. (1987). "Geometric, dynamic, orbital and photometric data on meteoroids from photographic fireball networks". *Bull. Astron. Inst. Cz.*, **38**, 222–234.

Jenniskens P., Nénon Q., Albers J., Gural P. S., Haberman B., Holman D., Morales R., Grigsby B. J., Samuels D. and Johannink C. (2016). "The established meteor showers as observed by CAMS". *Icarus*, **266**, 331–354.

Madiedo J. M. (2014). "Robotic systems for the determination of the composition of solar system materials by means of fireball spectroscopy". *Earth, Planets & Space*, **66**, 70.

Madiedo J. M. (2017). "Automated systems for the analysis of meteor spectra: The SMART Project". *Planetary and Space Science*, **143**, 238–244.

Madiedo J. M. (2015a). "Spectroscopy of a κ-Cygnid fireball afterglow". *Planetary and Space Science*, **118**, 90–94.

Madiedo J. M. (2015b). "The ρ-Geminid meteoroid stream: orbits, spectroscopic data and implications for its parent body". *Monthly Notices of the Royal Astronomical Society*, **448**, 2135–2140.

Madiedo J. M., Ortiz J. L., Organero F., Ana-Hernández L., Fonseca F., Morales N. and Cabrera-Caño J. (2015). "Analysis of Moon impact flashes detected during the 2012 and 2013 Perseids". *A&A*, **577**, A118.

Madiedo J. M., Ortiz J. L. and Morales N. (2018). "The first observations to determine the temperature of a lunar impact flash and its evolution". *Monthly Notices of the Royal Astronomical Society*, **480**, 5010–5016.

Madiedo J. M., Ortiz J. L., Morales N. and Santos-Sanz P. (2019a). "Multiwavelength observations of a bright impact flash during the 2019 January total lunar eclipse". *Monthly Notices of the Royal Astronomical Society*, **486**, 3380–3387.

Madiedo J. M., Ortiz J. L., Izquierdo J., Santos-Sanz P., Aceituno J., de Guindos E., Yanguas P., Palacian J., San Segundo A., and Avila D. (2021). "The Southwestern Europe Meteor Network: recent advances and analysis of bright fireballs recorded along April 2021". *eMetN*, **6**, 397–406.

Madiedo J. M., Ortiz J. L., Izquierdo J., Santos-Sanz P., Aceituno J., de Guindos E., Yanguas P., Palacian J., San Segundo A., Avila D., Tosar B., Gómez-Hernández A., Gómez-Martínez J., and García A. (2022). "The Southwestern Europe Meteor Network: development of new artificial intelligence tools and remarkable fireballs observed from January to February 2022". *eMetN*, **7**, 199–208.

Molau S. and Rendtel J. (2009). "A Comprehensive List of Meteor Showers Obtained from 10 Years of Observations with the IMO Video Meteor Network". *WGN, Journal of the International Meteor Organization*, **37**, 98–121.

Ortiz J. L., Madiedo J. M., Morales N., Santos-Sanz P. and Aceituno F. J. (2015). "Lunar impact flashes from Geminids: analysis of luminous efficiencies and the flux of large meteoroids on Earth". *Monthly Notices of the Royal Astronomical Society*, **454**, 344–352.

Radio meteors October 2022

Felix Verbelen

Vereniging voor Sterrenkunde & Volkssterrenwacht MIRA, Grimbergen, Belgium
felix.verbelen@skynet.be

An overview of the radio observations during October 2022 is given.

1 Introduction

The graphs show both the daily totals (*Figure 1 and 2*) and the hourly numbers (*Figure 3 and 4*) of "all" reflections counted automatically, and of manually counted "overdense" reflections, overdense reflections longer than 10 seconds and longer than 1 minute, as observed here at Kampenhout (BE) on the frequency of our VVS-beacon (49.99 MHz) during the month of October 2022.

The hourly numbers, for echoes shorter than 1 minute, are weighted averages derived from:

$$N(h) = \frac{n(h-1)}{4} + \frac{n(h)}{2} + \frac{n(h+1)}{4}$$

Local interference and unidentified noise remained moderate to low during most of the month. Lightning activity was observed on 5 days. Especially during the first half of the month there were several intense solar eruptions causing sometimes considerable noise (*Figures 5 and 6*) while solar activity remained quite low on 49.99 MHz during the second half of the month.

On October 20th, the Orionids reached here their maximum activity, showing a clearly increased number of overdense reflections, best seen in the daily totals. Over the entire month, 18 reflections longer than 1 minute were registered here.

Attached are selections of long reflections (*Figures 7 to 21*) and of "epsilons" (*Figures 22 to 33*). In addition to the usual graphs, you will also find the raw counts in cvs-format[16] from which the graphs are derived.

The table contains the following columns: day of the month, hour of the day, day + decimals, solar longitude (epoch J2000), counts of "all" reflections, overdense reflections, reflections longer than 10 seconds and reflections longer than 1 minute, the numbers being the observed reflections of the past hour.

[16] https://www.meteornews.net/wp-content/uploads/2022/11/202210_49990_FV_rawcounts.csv

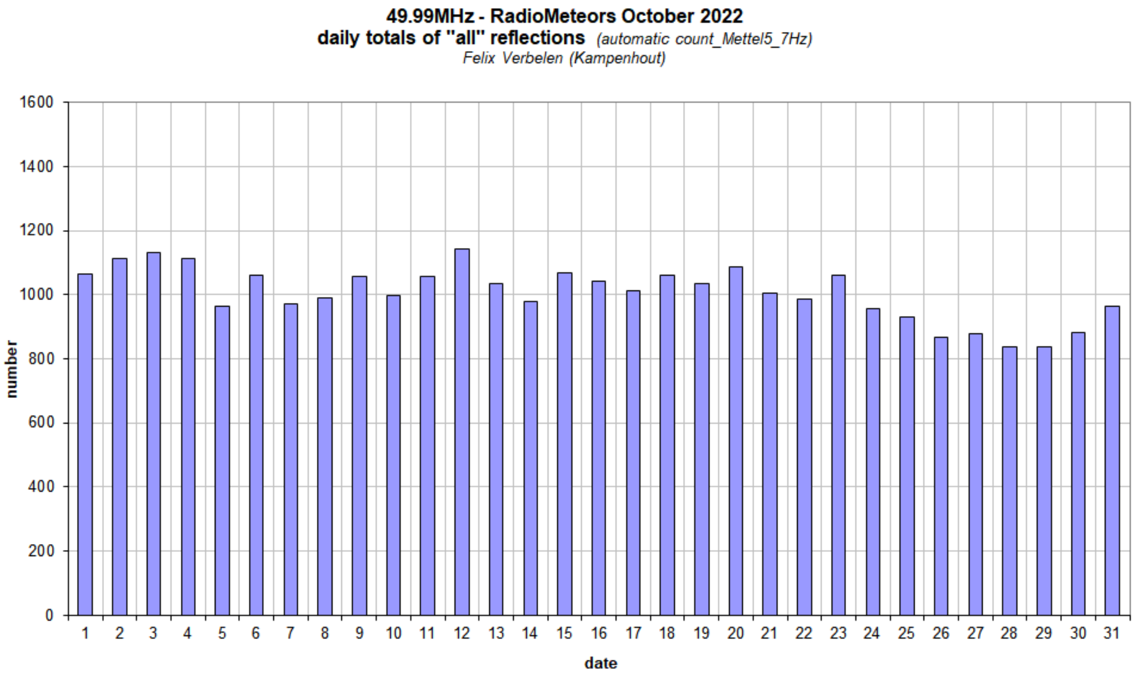

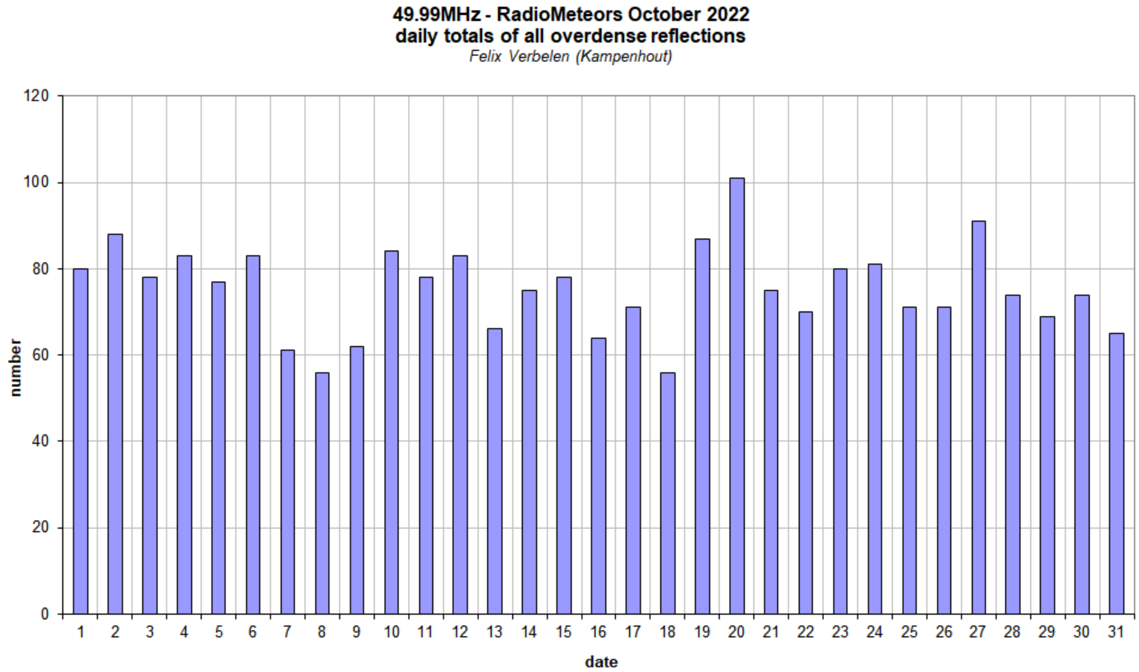

Figure 1 – The daily totals of "all" reflections counted automatically, and of manually counted "overdense" reflections, as observed here at Kampenhout (BE) on the frequency of our VVS-beacon (49.99 MHz) during October 2022.

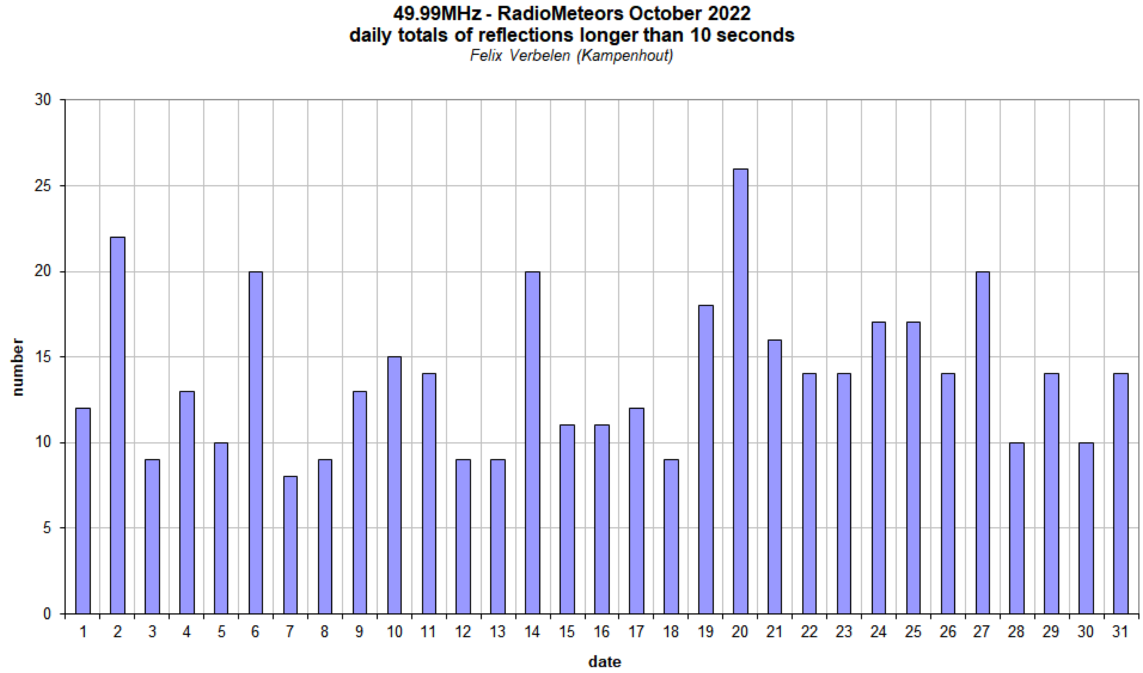

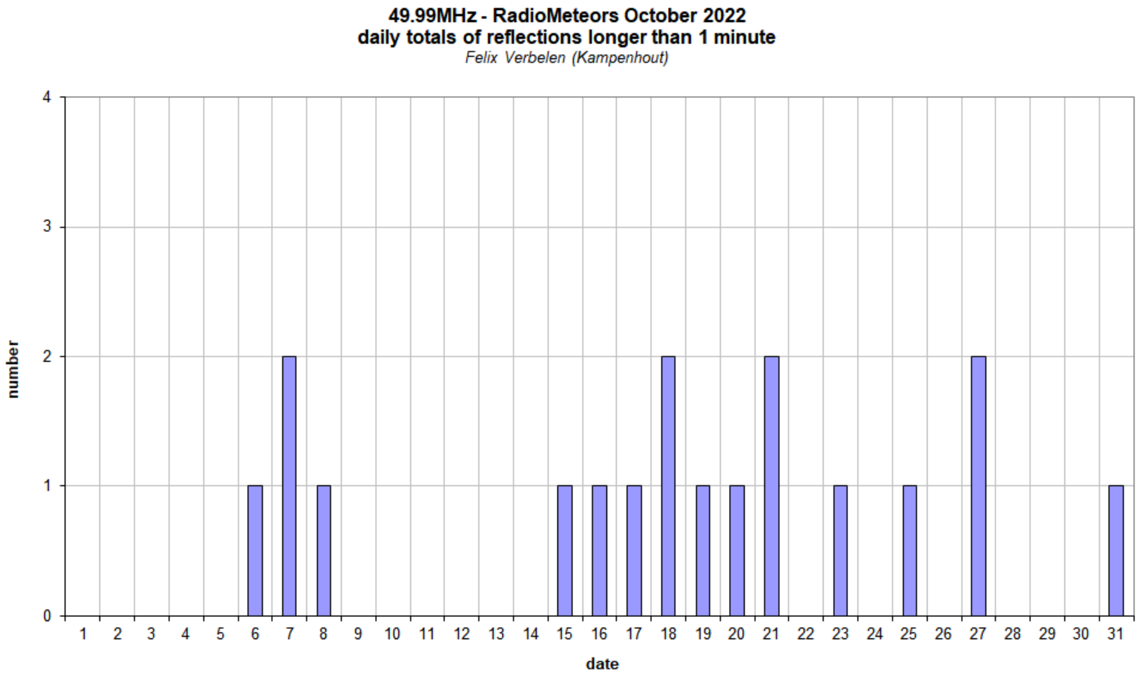

Figure 2 – The daily totals of overdense reflections longer than 10 seconds and longer than 1 minute, as observed here at Kampenhout (BE) on the frequency of our VVS-beacon (49.99 MHz) during October 2022.

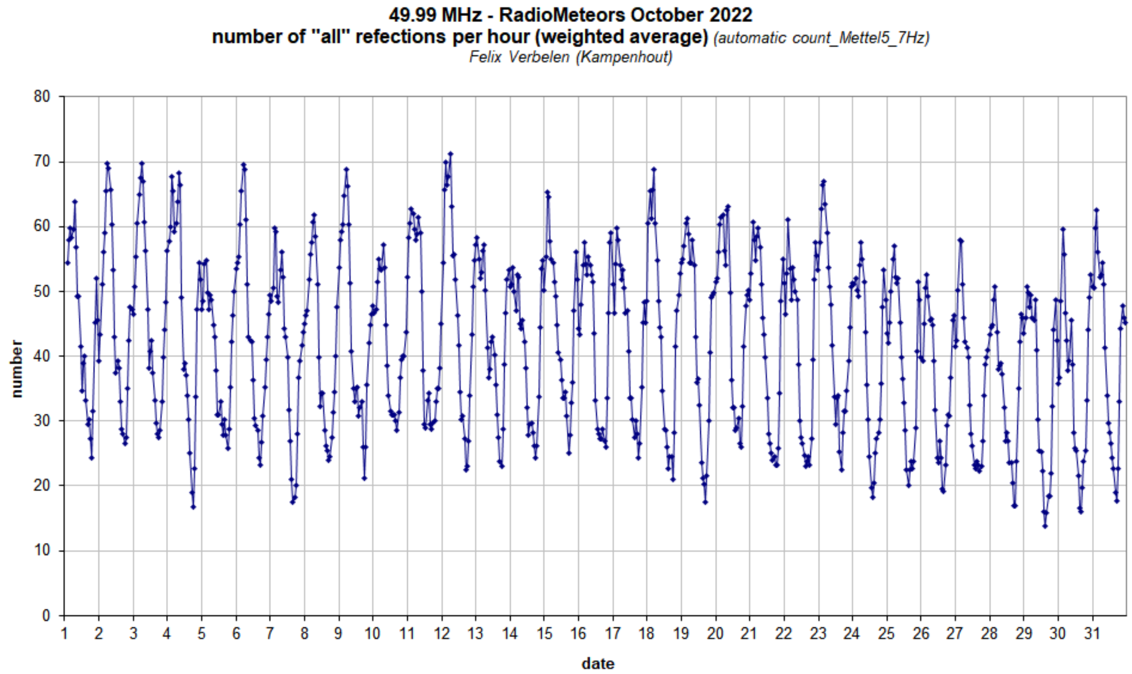

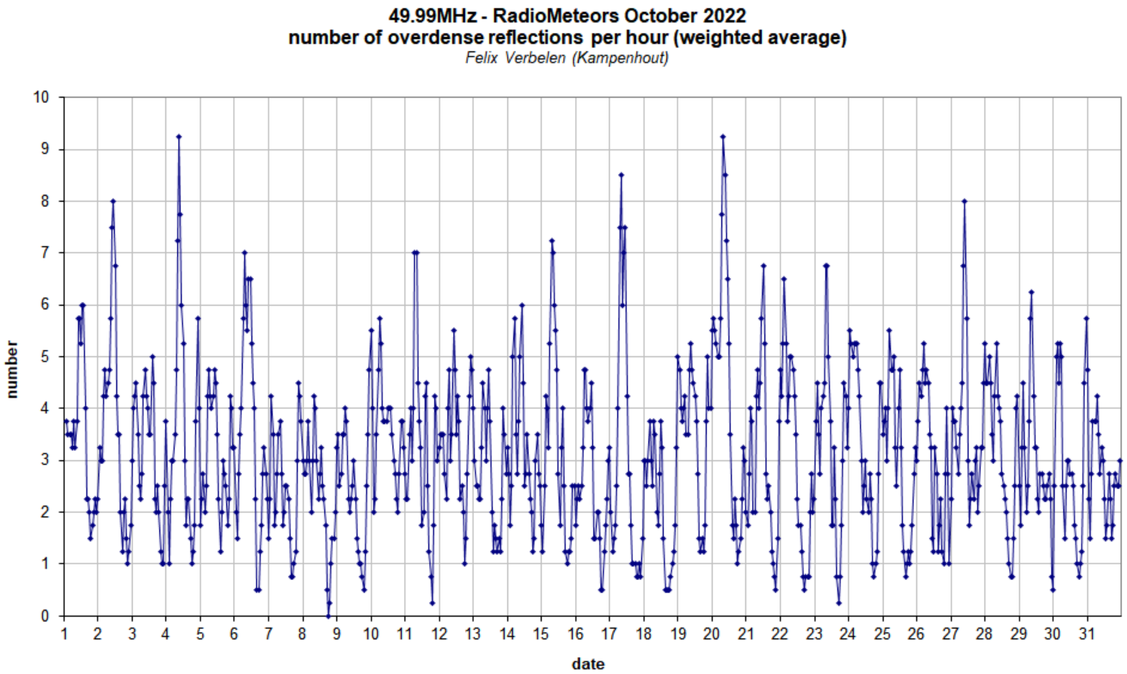

Figure 3 – The hourly numbers of "all" reflections counted automatically, and of manually counted "overdense" reflections, as observed here at Kampenhout (BE) on the frequency of our VVS-beacon (49.99 MHz) during October 2022.

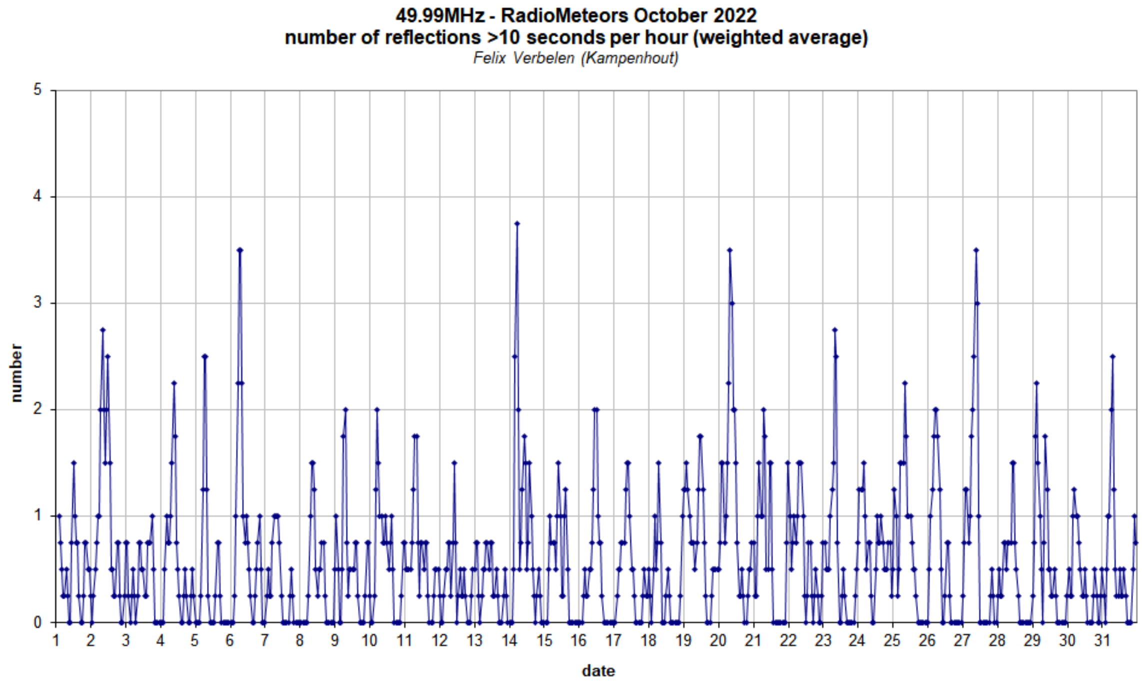

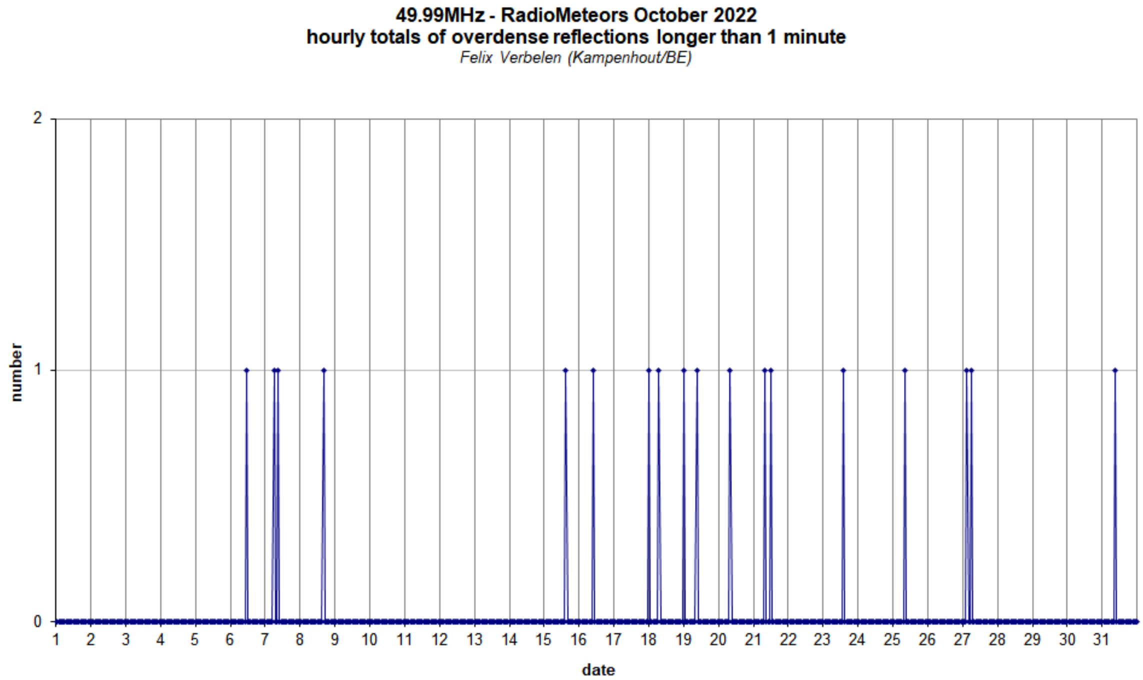

Figure 4 – The hourly numbers of overdense reflections longer than 10 seconds and longer than 1 minute, as observed here at Kampenhout (BE) on the frequency of our VVS-beacon (49.99 MHz) during October 2022.

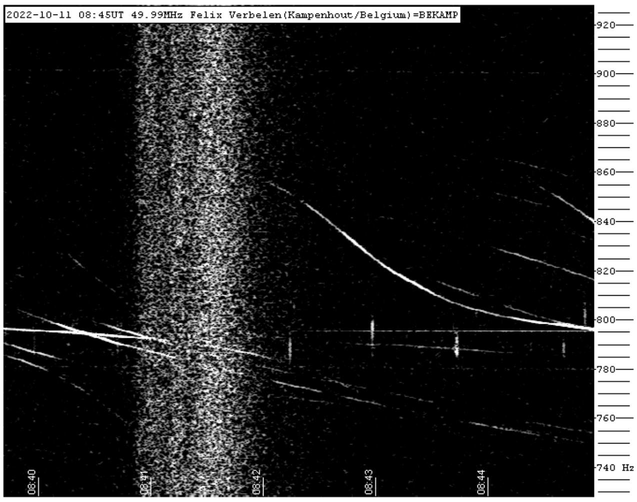

Figure 5 – Solar eruption 11 October 2022, 08^h45^m UT.

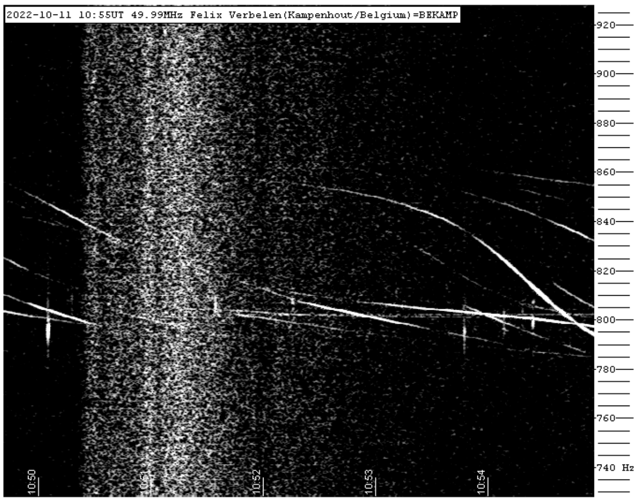

Figure 6 – Solar eruption 11 October 2022, 10^h55^m UT.

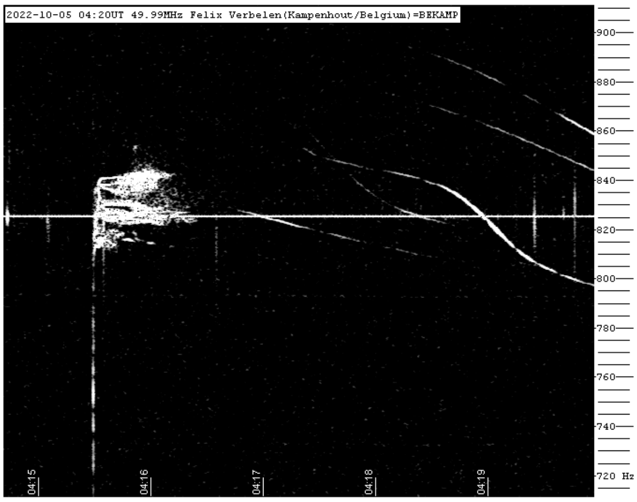

Figure 7 – Meteor reflection 5 October 2022, 04^h20^m UT.

Figure 8 – Meteor reflection 6 October 2022, 06^h15^m UT.

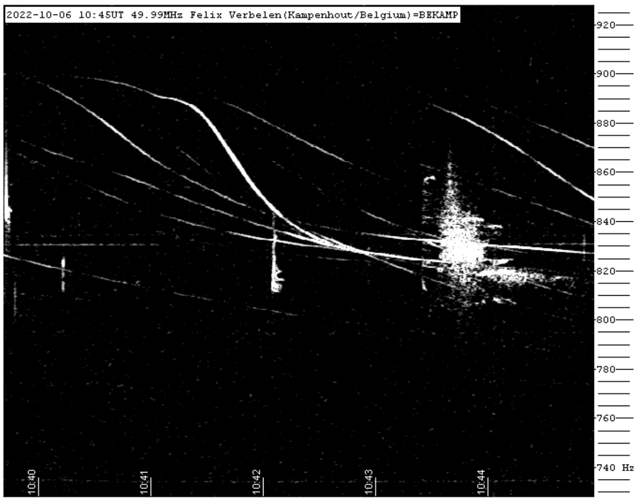

Figure 9 – Meteor reflection 6 October 2022, 10^h45^m UT.

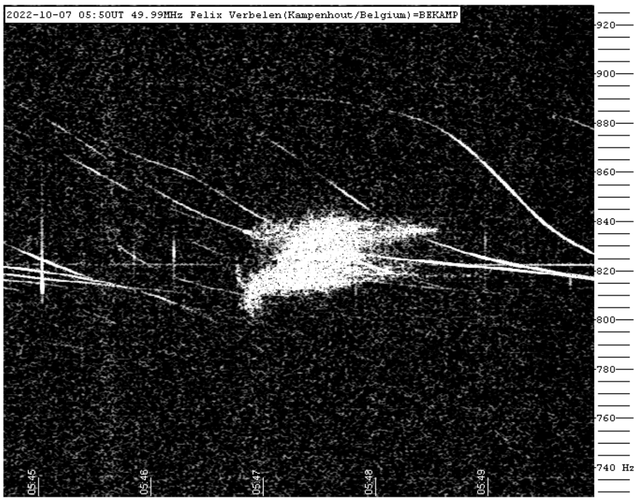

Figure 10 – Meteor reflection 7 October 2022, 05^h50^m UT.

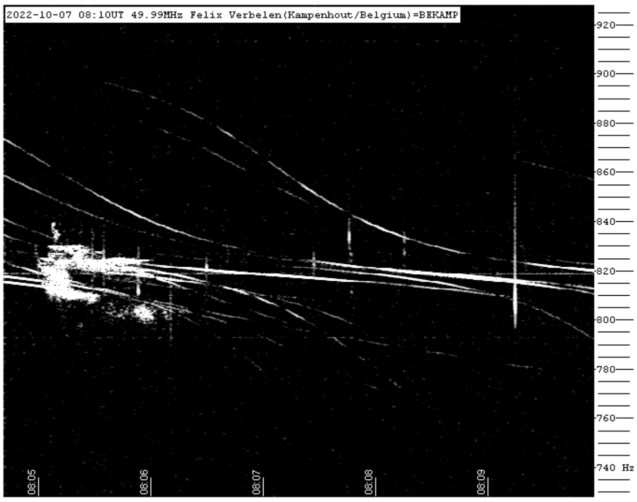

Figure 11 – Meteor reflection 7 October 2022, 08^h10^m UT.

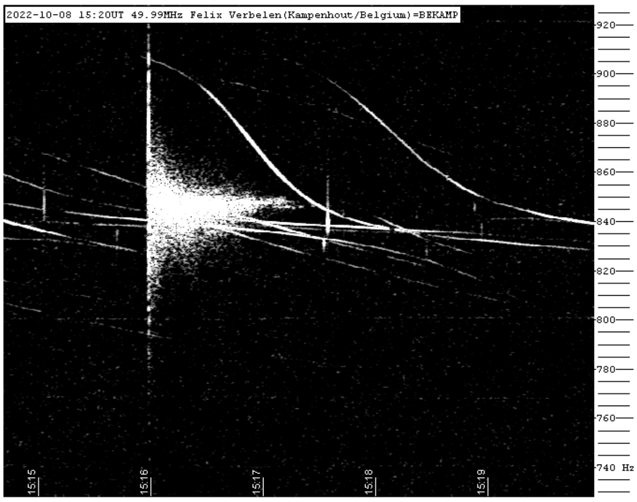

Figure 12 – Meteor reflection 8 October 2022, 15^h20^m UT.

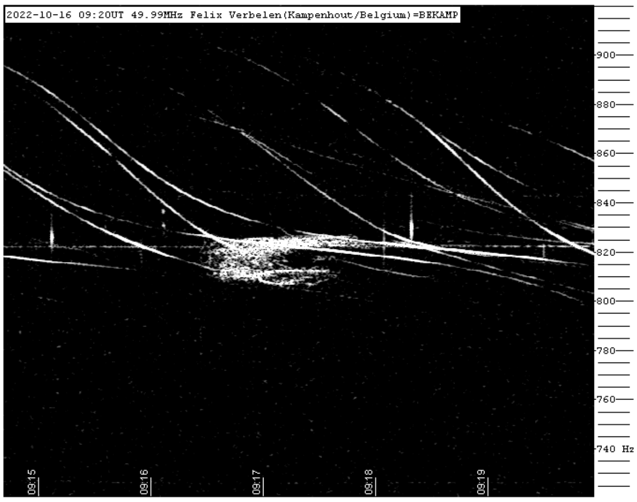

Figure 13 – Meteor reflection 16 October 2022, 09^h20^m UT.

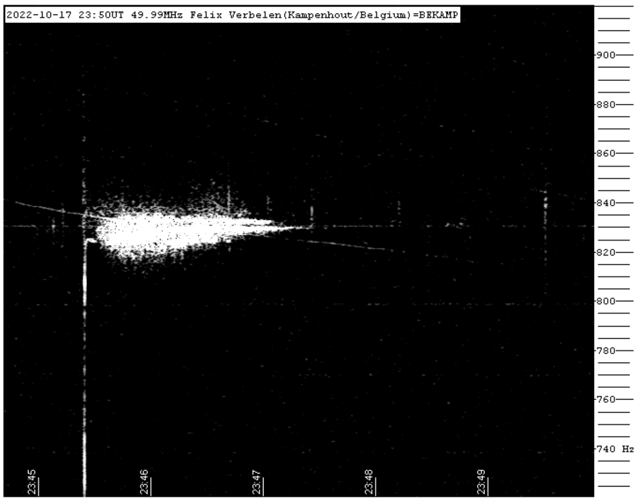

Figure 14 – Meteor reflection 17 October 2022, 23^h50^m UT.

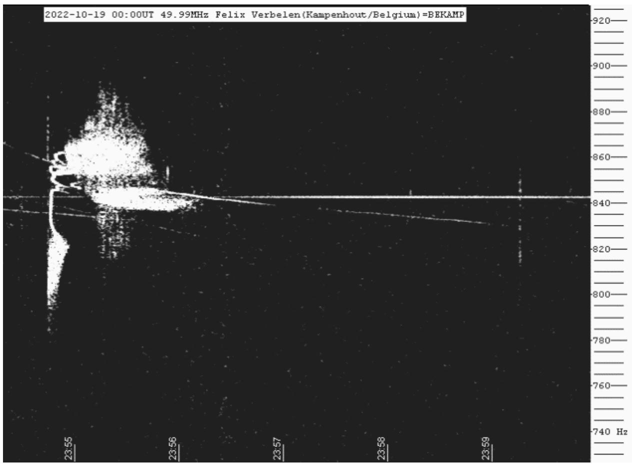

Figure 15 – Meteor reflection 19 October 2022, 00^h00^m UT.

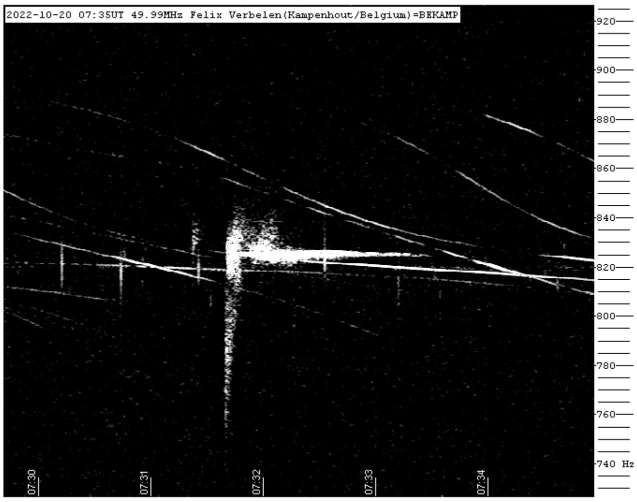

Figure 16 – Meteor reflection 20 October 2022, 07^h35^m UT.

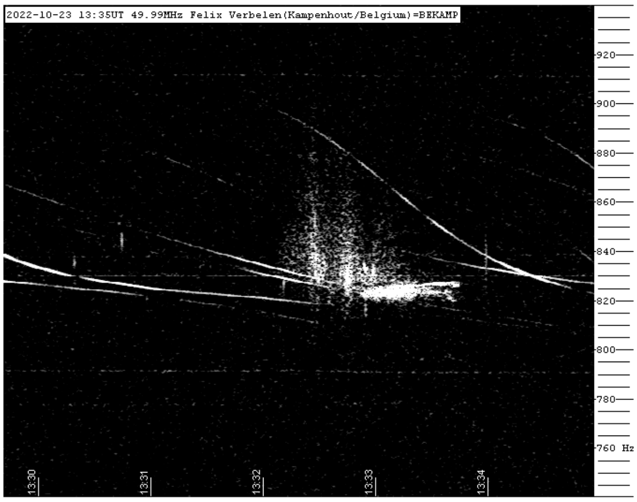

Figure 17 – Meteor reflection 23 October 2022, 13^{h}35^{m} UT.

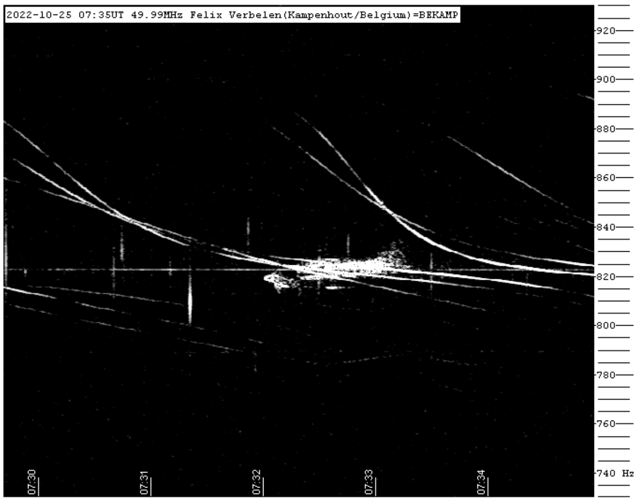

Figure 18 – Meteor reflection 25 October 2022, 07^{h}35^{m} UT.

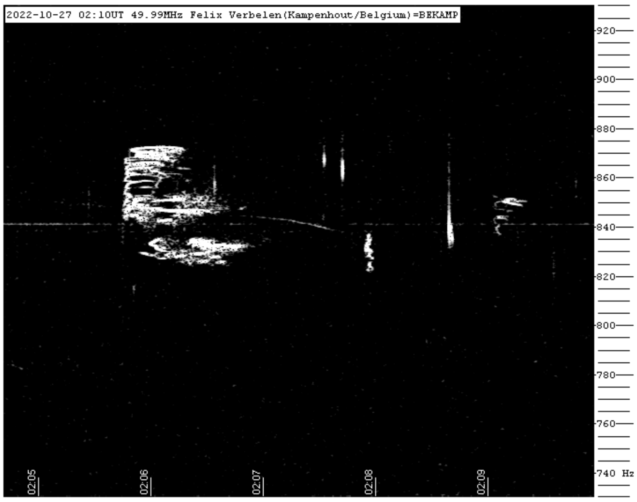

Figure 19 – Meteor reflection 27 October 2022, 02^{h}10^{m} UT.

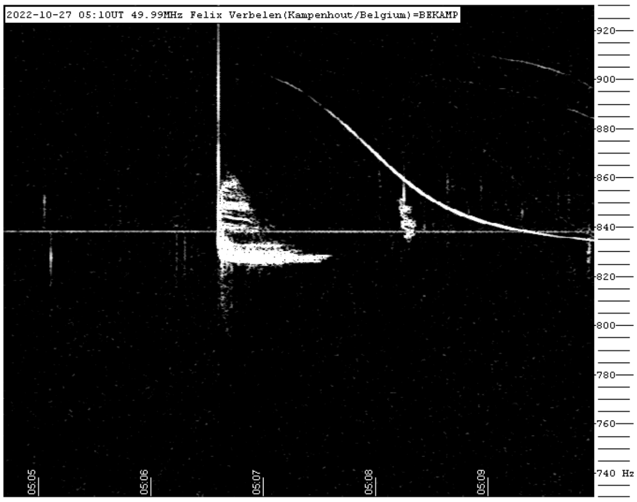

Figure 20 – Meteor reflection 27 October 2022, 05^{h}10^{m} UT.

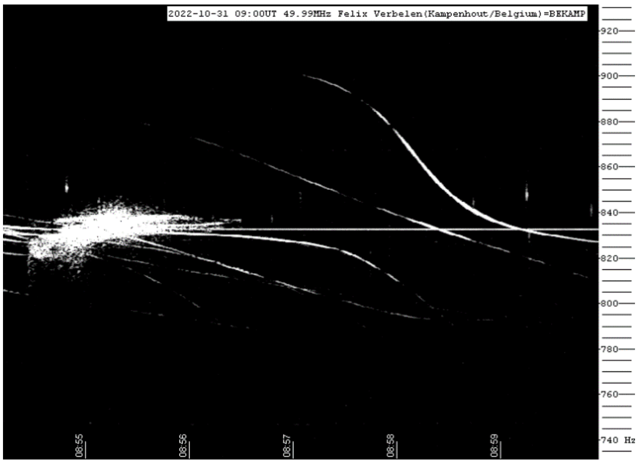

Figure 21 – Meteor reflection 31 October 2022, 09^{h}00^{m} UT.

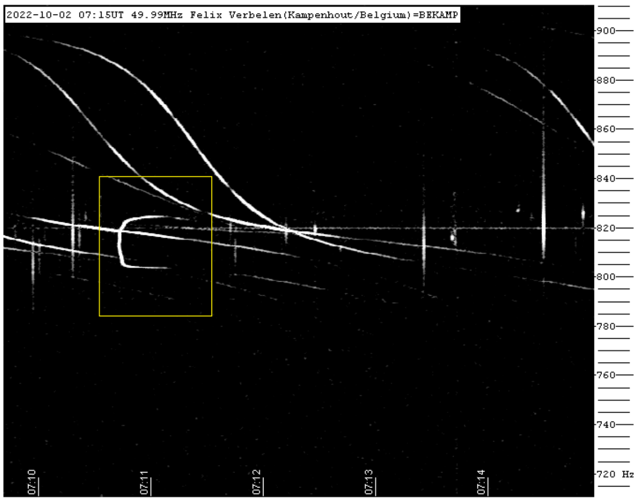

Figure 22 – Meteor reflection 02 October 2022, 07^{h}15^{m} UT.

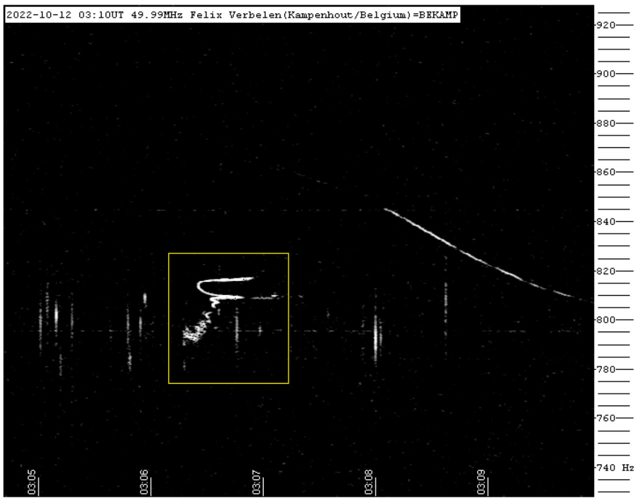

Figure 23 – Meteor reflection 12 October 2022, 03^h10^m UT.

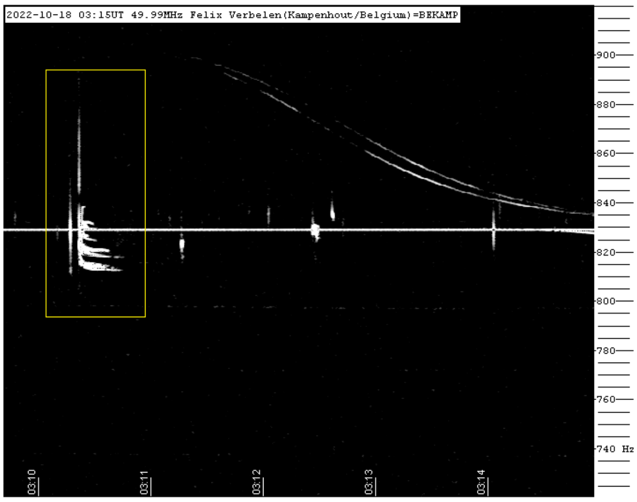

Figure 24 – Meteor reflection 18 October 2022, 03^h15^m UT.

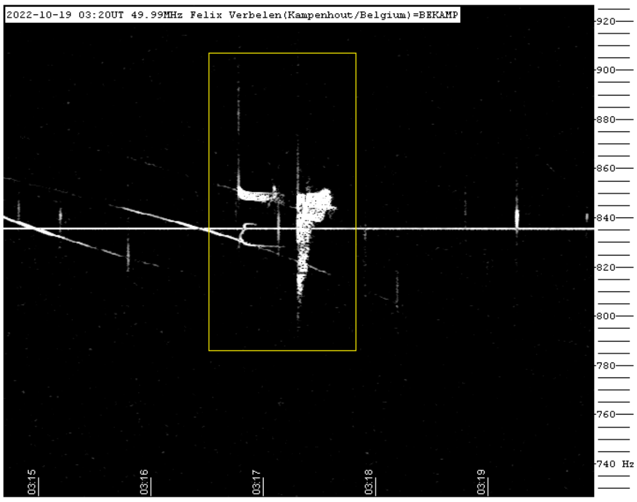

Figure 25 – Meteor reflection 19 October 2022, 03^h20^m UT.

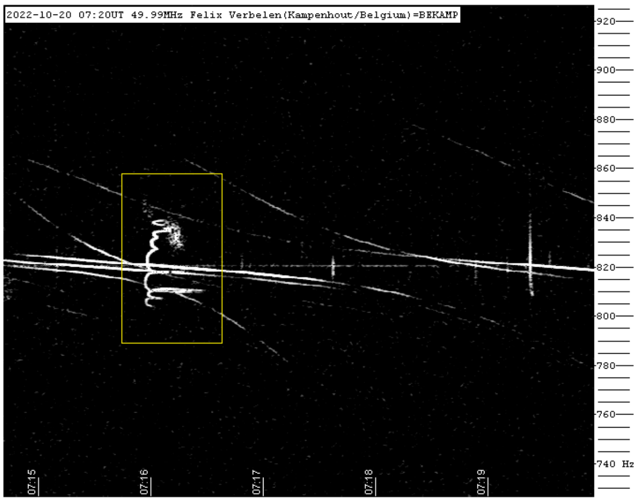

Figure 26 – Meteor reflection 20 October 2022, 07^h20^m UT.

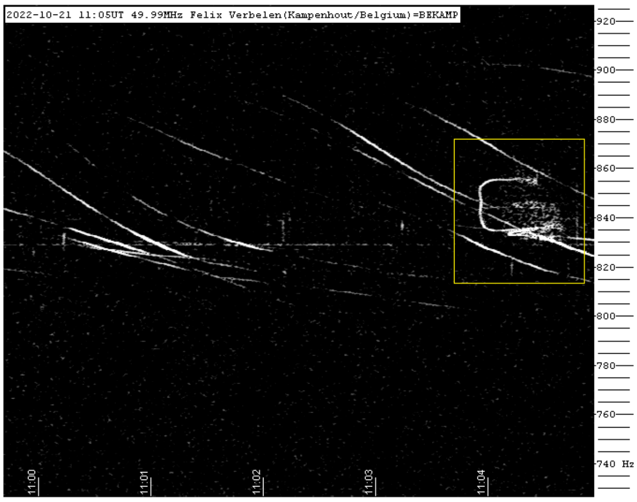

Figure 27 – Meteor reflection 21 October 2022, 11^h05^m UT.

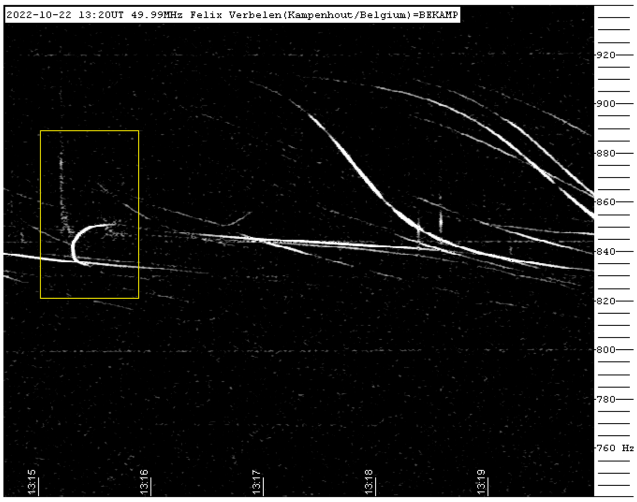

Figure 28 – Meteor reflection 22 October 2022, 13^h20^m UT.

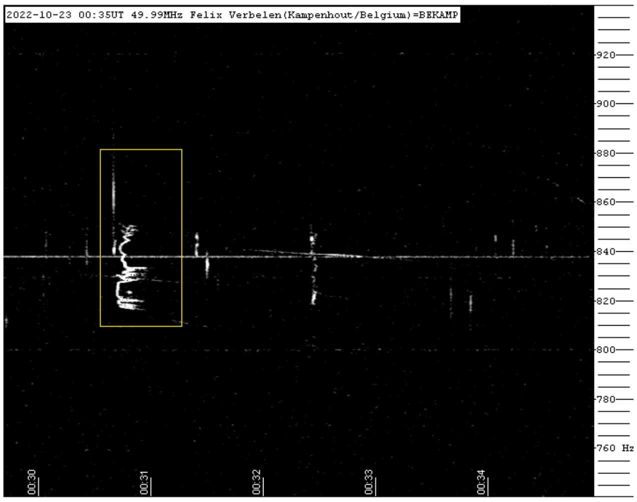

Figure 29 – Meteor reflection 23 October 2022, 00^{h}35^m UT.

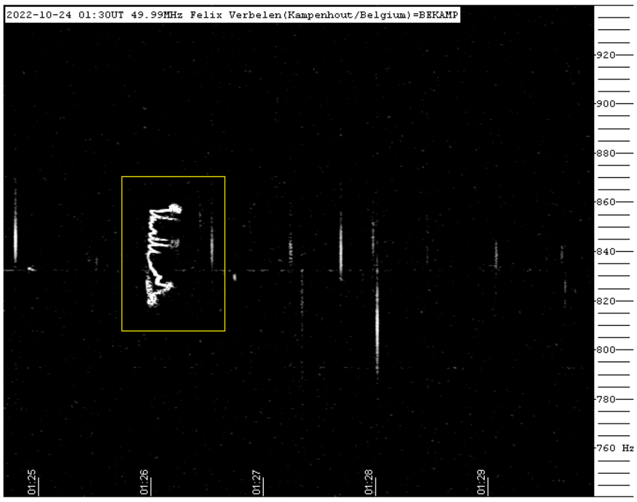

Figure 30 – Meteor reflection 24 October 2022, 01^{h}30^m UT.

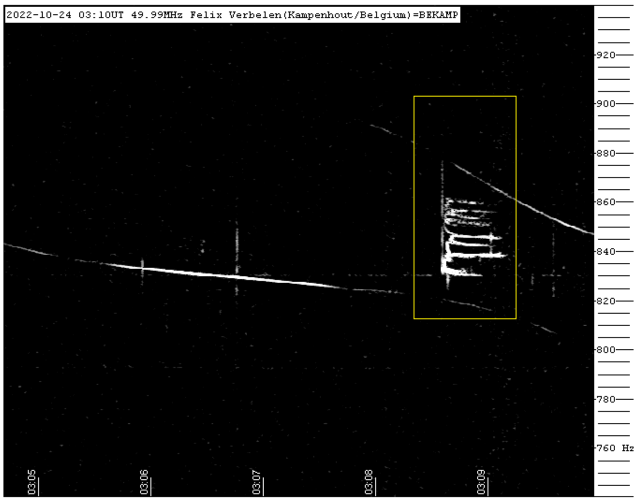

Figure 31 – Meteor reflection 24 October 2022, 03^{h}10^m UT.

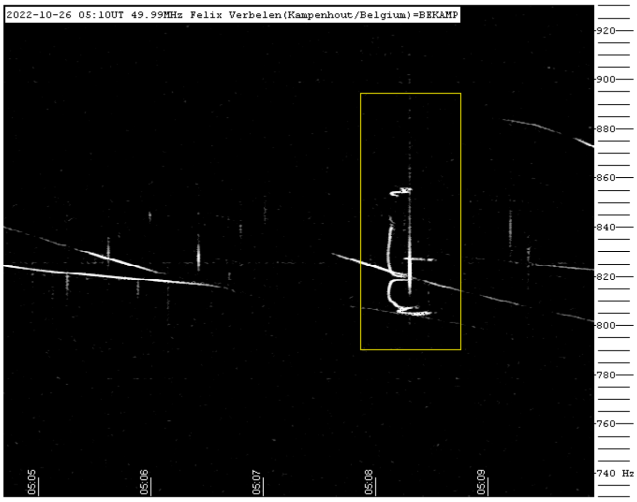

Figure 32 – Meteor reflection 26 October 2022, 05^{h}10^m UT.

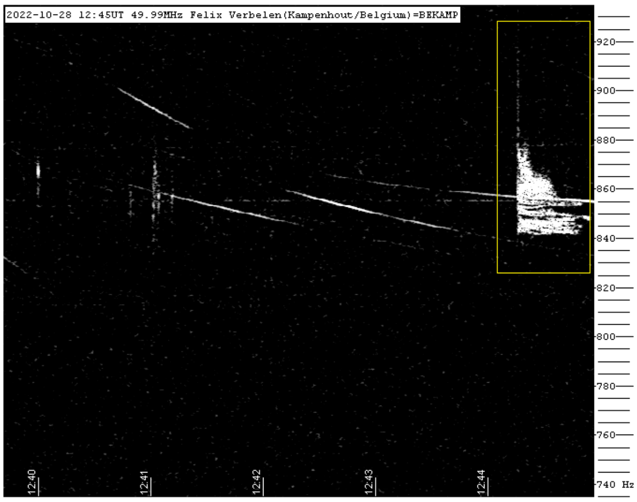

Figure 33 – Meteor reflection 28 October 2022, 12^{h}45^m UT.

Radio meteors November 2022

Felix Verbelen

Vereniging voor Sterrenkunde & Volkssterrenwacht MIRA, Grimbergen, Belgium
felix.verbelen@skynet.be

An overview of the radio observations during November 2022 is given.

1 Introduction

The graphs show both the daily totals (*Figure 1 and 2*) and the hourly numbers (*Figure 3 and 4*) of "all" reflections counted automatically, and of manually counted "overdense" reflections, overdense reflections longer than 10 seconds and longer than 1 minute, as observed here at Kampenhout (BE) on the frequency of our VVS-beacon (49.99 MHz) during the month of November 2022.

The hourly numbers, for echoes shorter than 1 minute, are weighted averages derived from:

$$N(h) = \frac{n(h-1)}{4} + \frac{n(h)}{2} + \frac{n(h+1)}{4}$$

Local interference and unidentified noise remained moderate to low for most of the month. Only minimal lightning activity was observed on 2 days. Solar activity remained low at 49.99 MHz, with only a few short bursts.

Two periods of increased meteor activity stand out: the Taurids at the beginning of the month and the Leonids in the days before and after November 18th. However, the actual course of the observed reflections is peculiar, with an unexplained drop on 18 November on the one hand and an increase in the underdenses in the following days. These peculiarities may be due to material problems (beacon or receiver installation) or to atmospheric conditions, although there are no direct indications of this; further research and comparison with the results of other observers is therefore necessary.

Over the entire month, 26 reflections longer than 1 minute were registered here. Attached are selections of long reflections (*Figures* 5 to 14) and of a number of interesting "epsilons" (*Figures* 15 to 25). In addition to the usual graphs, you will also find the raw counts in cvs-format[17] from which the graphs are derived.

The table contains the following columns: day of the month, hour of the day, day + decimals, solar longitude (epoch J2000), counts of "all" reflections, overdense reflections, reflections longer than 10 seconds and reflections longer than 1 minute, the numbers being the observed reflections of the past hour.

[17] https://www.meteornews.net/wp-content/uploads/2022/12/202211_49990_FV_rawcounts.csv

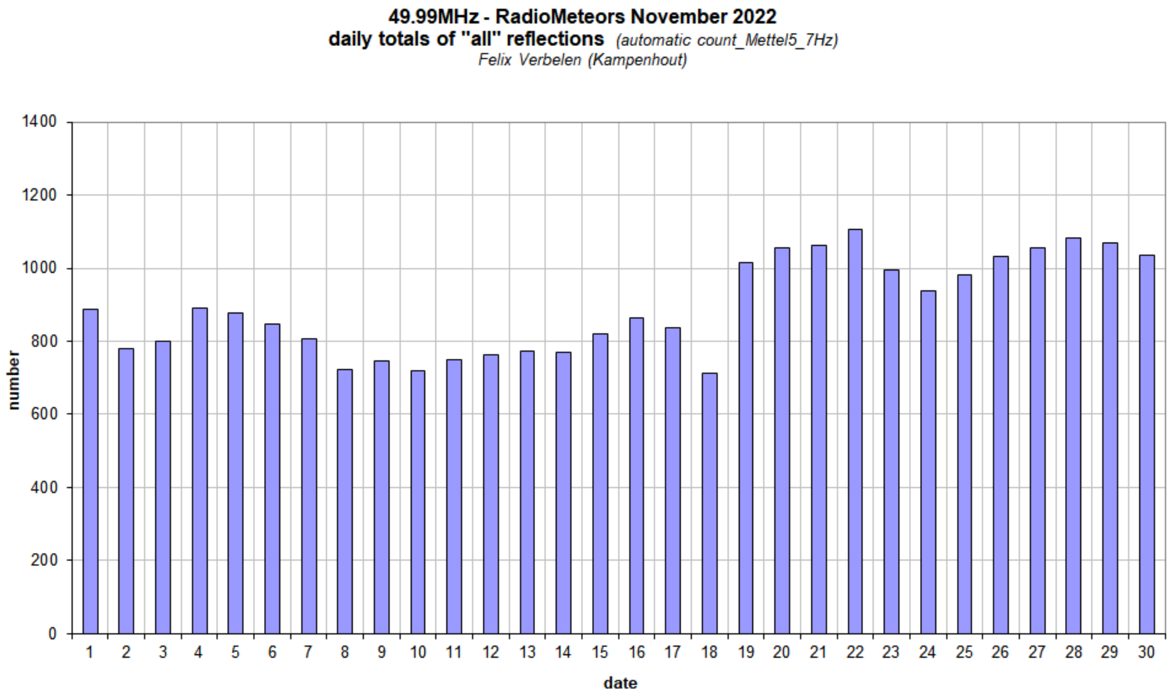

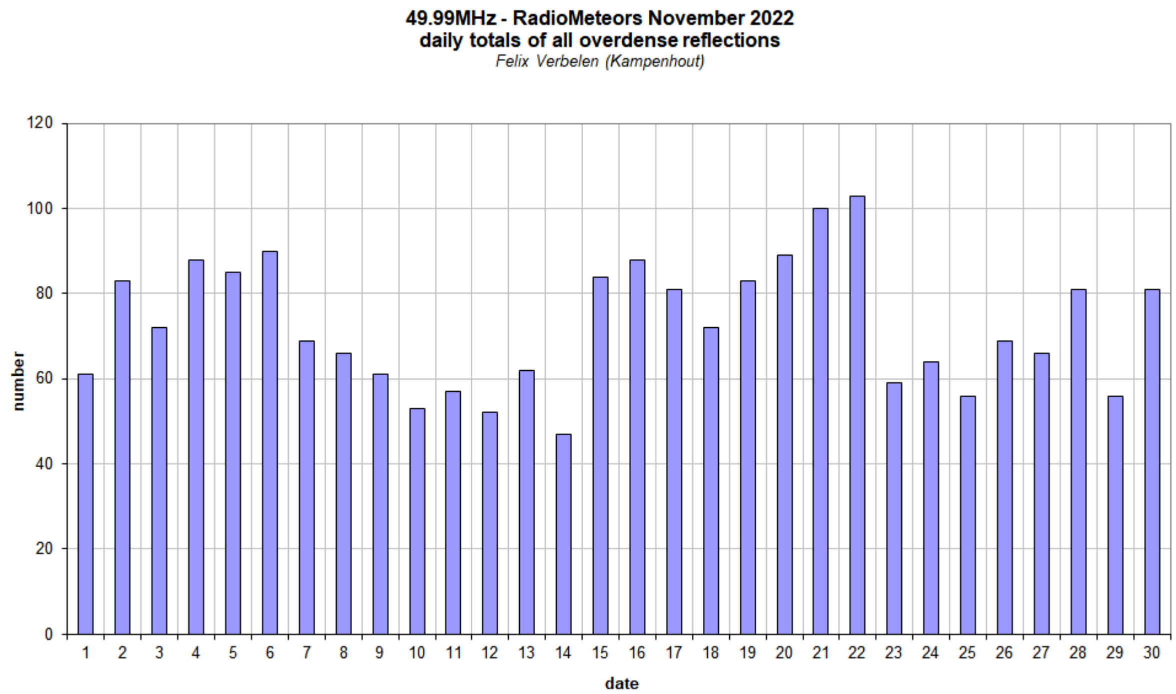

Figure 1 – The daily totals of "all" reflections counted automatically, and of manually counted "overdense" reflections, as observed here at Kampenhout (BE) on the frequency of our VVS-beacon (49.99 MHz) during November 2022.

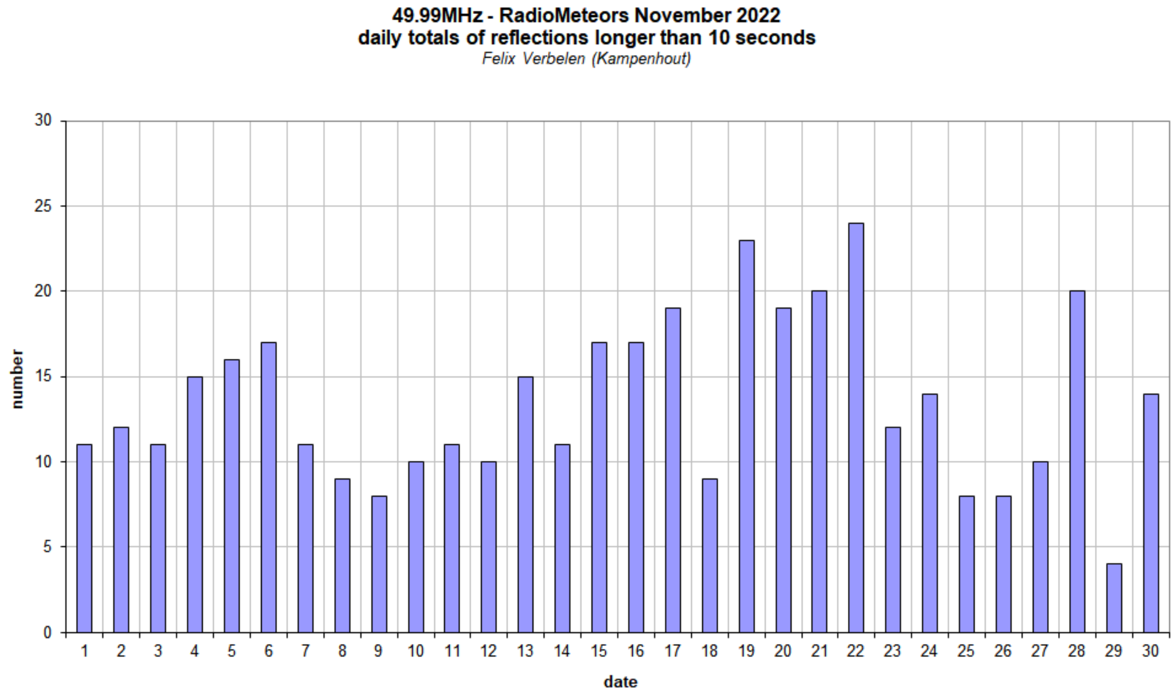

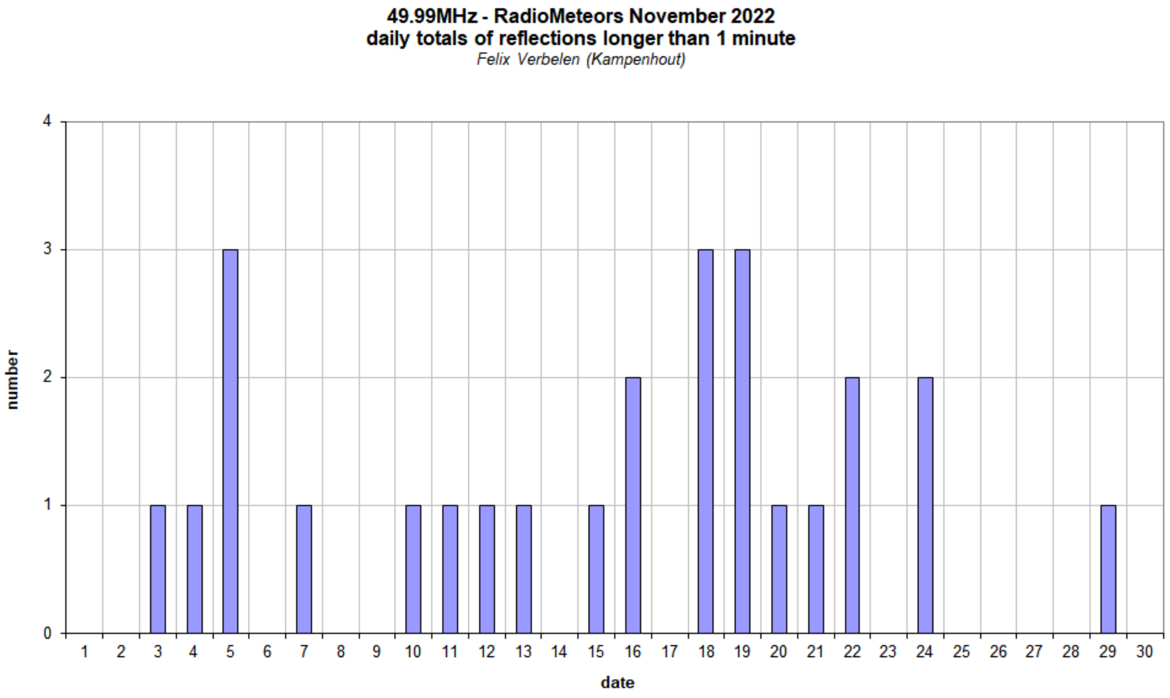

Figure 2 – The daily totals of overdense reflections longer than 10 seconds and longer than 1 minute, as observed here at Kampenhout (BE) on the frequency of our VVS-beacon (49.99 MHz) during November 2022.

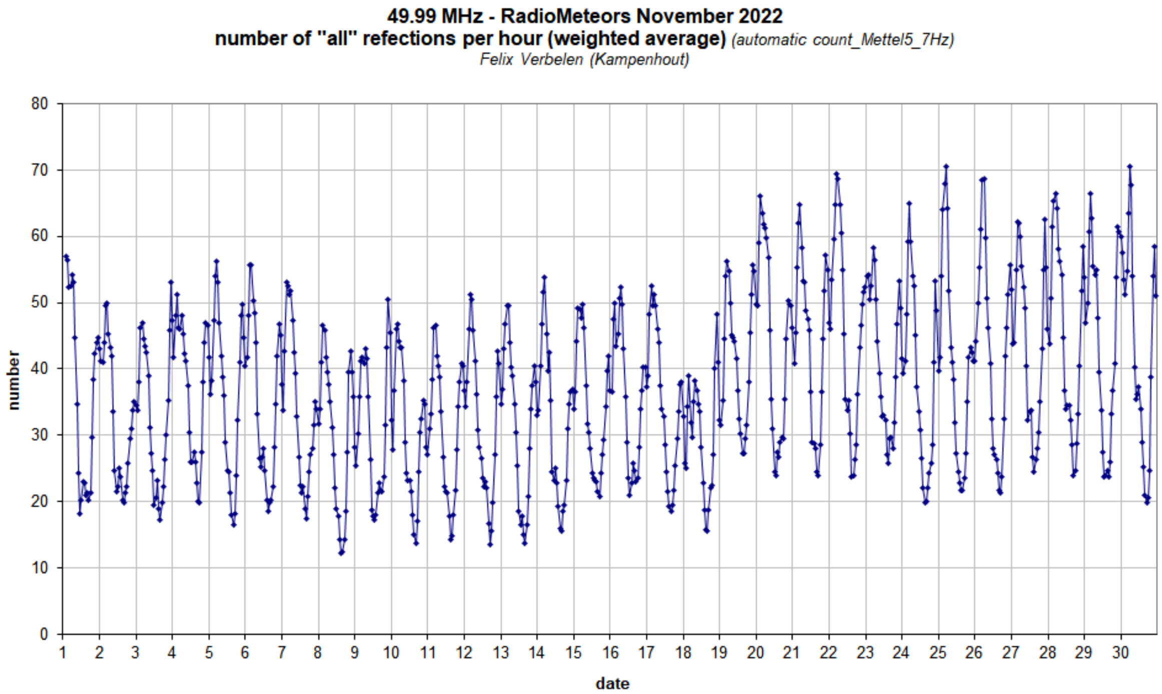

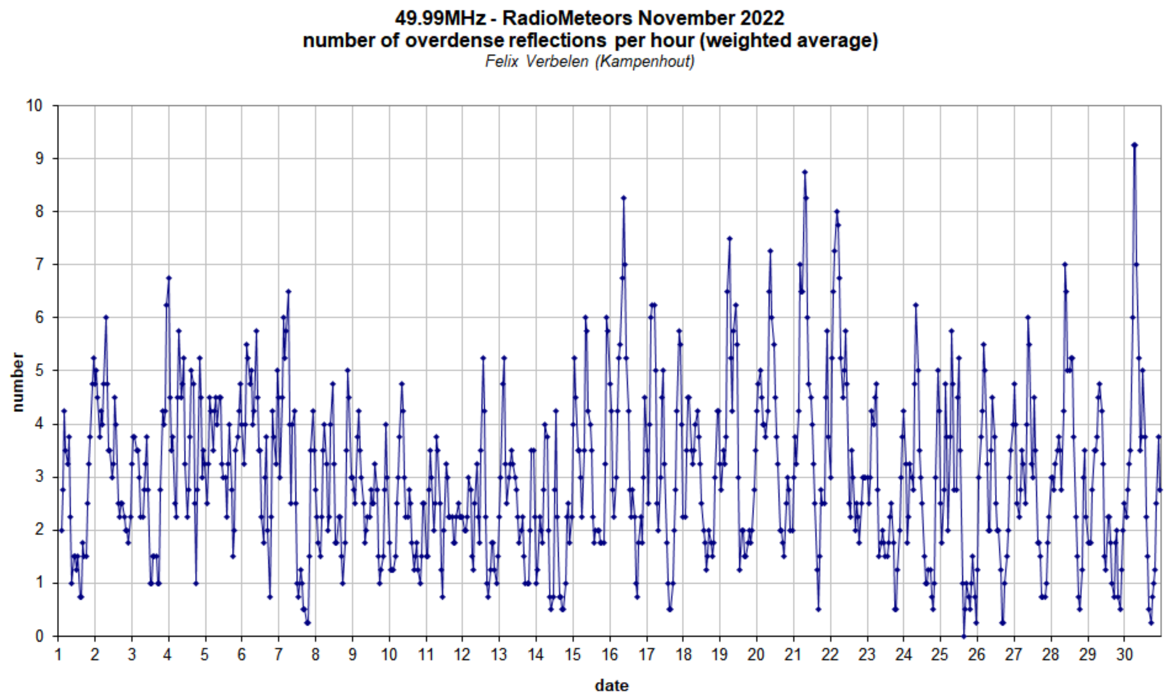

Figure 3 – The hourly numbers of "all" reflections counted automatically, and of manually counted "overdense" reflections, as observed here at Kampenhout (BE) on the frequency of our VVS-beacon (49.99 MHz) during November 2022.

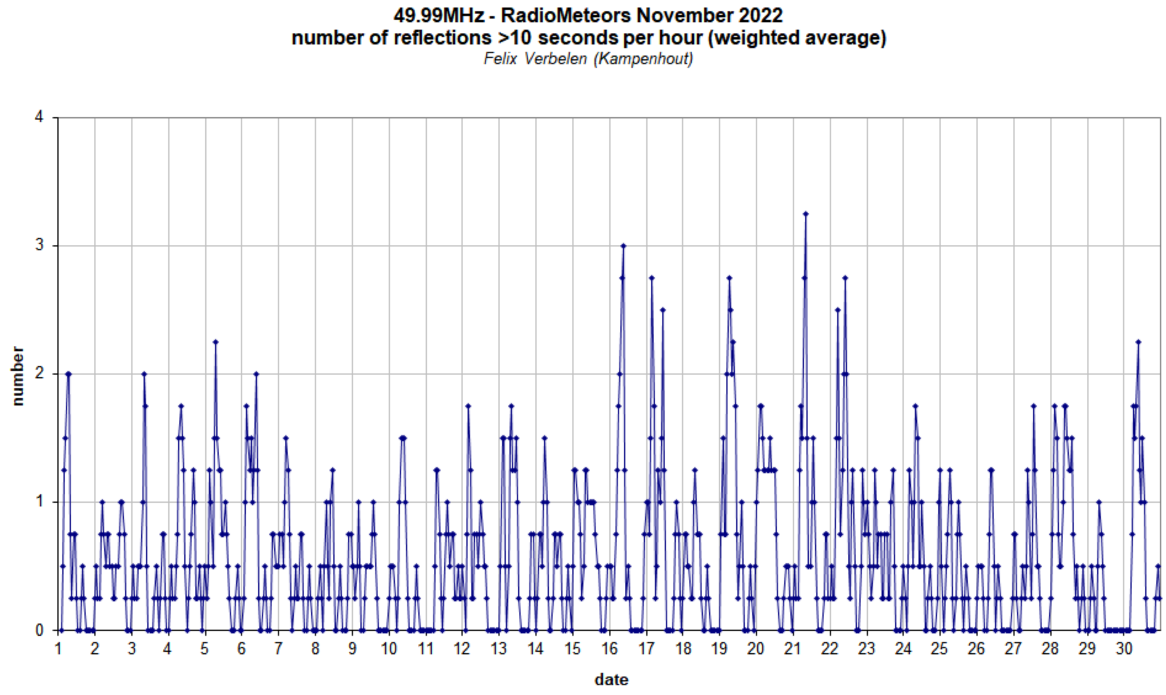

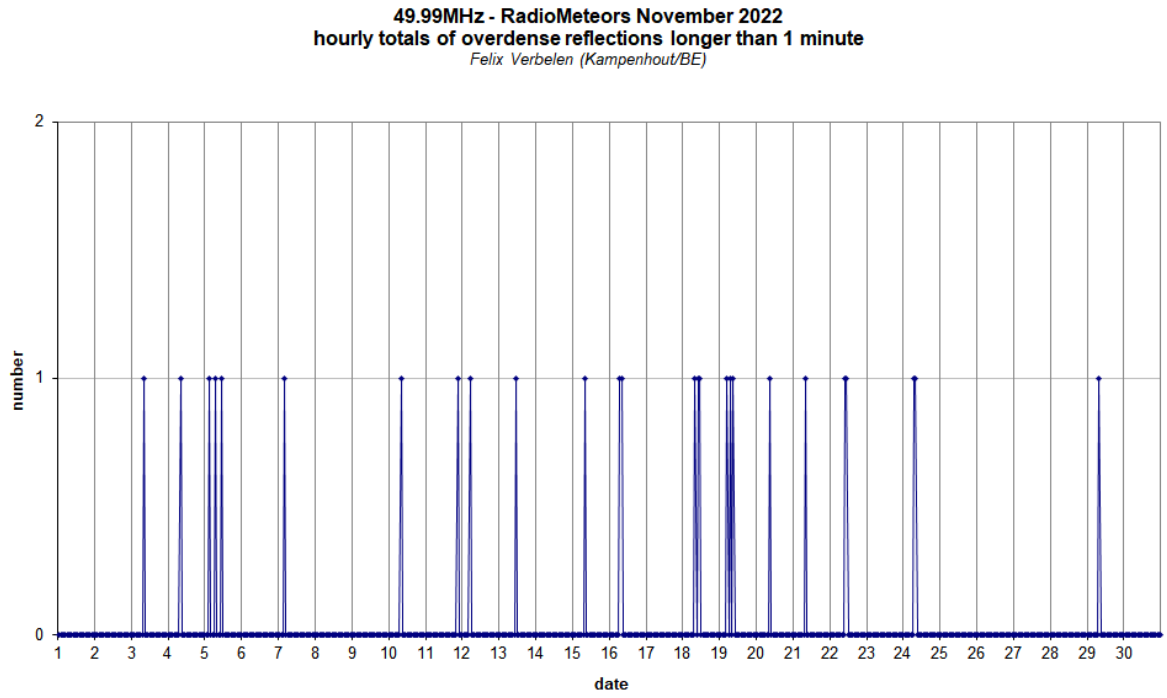

Figure 4 – The hourly numbers of overdense reflections longer than 10 seconds and longer than 1 minute, as observed here at Kampenhout (BE) on the frequency of our VVS-beacon (49.99 MHz) during November 2022.

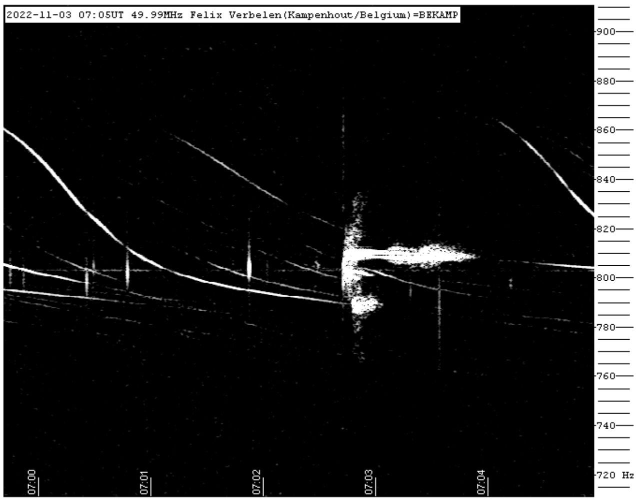

Figure 5 – Meteor reflection 03 November 2022, 07ʰ05ᵐ UT.

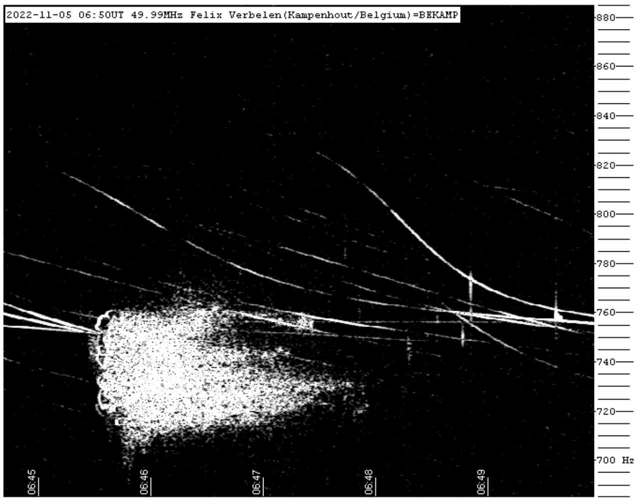

Figure 6 – Meteor reflection 05 November 2022, 06ʰ50ᵐ UT.

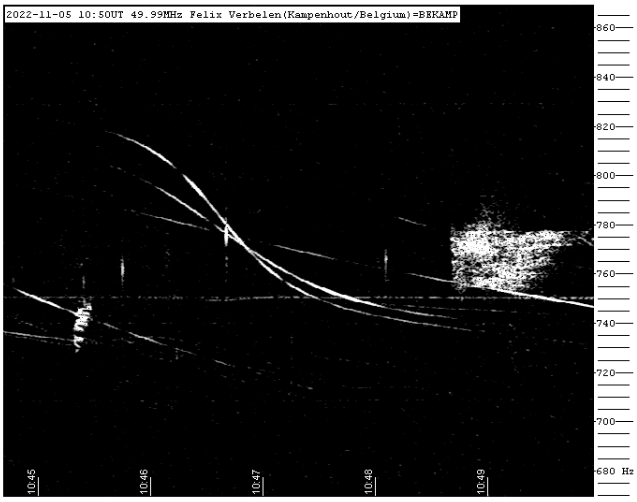

Figure 7 – Meteor reflection 05 November 2022, 10ʰ50ᵐ UT.

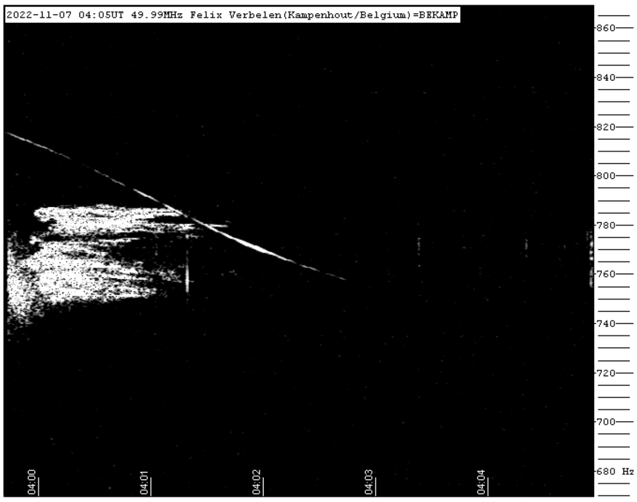

Figure 8 – Meteor reflection 07 November 2022, 04ʰ05ᵐ UT.

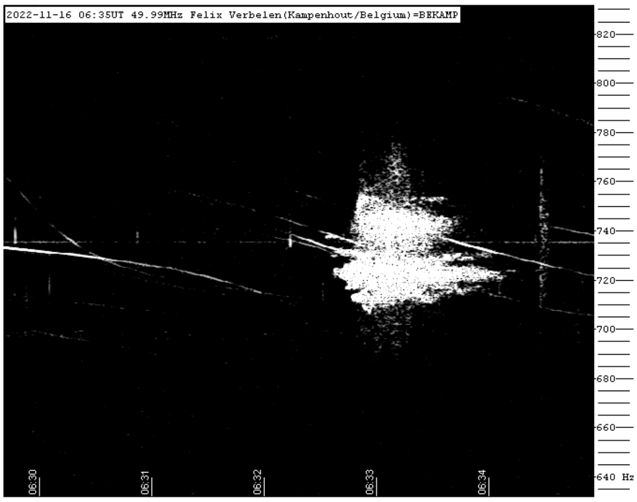

Figure 9 – Meteor reflection 16 November 2022, 06ʰ35ᵐ UT.

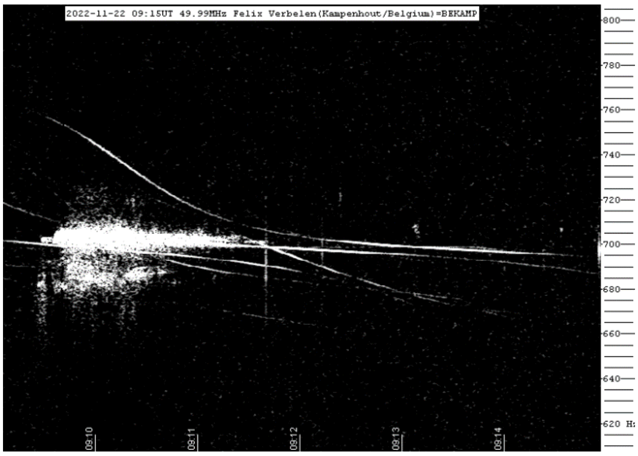

Figure 10 – Meteor reflection 22 November 2022, 09ʰ15ᵐ UT.

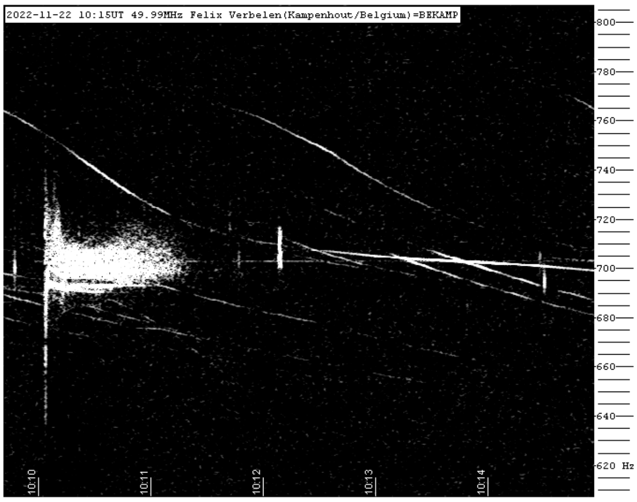

Figure 11 – Meteor reflection 22 November 2022, 10^{h}15^{m} UT.

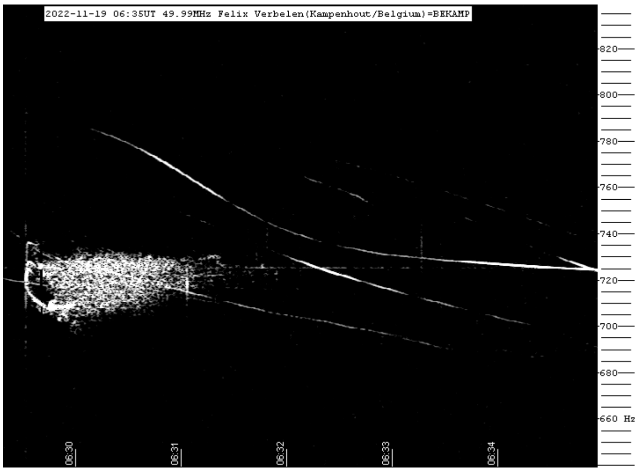

Figure 12 – Meteor reflection 19 November 2022, 06^{h}35^{m} UT.

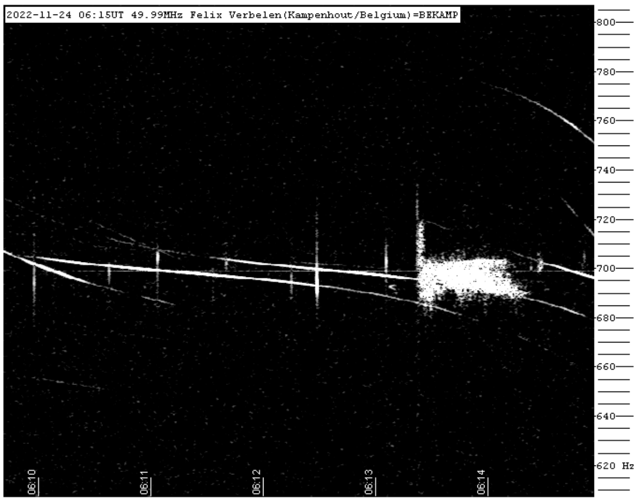

Figure 13 – Meteor reflection 24 November 2022, 06^{h}15^{m} UT.

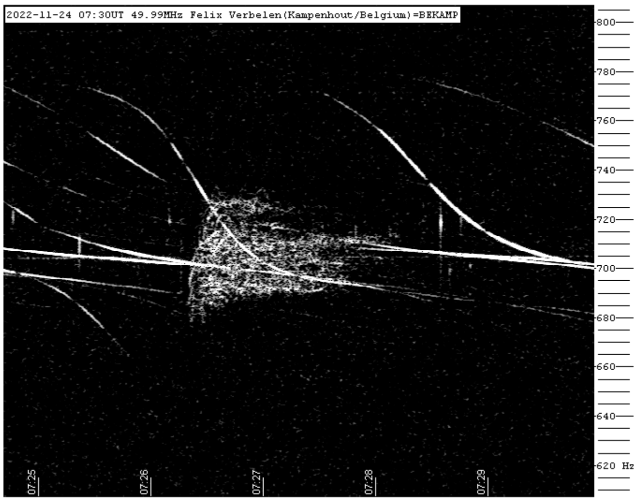

Figure 14 – Meteor reflection 24 November 2022, 07^{h}30^{m} UT.

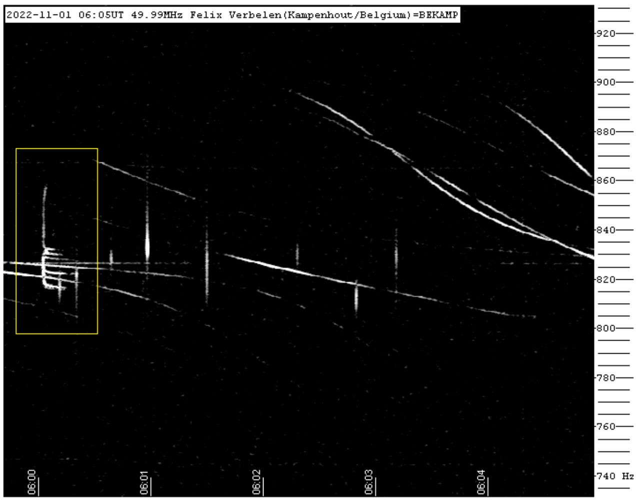

Figure 15 – Meteor reflection 01 November 2022, 06^{h}05^{m} UT.

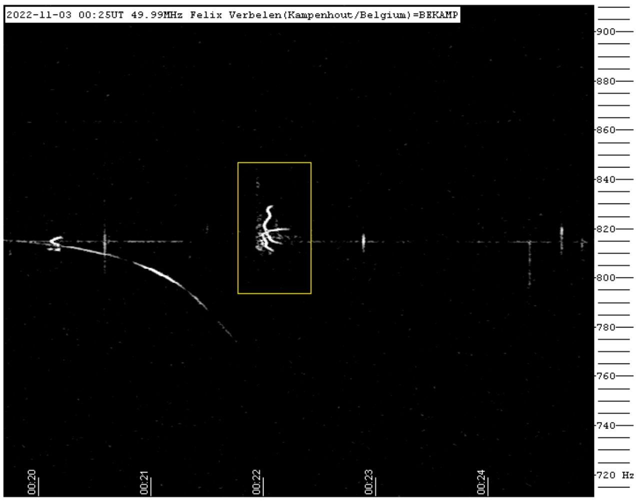

Figure 16 – Meteor reflection 03 November 2022, 00^{h}25^{m} UT.

Figure 17 – Meteor reflection 04 November 2022, 06^{h}45^m UT.

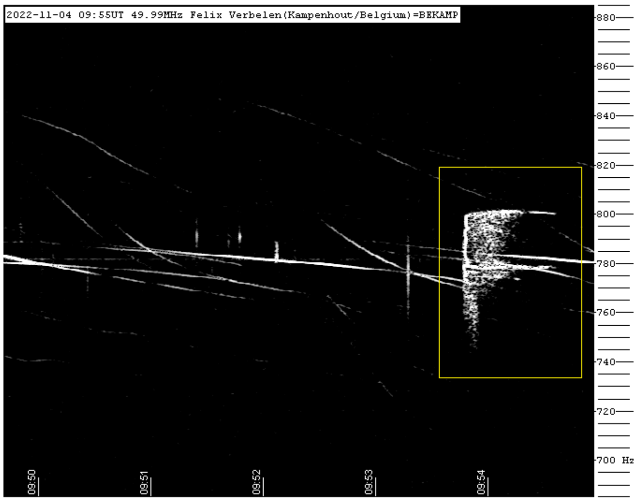

Figure 18 – Meteor reflection 04 November 2022, 09^{h}55^m UT.

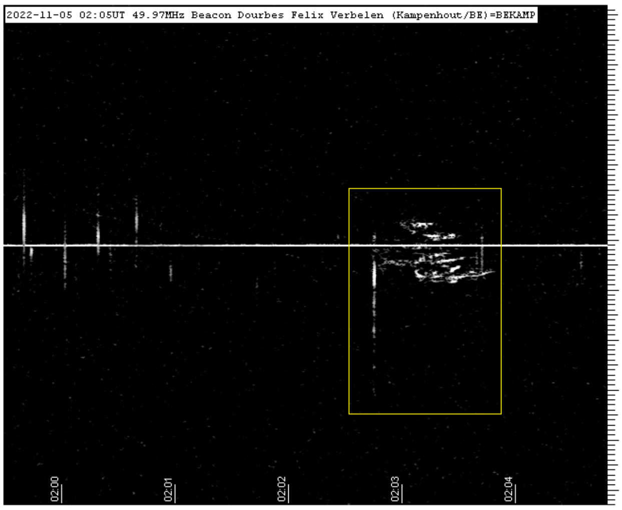

Figure 19 – Meteor reflection 05 November 2022, 02^{h}05^m UT.

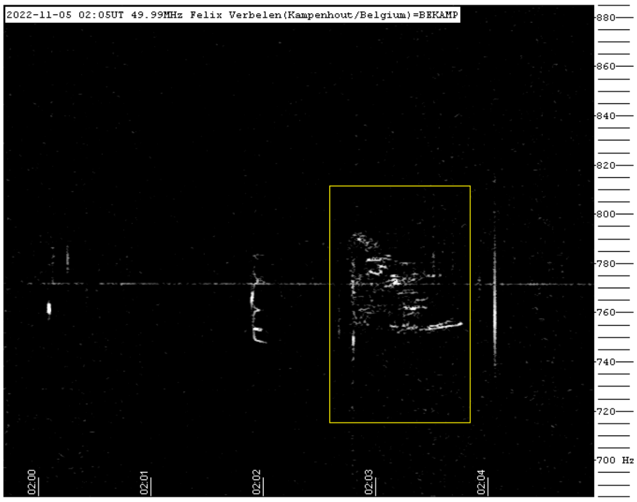

Figure 20 – Meteor reflection 05 November 2022, 02^{h}05^m UT.

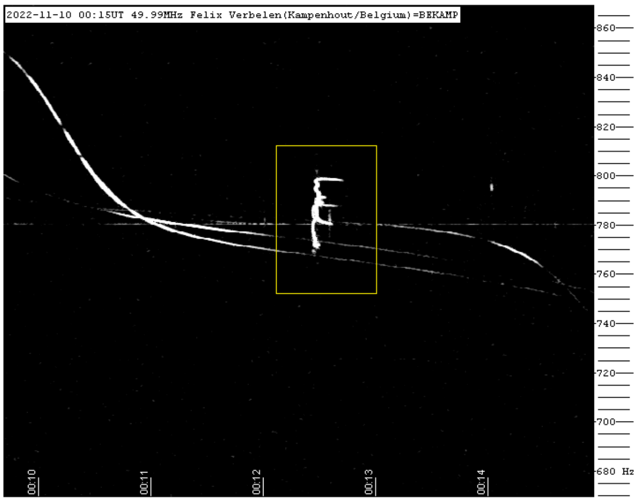

Figure 21 – Meteor reflection 10 November 2022, 00^{h}15^m UT.

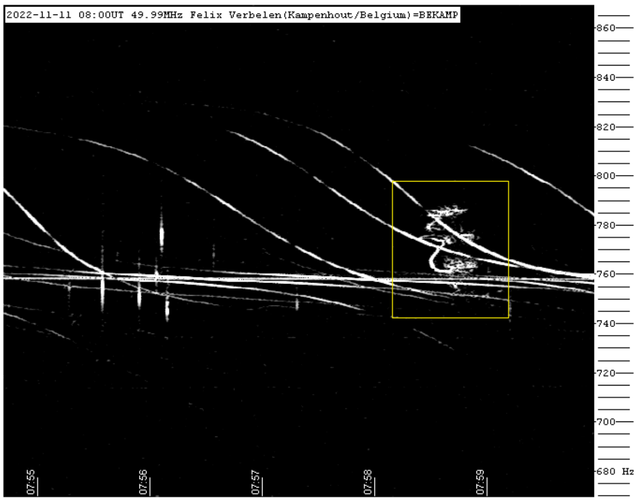

Figure 22 – Meteor reflection 11 November 2022, 08^{h}00^m UT.

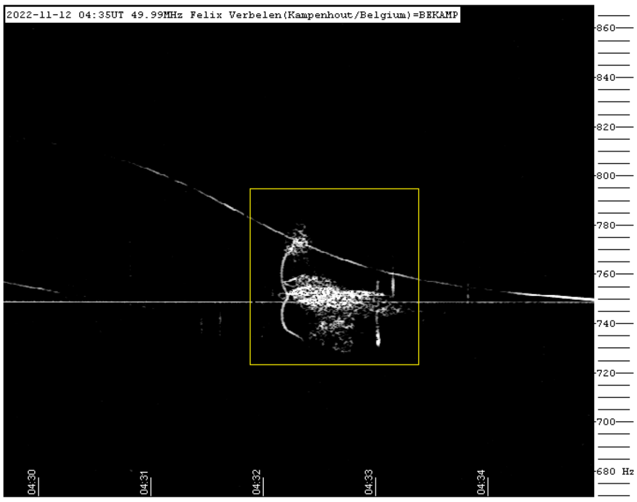

Figure 23 – Meteor reflection 12 November 2022, 04^h35^m UT.

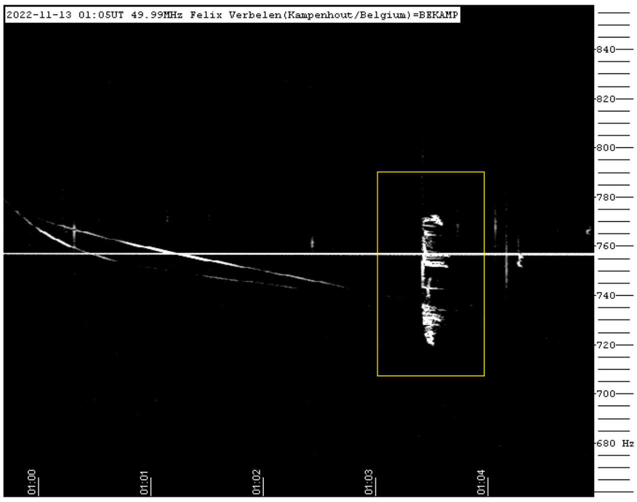

Figure 24 – Meteor reflection 13 November 2022, 01^h05^m UT.

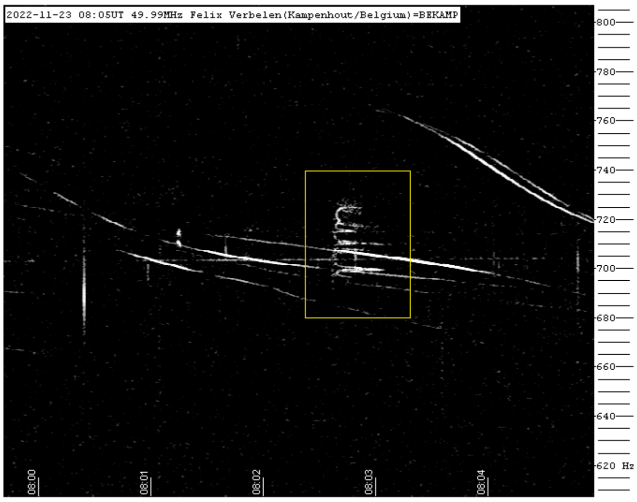

Figure 25 – Meteor reflection 23 November 2022, 08^h05^m UT.

October 2022 report CAMS BeNeLux

Carl Johannink

Am Ollenkamp 4, 48599 Gronau, Germany
c.johannink@t-online.de

A summary of the activity of the CAMS BeNeLux network during the month of October 2022 is presented. This month we collected a total of 32170 multi-station meteors resulting in 9749 orbits.

1 Introduction

Sporadic meteor activity is now nearly reaching its highest level, but there are also several meteor streams visible, reaching their high activity towards the end of this month, like the Orionids and the Taurids.

Meanwhile we can observe for more than 12 hours at our latitudes (50°–53° north). This makes this month one of the most attractive months to observe meteors, therefore, we were curious to see the results.

2 October 2022 statistics

October 2022 showed a very stable weather pattern. The BeNeLux had many complete clear, or at least partly clear nights. As a result, we could collect a substantial number of orbits in every night this month, except for October 13–14. Skies remained mostly cloudy in our regions. Only 63 meteors were captured by all cameras this night, but none of them was simultaneous from at least two different sites.

A total of 32170 meteors were detected this month, resulting in a record amount of 9749 orbits, see *Figure 1*. In several nights, October 2–3, 6–7, 8-9, 18–19, 21–22, 23–24, 26–27 and 27–28 the number of orbits was more than 500. The highest number of orbits was collected during October 23–24 with 814 orbits in this single night.

It was striking to see that more than 56% of all orbits were captured by at least 3 cameras during this month. This is an indication that the sky over the BeNeLux is well covered by our network.

For the first time, we could receive results from a station in Luxembourg. *Philippe Schaack* is running an RMS camera LU0001 (CAMS 3952) from Roodt-sur-Syre since October 19.

On average 86.4 cameras were active at 31 stations in the BeNeLux during this month. At least 68 cameras (October 14–15) and a maximum of 94 cameras (October 8–9 and 9–10) were active. These numbers are slightly better than last month (*Figure 1* and *Table 1*).

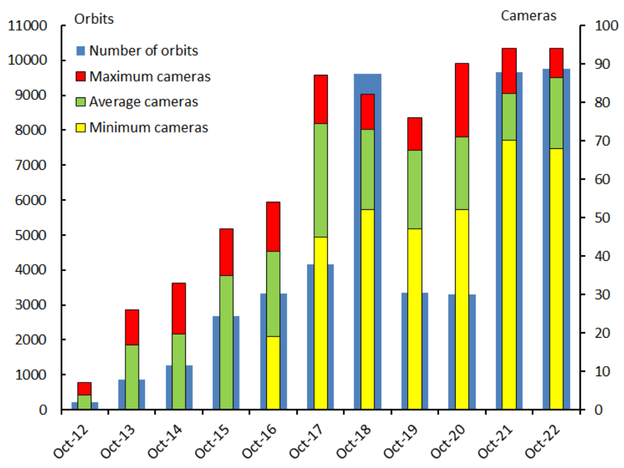

Figure 1 – Comparing October 2022 to previous months of October in the CAMS BeNeLux history. The blue bars represent the number of orbits, the red bars the maximum number of cameras capturing in a single night, the green bar the average number of cameras capturing per night and the yellow bar the minimum number.

Table 1 – Number of orbits and active cameras in the BeNeLux during October 2012–2022.

Year	Nights	Orbits	Stations	Max. Cams	Min. Cams	Mean Cams
2012	16	220	6	7	–	3.9
2013	20	866	10	26	–	16.8
2014	22	1262	14	33	–	19.7
2015	24	2684	15	47	–	34.8
2016	30	3335	19	54	19	41.3
2017	29	4163	22	87	45	74.4
2018	29	9611	21	82	52	73.0
2019	29	3344	20	76	47	67.5
2020	29	3305	23	90	52	70.9
2021	29	9669	26	94	70	82.2
2022	30	9749	31	94	68	86.4
Total	287	48208				

3 Focus on a minor shower

In the past, around October 5 there have been sometimes reports about a substantial meteor activity from the Draconid/Camelopardalid region (Jenniskens, 2005; 2006). Based on the high activity in October 2005 this minor shower was listed as an 'established shower' in the IAU as October Camelopardalids, OCT#281 (Jenniskens 2005).

In 2018 higher activity of this meteoroid stream was mentioned again at this date (Roggemans et al., 2019). However, from CAMS data it is clear that we can see meteors from this minor shower in every year.

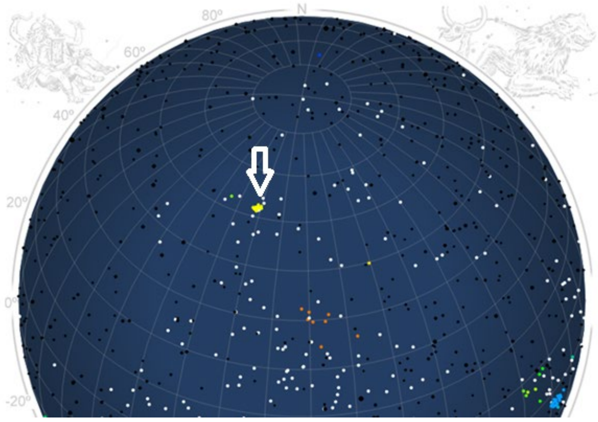

Figure 2 – Radiant plot for CAMS BeNeLux data on 2022 October 5–6.

Table 2 – Number of OCT#281 meteors during 2022 October 5–6 (data CAMS BeNeLux).

UT	$\lambda_\odot$ (°)	OCT	Comment
20^h54^m	192.2892	–	First orbit
23^h07^m–23^h36^m	192.38–192.40	1	
23^h36^m–00^h06^m	192.40–192.42	0	
00^h06^m–00^h35^m	192.42–192.44	0	
00^h35^m–01^h04^m	192.44–192.46	0	
01^h04^m-01^h33^m	192.46–192.48	0	
01^h33^m–02^h02^m	192.48–192.50	0	
02^h02^m–02^h31^m	192.50–192.52	1	
02^h31^m–03^h00^m	192.52–192.54	3	
03^h00^m–03^h30^m	192.54–192.56	0	
03^h30^m–03^h59^m	192.56–192.58	2	
03^h59^m–04^h28^m	192.58–192.60	3	
04^h28^m–04^h58^m	192.60-192.62	3	
04^h58^m	192.6207	–	Last orbit

Figure 2 shows a nice compact radiant near RA = 165° and Decl. = +78° (yellow dots) on 2022 October 5–6 (data CAMS BeNeLux). The first OCT meteor was captured at $23^h22^m59^s$ UT by Bart Dessoy (Zoersel, Belgium), Steve Rau (Zillebeke, Belgium), Steve Rau (Oostende, Belgium) and Adriana and Paul Roggemans (Mechelen, Belgium). The last OCT meteor that night was captured at $04^h46^m24^s$ UT by Luc Gobin (Mechelen, Belgium), Hervé Lamy (Ukkel, Belgium) and Pierre-Yves Péchart (Hagnicourt, France).

In *Table 2* we see the number of OCT-meteors during this night in intervals of 30 minutes. Triggered by good observing conditions, visual observers *Michel Vandeputte* and *Koen Miskotte* decided to make observations this night. They also looked whether they could detect visually activity from this shower. They made the following comments: "*The most striking aspect of these meteors is their medium speed. Visual observers, who are not aware of activity of this shower, will certainly classify these meteors as sporadic*".

It is interesting to look whether the display of the activity, visible in the CAMS data (*Table 2*), is also visible in the data of Michel and Koen. Their results are as follows:

MISKO

- 02^h09^m–03^h10^m UT 1 OCT +3
- 03^h10^m–04^h20^m UT 3 OCT +2 ; +3 ; +4

VANMC

- 01^h30^m–02^h30^m UT 1 OCT +3
- 02^h30^m–03^h30^m UT 2 OCT +3, +2
- 03^h30^m–04^h30^m UT 2 OCT +3, +2

From this data we can say that for these visual observers the activity is more or less in agreement with CAMS data.

This is a nice confirmation that an attentive observer, who is aware of activity of a minor stream, can monitor this stream also.

4 Conclusion

The results for October 2022 are the best in 11 years of the CAMS BeNeLux network for this month.

Acknowledgment

In October 2022 the CAMS BeNeLux network was operated by the following volunteers:

Hans Betlem (Woold, Netherlands, CAMS 3071, 3072 and 3073), *Jean-Marie Biets* (Wilderen, Belgium, CAMS 379, 380, 381 and 382), *Ludger Boergerding* (Holdorf, Germany, RMS 3801), *Günther Boerjan* (Assenede, Belgium, RMS 3823), *Martin Breukers* (Hengelo, Netherlands, CAMS 320, 321, 322, 323, 324, 325, 326 and 327, RMS 319, 328 and 329), *Seppe Canonaco* (Genk, RMS 3818 and 3819), *Pierre de Ponthiere* (Lesve, Belgium, RMS 3816 and 3826), *Bart Dessoy* (Zoersel, Belgium, CAMS 397, 398, 804, 805, 806, 3888 and RMS 3827), *Tammo Jan Dijkema* (Dwingeloo, Netherlands, RMS 3199), *Isabelle Ansseau, Jean-Paul Dumoulin, Dominique Guiot* and *Christian Walin* (Grapfontaine, Belgium, CAMS 814 and 815, RMS 3814 and 3817), *Uwe Glässner* (Langenfeld, Germany, RMS 3800), *Luc Gobin* (Mechelen, Belgium, CAMS 3890, 3891, 3892 and 3893), *Tioga Gulon* (Nancy, France, CAMS 3900 and 3901),

Robert Haas (Alphen aan de Rijn, Netherlands, CAMS 3160, 3161, 3162, 3163, 3164, 3165, 3166 and 3167), *Robert Haas* (Texel, Netherlands, CAMS 810, 811, 812 and 813), *Kees Habraken* (Kattendijke, Netherlands, RMS 3780 and 3781), *Klaas Jobse* (Oostkapelle, Netherlands, CAMS 3030, 3031, 3032, 3033, 3034, 3035, 3036 and 3037), *Carl Johannink* (Gronau, Germany, CAMS 3100, 3101, 3102), *Reinhard Kühn* (Flatzby, Germany, RMS 3802), *Hervé Lamy* (Dourbes, Belgium, CAMS 394 and 395, RMS 3825), *Hervé Lamy* (Humain, Belgium, RMS 3821), *Hervé Lamy* (Ukkel, Belgium, CAMS 393), *Koen Miskotte* (Ermelo, Netherlands, CAMS 3051, 3052, 353 and 354), *Pierre-Yves Péchart* (Hagnicourt, France, RMS 3902 and 3903), *Tim Polfliet* (Gent, Belgium, CAMS 396, RMS 3820), *Steve Rau* (Oostende, Belgium, RMS 3822), *Steve Rau* (Zillebeke, Belgium, CAMS 3850 and 3852, RMS 3851 and 3853), *Paul and Adriana Roggemans* (Mechelen, Belgium, RMS 3830 and 3831, CAMS 3832, 3833, 3834, 3835, 3836 and 3837), *Jim Rowe* (Eastbourne, Great Britain, RMS 3829), *Philippe Schaack* (Roodt-sur-Syre, Luxemburg, RMS 3952), *Hans Schremmer* (Niederkruechten, Germany, CAMS 803), *Erwin van Ballegoij* (Heesh, Netherlands CAMS 3148 and 3149).

References

Jenniskens P., Moilanen J., Lyytinen E., Yrjölä I. and Brower J. (2005). "The 2005 October 5 outburst of October Camelopardalids". *WGN, Journal of the International Meteor Organization*, **33**, 125–128.

Jenniskens P. (2006). Meteor Showers and their Parent Comets. ISBN 0521853494. Cambridge, UK: Cambridge University Press. Pages 528–530.

Jenniskens P., Gural P. S., Grigsby B., Dynneson L., Koop M. and Holman D. (2011). "CAMS: Cameras for Allsky Meteor Surveillance to validate minor meteor showers". *Icarus*, **216**, 40–61.

Roggemans P., Johannink C., Cambell-Burns P. (2019). "October Camelopardalids (OCT#281)". *eMetN*, **4**, 65–73.

November 2022 report CAMS BeNeLux

Carl Johannink

Am Ollenkamp 4, 48599 Gronau, Germany
c.johannink@t-online.de

A summary of the activity of the CAMS BeNeLux network during the month of November 2022 is presented. This month we collected a total of 17401 multi-station meteors resulting in 5635 orbits.

1 Introduction

In November the chances for long periods of clear weather are getting rather small. Only under specific favorable circumstances the BeNeLux can count on a longer series of clear nights.

Meteor activity is still very high this month, due to high sporadic activity and the visibility of meteoroid streams like the Taurids and the Leonids. So, it is interesting to see what this month would bring us.

2 November 2022 statistics

Until November 25, weather remained stable, with lots of sunshine, resulting in good results for our network. Afterwards, the weather turned more and more gloomy. Only a handful of orbits in this period could be collected. Not a single orbit could be obtained during November 27–28.

This month CAMS BeNeLux collected a total of 17401 multi-station meteors, resulting in 5635 orbits. This is a second-best score for this month. Only in November 2018 more orbits were collected (*Figure 1* and *Table 1*).

In particular November 4–5, 11–12 and 13–14 got good results with more than 500 orbits in each night, due to clear conditions in these nights. The highest number of orbits were collected on November 13–14, 576 orbits.

52% of all orbits were collected by at least 3 stations. Once again, like in October, this emphasizes good coverage of the skies over the BeNeLux. On average 86.2 cameras were active each night, with a maximum of 94 cameras and a minimum of 69 cameras. These numbers are comparable to the situation of previous month. We hope that the camera stations such as Terschelling and Burlage can rejoin the efforts of the network soon.

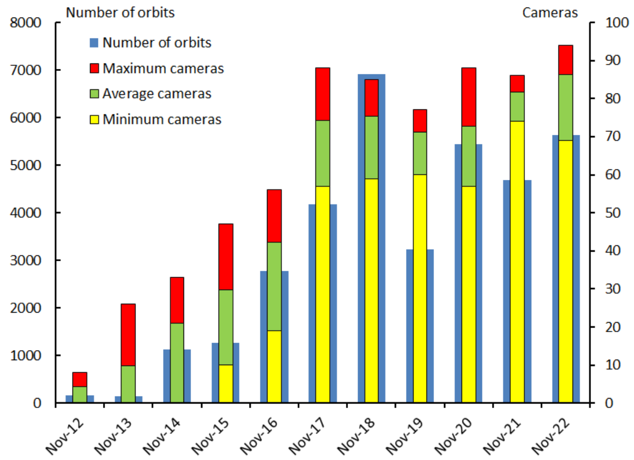

Figure 1 – Comparing November 2022 to previous months of November in the CAMS BeNeLux history. The blue bars represent the number of orbits, the red bars the maximum number of cameras capturing in a single night, the green bar the average number of cameras capturing per night and the yellow bar the minimum number.

Table 1 – Number of orbits and active cameras in the BeNeLux during November 2012–2022.

Year	Nights	Orbits	Stations	Max. Cams	Min. Cams	Mean Cams
2012	14	165	6	8	–	4.4
2013	13	142	10	26	–	9.8
2014	24	1123	14	33	–	21.1
2015	23	1261	15	47	10	29.8
2016	24	2769	19	56	19	42.2
2017	26	4182	22	88	57	74.2
2018	28	6916	21	85	59	75.3
2019	27	3237	20	77	60	71.1
2020	28	5441	23	88	57	72.6
2021	24	4691	26	86	74	81.6
2022	29	5635	31	94	69	86.2
Total	260	35562				

3 Conclusion

Results for November 2022 are among the best in the 11 years of the existance of the CAMS BeNeLux network.

Acknowledgment

Many thanks to all operators in the CAMS BeNeLux network for their work and quick delivery of data. In November 2022 the CAMS BeNeLux network was operated by the following volunteers:

Hans Betlem (Woold, Netherlands, CAMS 3071, 3072 and 3073), *Jean-Marie Biets* (Wilderen, Belgium, CAMS 379, 380, 381 and 382), *Ludger Boergerding* (Holdorf, Germany, RMS 3801), *Günther Boerjan* (Assenede, Belgium, RMS 3823), *Martin Breukers* (Hengelo, Netherlands, CAMS 320, 321, 322, 323, 324, 325, 326 and 327, RMS 319, 328 and 329), *Seppe Canonaco* (Genk, RMS 3818 and 3819), *Pierre de Ponthiere* (Lesve, Belgium, RMS 3816 and 3826), *Bart Dessoy* (Zoersel, Belgium, CAMS 397, 398, 804, 805, 806, 3888 and RMS 3827), *Tammo Jan Dijkema* (Dwingeloo, Netherlands, RMS 3199), *Isabelle Ansseau, Jean-Paul Dumoulin, Dominique Guiot* and *Christian Walin* (Grapfontaine, Belgium, CAMS 814 and 815, RMS 3814 and 3817), *Uwe Glässner* (Langenfeld, Germany, RMS 3800), *Luc Gobin* (Mechelen, Belgium, CAMS 3890, 3891, 3892 and 3893), *Tioga Gulon* (Nancy, France, CAMS 3900 and 3901), *Robert Haas* (Alphen aan de Rijn, Netherlands, CAMS 3160, 3161, 3162, 3163, 3164, 3165, 3166 and 3167), *Robert Haas* (Texel, Netherlands, CAMS 810, 811, 812 and 813), *Kees Habraken* (Kattendijke, Netherlands, RMS 3780 and 3781), *Klaas Jobse* (Oostkapelle, Netherlands, CAMS 3030, 3031, 3032, 3033, 3034, 3035, 3036 and 3037), *Carl Johannink* (Gronau, Germany, CAMS 3100, 3101, 3102), *Reinhard Kühn* (Flatzby, Germany, RMS 3802), *Hervé Lamy* (Dourbes, Belgium, CAMS 394 and 395, RMS 3825), *Hervé Lamy* (Humain, Belgium, RMS 3821), *Hervé Lamy* (Ukkel, Belgium, CAMS 393), *Koen Miskotte* (Ermelo, Netherlands, CAMS 3051, 3052, 353 and 354), *Pierre-Yves Péchart* (Hagnicourt, France, RMS 3902 and 3903), *Tim Polfliet* (Gent, Belgium, CAMS 396, RMS 3820), *Steve Rau* (Oostende, Belgium, RMS 3822), *Steve Rau* (Zillebeke, Belgium, CAMS 3850 and 3852, RMS 3851 and 3853), *Paul and Adriana Roggemans* (Mechelen, Belgium, RMS 3830 and 3831, CAMS 3832, 3833, 3834, 3835, 3836 and 3837), *Jim Rowe* (Eastbourne, Great Britain, RMS 3829), *Philippe Schaack* (Roodt-sur-Syre, Luxemburg, RMS 3952), *Hans Schremmer* (Niederkruechten, Germany, CAMS 803), *Erwin van Ballegoij* (Heesh, Netherlands CAMS 3148 and 3149).

The mission of MeteorNews is to offer fast meteor news to a global audience, a swift exchange of information in all fields of active amateur meteor work without editing constraints. MeteorNews is freely available without any fees. To receive a notification: https://www.meteornews.net/newsletter-signup/.

You are welcome to contribute to MeteorNews on a regular or casual basis, if you wish to. Anyone can become an author or editor, send an email to us. For more info read: https://meteornews.net/writing-content-for-emeteornews/

MeteorNews account manager: Richard Kacerek rickzkm@gmail.com.

The running costs for website hosting are covered by a team of sponsors. We want to thank the 2022-2023 sponsors: Anonymous (3x), Mikhail Bidnichenko, Gaetano Brando, Trevor C, Nigel Cunnington, Kevin Heider, Paul Hyde, K. Jamrogowicx, Dave Jones, Richard Kacerek, Richard Lancaster, Joseph Lemaire, Mark McIntyre, Hiroshi Ogawa, Paul Mohan, Stan Nelson, Lubos Neslusan, BillR, Whitham D. Reeve, John Schlin, Ann Schroyens and Denis Vida.

Financial support is still needed and welcome:
https://www.justgiving.com/crowdfunding/meteor-news?utm_term=JJBjmJpzV

Contributing to this issue:

- Aceituno J.
- Aimee A.I.
- Ávila D.
- de Guindos E.
- García A.
- Gómez-Hernández A.
- Gómez-Martínez J.
- Izquierdo J.
- Johannink C.
- Kacerek R.
- Landy-Gyebnar M.
- Madiedo J.M.
- Maslov M.
- Ogawa H.
- Ortiz J.L.
- Palacián J.
- Roggemans P.
- San Segundo A.
- Santos-Sanz P.
- Šegon D.
- Sekiguchi T.
- Sugimoto H.
- Tosar B.
- Verbelen F.
- Vida D.
- Yanguas P.

ISSN 2570-4745 Online publication https://meteornews.net

Listed and archived with ADS Abstract Service: https://ui.adsabs.harvard.edu/search/q=eMetN

MeteorNews Publisher:

Valašské Meziříčí Observatory, Vsetínská 78, 75701 Valašské Meziříčí, Czech Republic